Fronts and Frontogenesis as Revealed by High Time Resolution Data

Albert E. Frank and David A. Barber

AUGUST 1977

NASA

NASA Reference Publication 1005

Fronts and Frontogenesis as Revealed by High Time Resolution Data

Albert E. Frank and David A. Barber

George C. Marshall Space Flight Center
Marshall Space Flight Center, Alabama

TABLE OF CONTENTS

LIST OF ILLUSTRATIONS

List of Illustrations -- continued

FRONTS AND FRONTOGENESIS AS REVEALED BY HIGH TIME RESOLUTION DATA

PURPOSE OF THE STUDY

Fronts, which are sloping stable layers characterized by large values of baroclinity and horizontal and vertical wind shear, are typical features of the atmosphere. Indeed, the rotating pan experiments of Fultz (1952), Faller (1956), and others suggest that fronts necessarily occur in a rotating, differentially heated fluid. The well known association of fronts with cyclones, jet streams, and cloud and precipitation systems shows the importance of understanding the dynamics and structure of fronts.

Years of study have resulted in knowledge of the basic features of fronts and the processes responsible for their formation and dissolution. However, much uncertainty remains about significant details of fronts and frontogenesis. In this report, a unique set of data will be studied in hopes of clarifying some of these uncertainties. Specifically, the purposes of this study are:

1. To use high time resolution data to produce analyses which will show frontal evolution on a time scale not usually obtainable.

2. To employ these analyses to determine the processes responsible for the observed changes in the fronts being studied.

3. To compare and contrast these results with those
    obtained by other investigators.

HISTORICAL REVIEW OF FRONTAL CONCEPTS

Concepts Prior to 1948

Prior to the second decade of this century, meterologists had little conception of the fundamental atmospheric structure that we today call a front. Fronts were implicit in many of the cyclone models of the 1880's which regarded storms to be regions of conflicting air masses. The cold front was clearly described by Espy (1850) and several others some 20 years later. (The warm front went unrecognized due to the exclusion of all variables except sea level isobars from meteorological analyses.) Even as early as 1820, Howard (1820) described how an advancing mass of cold air would lift an opposing warm air mass, causing vast areas of clouds and precipitation. However, no model existed which could explain the relation of fronts to weather systems nor the processes that cause fronts to form.

Bjerknes (1918) provided the first reasonably complete picture of the nature of the wave cyclone and of the fronts which are an integral part of it. Using a dense network of surface data, he found the zones of confluence associated with the warm and cold fronts, and noted the temperature gradient across these regions. The now well known pattern of clouds and precipitation was described and related to lifting of the air by the fronts. Bjerknes also explained

how the temperature contrast across the fronts could be
utilized by the storm as a source of energy and showed that
the circulation about the cyclone transported heat to re-
gions of cold air. That is, fronts and the cyclones as-
sociated with them were shown to be an integral part of the
general circulation.

Further advances followed in short order. In 1919,
Bergeron discovered the occlusion process. Bjerknes and
Solberg (1921) presented their model of the life cycle of a
typical extratropical cyclone, from nascent wave to fully
occluded and dissipating vortex. They described the two
types of occluded fronts and noted the existence of second-
ary cold fronts in the cold air behind the storm. The polar
front was defined and described, and methods for its analy-
sis were given. Cyclone families were also described, and
their role in the general circulation and heat transport
discussed at length.

Bergeron (1928) was the first to attend to the problem
of how fronts form or dissipate. He showed that a station-
ary field of deformation acting upon a linear field of
potential temperature will concentrate the isentropes along
the axis of dilatation. Though this was an important
demonstration of how frontogenesis could occur, it was a
rather idealized case. Petterssen (1936) studied nonlinear
fields and found that concentration of conservative atmos-
pheric properties can occur in a nonstationary field of

deformation. However, the line of maximum gradient of the prescribed property is no longer found to coincide with the axis of dilatation. Also, the isopleths of the variable under study undergo contraction only if they are oriented within a certain angle (usually 45°) of the axis of dilatation. A further contribution of this paper was to define frontogenesis in concrete terms, namely the total time rate of change of the gradient of a conservative atmospheric property. Petterssen's and Bergeron's work showed that fronts are formed where two air masses are brought into juxtaposition by the action of the winds.

A later paper by Petterssen and Austin (1942) studied frontogenesis from the point of view of the production and maintenance of cyclonic vorticity. An important result of this study is that in the presence of friction, more than just deformation is necessary for the preservation of the surface front; namely, horizontal convergence is required to maintain the field of vorticity.

This paper is noteworthy because it was the first (and for some years, the only) treatment of the development of fronts from a dynamical point of view. Until the end of World War II, frontogenesis studies were characteristically limited to studying the kinematics of the flow in the vicinity of surface fronts. As late as 1940, Petterssen (1940) stated, "there can be little doubt that frontogenesis is mainly a kinematic phenomenon". The major advances

in the study of fronts and frontogenesis that began to oc-
cur in the late 1940's resulted from two important changes
in the field of meteorology.

The first of these changes was an improvement in the
character and quantity of meteorological data. The need for
improved weather forecasts in the war years and the develop-
ment of a practical and reliable radiosonde led to the
establishment of a vastly expanded network of regular upper
air observations. For the first time, meteorologists could
study deep layers of the atmosphere over large areas on a
continuing basis. Hence, subsequent articles no longer con-
fined themselves to examining surface fronts, and the com-
plexity of atmospheric structures began to be revealed.

The second major influence on frontal studies was the
development of the Chicago School of Meteorology and its
emphasis on atmospheric dynamics. The discovery of the jet
stream had profound implications for all later investiga-
tions of atmospheric fronts.

More Recent Studies

In the light of these changes in meteorological methods
and philosophy, the important paper by Miller (1948) can be
interpreted as a bridge between the older ideas and subse-
quent concepts of processes affecting frontal intensity.
Following Petterssen's definition of frontogenesis, Miller
derived a kinematic equation for frontogenesis in three

dimensions. Miller's equation is

$$F_3 = (\cos\,\alpha\,\frac{\partial}{\partial x} + \sin\,\alpha\,\frac{\partial}{\partial z})\,\overset{B\qquad C}{\frac{dS}{dt}} - (u_x S_x + w_x S_z)\cos\,\alpha$$

$$\overset{D\qquad\quad E}{- (u_z S_x + w_z S_z)\sin\,\alpha}$$

where the y-axis is tangential to the surfaces of conservative property S, and α is the angle between the gradients of S and the x-axis.

The interpretation of the terms of the equation is as follows:

A) Spatial variations in the total time derivative of the conservative property being studied.

B) Confluence of the flow across the front.

C) Variations in the vertical velocity across the front.

D) Vertical shear of the flow normal to the front.

E) Confluence of the vertical velocity.

These processes are illustrated schematically in figure 1.

At about this same time, Palmén (1948) and Palmén and Newton (1948) described the structure of the polar front as shown by analyses of cross sections and of the 500 mb surface. The front was shown to be a sloping layer of high thermal stability and large horizontal temperature gradient extending through a deep layer of the troposphere (though not, on their analyses, above 400 mb). The warm and cold
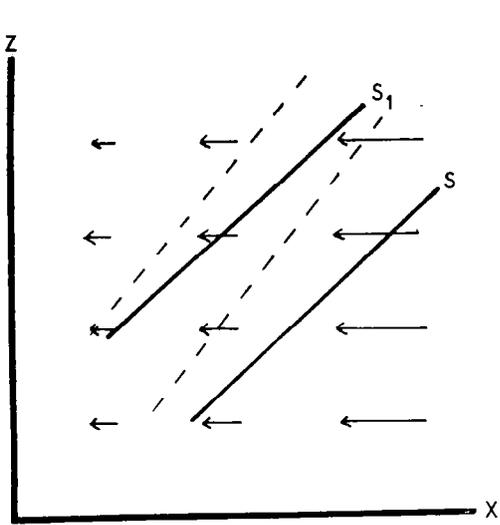
Illustration of frontogenetic effect of term B of Miller's equation.
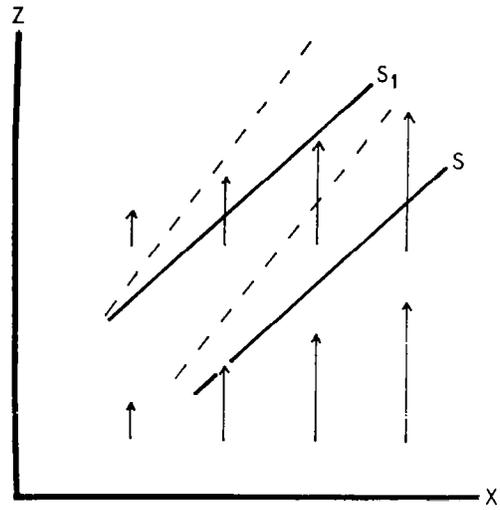
Illustration of frontogenetic effect of term C of Miller's equation.
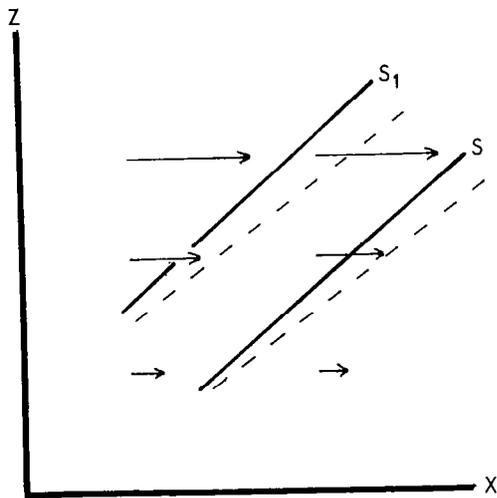
Illustration of frontogenetic effect of term D of Miller's equation.
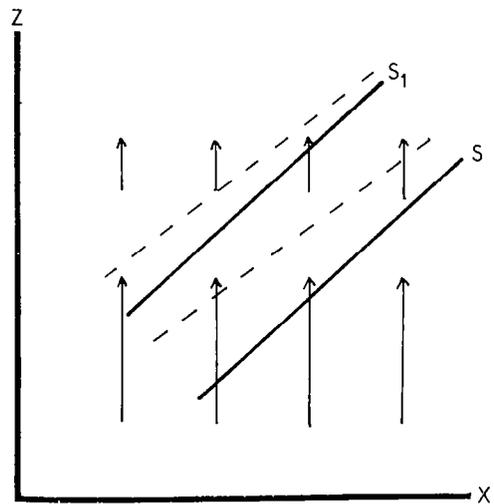
Illustration of frontogenetic effect of term E of Miller's equation.

Figure 1.   Illustration of terms of Miller's (1948) fronto-genesis equation.

air masses on either side of the front possessed substantial baroclinity.[1]

A narrow current of high speed westerly flow (the jet stream) was found near the level of the tropopause and above the location where the frontal surface intercepted the 500-600 mb level. The tropopause was found to be low in the cold air, high in the warm air, and indistinct in the vicinity of the front.

The failure to identify the front in the thermal field of the uppermost troposphere is significant, for as Berggren (1952) showed, the atmosphere near the level of maximum wind is nearly barotropic, and the front there is recognized as a region of large horizontal wind shear. Therefore, a frontogenetic process near the tropopause is one that must concentrate shear.

The first paper to study upper-level frontogenesis was by Reed and Sanders (1953). They applied Miller's equations to a case of intense upper level frontogenesis and found that nearly all of the development (near 400mb) in their case could be accounted for by variations in a direction normal to the front in the magnitude of the vertical velocity (this effect will henceforth be referred to as the "tilting" effect and its mathematical representation as the

---

[1] This paper will follow the conventions of Godson (1951) and call such broad regions of baroclinity lacking sharp boundaries "frontal zones," while the terms "front" or "hyperbaroclinic zone" will be reserved for the well defined layers of more intense baroclinity.

"tilting term."). The upper front was found to be a region of sinking motion with the strongest subsidence near the warm edge of the front. This intensifies the temperature gradient due to transverse differences in adiabatic warming and increases the vorticity (wind shear) by tilting a previously horizontal axis of vorticity such that it gains a component about a vertical axis. Reed and Sanders conclude that their front was a "portion of the lower stratosphere which underwent strong subsidence with the tropopause assuming the character and appearance of a frontal surface."

Reed (1955) studied another case of intense upper level frontogenesis and verified the results of the aforementioned paper; i.e., the front intensified (between 300 and 500 mb) due to variations in the vertical velocity across the front. He pointed out that this meant that a front need not be considered as separating air masses of different origins, but can arise within a body of air of uniform temperature (specifically the polar air mass). He concluded on the basis of the conservation of potential vorticity that the front formed due to the folding of the tropopause "with a thin tongue of stratospheric air slicing down into the troposphere," in this case, down to 700 or 800 mb.

Palmén and Newton (1969) argue against such a deep extrusion of stratospheric air and instead consider a limited descent of air from the stratosphere to be "a

necessary accompaniment of the vertical circulations con-
necting the frontogenetic processes near the level of maxi-
mum wind and in the middle troposphere." The presence of
stratospheric air in upper level fronts is strongly sup-
ported by analyses of potential vorticity and radioactivity
(Danielsen, 1964) and potential vorticity and ozone
(Shapiro, 1974) in the vicinity of these fronts. The ex-
treme dryness of high altitude fronts can also be inter-
preted as being due to descent of air within these regions
(Sanders, 1955).

Newton (1954) examined the frontolytic processes at
the exit region of a front that was wrapped around the west
side of a trough. Miller's equations again formed the
basis for the equations that Newton used to study time
changes of horizontal temperature gradient, thermal stabi-
lity, absolute vorticity, and vertical shear following the
motion. An important conclusion is that the processes res-
ponsible for frontogenesis are different at different
altitudes in the troposphere. Like Reed and Reed and
Sanders, Newton found the tilting term to be important in
the middle troposphere (near 500 mb). A difference between
this study and those already mentioned, though, is that the
tilting term is not dominant but is one of many processes
affecting the intensity of the front. Diffluence of the
flow normal to the front and differences in temperature ad-
vection across the front are of comparable significance

with tilting for changing the horizontal temperature
gradient. Tilting is also very important for changing the
absolute vorticity, but the effects of horizontal diver-
gence are considerable. Vertical shear of the wind is
found to be responsible for most of the changes of stabi-
lity in this case. The time rate of change of the vertical
shear of the flow parallel to the front is shown to be
essentially a non-geostrophic process. At the maximum wind
level, where the vertical velocity is zero, there can be
no tilting. Here, horizontal divergence is the dominant
frontolytic process.

Newton suggested that vertical motion near the surface
is sufficiently damped that frontogenesis there is due to
horizontal advections in a field of deformation. That this
assumption is incorrect is clearly shown by Sanders (1955).
His study of an intense low level front demonstrates that
near the ground, the front is a line of strong convergence
with an intense "jet" of rising warm air just above the
surface front. The strong gradient of vertical motion
across the front produces tilting which is frontogenetic in
the warm air just ahead of the front and frontolytic with-
in the front itself. The frontogenetic effect of con-
fluence is strongest within the front at the surface and
decreases rapidly upward through the front. The net effect
is for warm air to be entrained into the front and to
undergo strong frontogenesis (with respect to the

horizontal temperature gradient and absolute vorticity) in the lower levels. As this air rises and moves into the cold air, it experiences individual frontolysis.

Not only are the processes acting on low level fronts different from those for fronts aloft, but the structures of the two types of fronts are also dissimilar. The low level front is typically shallow with the smallest width and largest gradients at the surface. The gradients and slope of the front decrease and the width of the front increases upwards. Sanders further notes, "there appears to be no reason why the two types of zone should adjoin directly in space, even when they are simultaneously present in the same general region."

Confluence acting through a deep layer of the troposphere will increase the layer-averaged horizontal temperature gradient and therefore increase the magnitude of the thermal wind. If the temperature advections in the layer proceed at a fast enough pace, the flow may be unable to adjust itself rapidly enough to the changing pressure gradient, with resultant flow across the contours toward low pressure. The cross-contour flow will have the largest magnitude near the region of maximum wind, and its speed will decrease away from the jet. The result will be divergence aloft and rising motion in the warm air. Continuity considerations require sinking in the cold air. The role of such a circulation was examined by Sawyer (1956). He

constructed trajectories in the vicinity of fronts and found many of the fronts to be regions of confluence, particularly in the lower levels. Sawyer points out that the direct circulation described above would be frontolytic and states that the existence of the front is maintained by the continuing juxtaposition of air masses of different origins through confluence. It is significant for this hypothesis that the one front in his sample which showed no confluence also lacked a well-defined frontal cloud system.

Sawyer modeled the circulation in a zone of confluence with the flow along the isotherms being geostrophic with a transverse ageostrophic component superimposed. He obtained rising motion in the warm air and sinking motion in the cold air. The strength of the vertical motions on both sides of the front, but especially in the warm air, was intensified when condensation and neutral stability were present in the warm air. The intensity of the frontogenesis was greatest in the upper and lower troposphere and small in the middle levels. Eliassen (1962) studied a similar circulation allowing the direction of the geostrophic wind to vary with height and confirmed Sawyer's basic results. Both noted that the release of latent heat of condensation in the warm air acts to compensate the dissipative effect of the thermally direct circulation.

Bosart (1970) studied frontogenesis using three-hourly upper-air data of the AVE I Experiment. The results of his

study are illuminating in helping to resolve the apparent
contradictions between frontogenesis due to thermally
di____t circulations and that associated with thermally in-
direct circulations. He found that

> in the current case the initial frontogenetic
> mechanism arises from the cross-stream
> gradient of vertical velocity with the
> strongest subsidence on the warm side of
> the baroclinic zone. Horizontal confluence
> became a frontogenetic factor in the later
> stages... The change from a thermally in-
> direct to a thermally direct circulation is
> controlled by the passage of a short wave
> containing the baroclinic zone around the
> bottom of the long wave trough.

This result is consistent with the reasoning of Palmen and
Newton (1969) that descent of warm air on the east side of
the ridge is frontogenetic, while ascent of the warm air
downstream from a trough is frontolytic. Bosart also pre-
sents evidence for the descent of stratospheric air to low
altitudes (650) mb during the development of the front.

The uncertainty of frontal structure near the level of
the tropopause has already been mentioned. Berggren (1952)
found at this level a narrow (100km) zone of large cyclonic
wind shear continuous with and of similar intensity to that
in the hyperbaroclinic zone of lower levels. He inter-
preted the tropopause here to be broken and the front to
extend up into the stratosphere at an inclination opposite
to that in the troposphere (see figure 2).
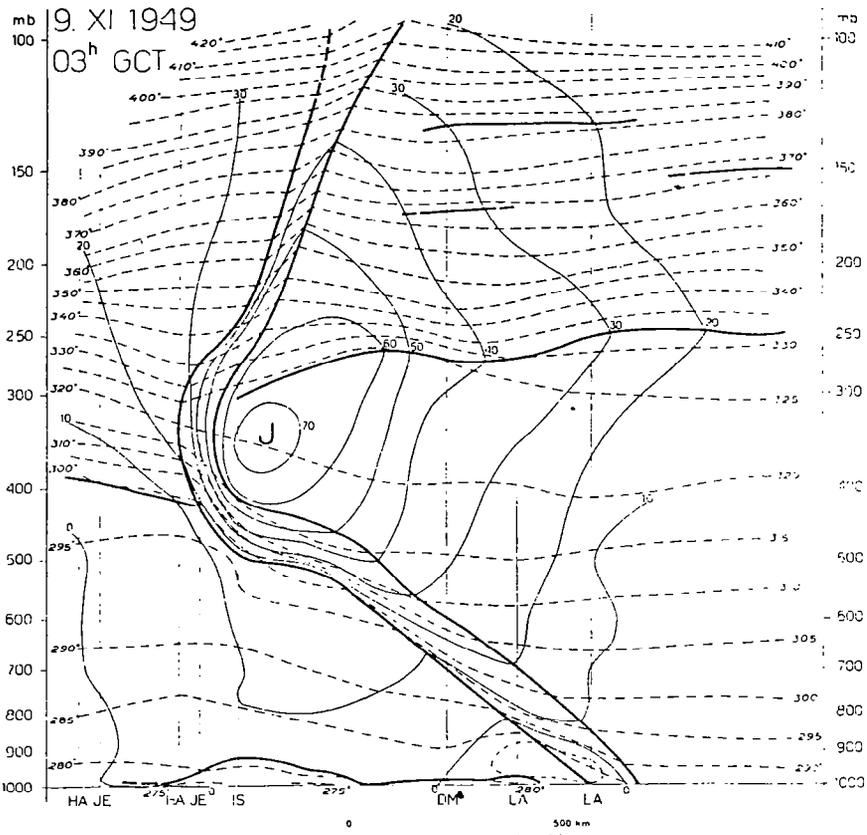
Figure 2. Frontal analysis from Berggren (1952). Isentropes (°K), thin, dashed lines; isotachs (m sec^{-1}), thin, solid lines; inversions, tropopauses, and frontal boundaries, heavy, solid lines.

Reed and Danielsen (1959) studied five cases of pronounced upper fronts and constructed the composite diagrams of figure 3. They merged the upper and lower surfaces of the front with the warm and cold air tropopause, respectively. Though they considered the front at high levels to be a zone of large cyclonic shear, their model possesses a smaller horizontal gradient of potential vorticity near the tropopause than does that of Berggren. Reed and Danielsen also subscribed to the concept of a causal link between the formation of an upper-level front and the downward extrusion of stratospheric air, and regarded the tropopause to fold as the extrusion occurred.

Recent work corroborates some aspects of each interpretation. Shapiro (1976), using data collected by radiosonde ascents and aircraft flights, documented several instances of "a 100 km scale cyclonic shear zone within the stratosphere which is continuous with the upper portion of the tropospheric frontal zone." This zone was embedded within a potential vorticity field whose structure is compatible with the folded tropopause of Reed and Danielsen. Bosart (1970) also finds evidence supportive of the interpretation of a folding of the tropopause surface.

Shapiro hypothesizes that ageostrophic convergence in the geostrophic confluence about a forming jet streak leads to sufficient increase in the vertical wind shear for turbulence to occur. The vertical profile of turbulent heat
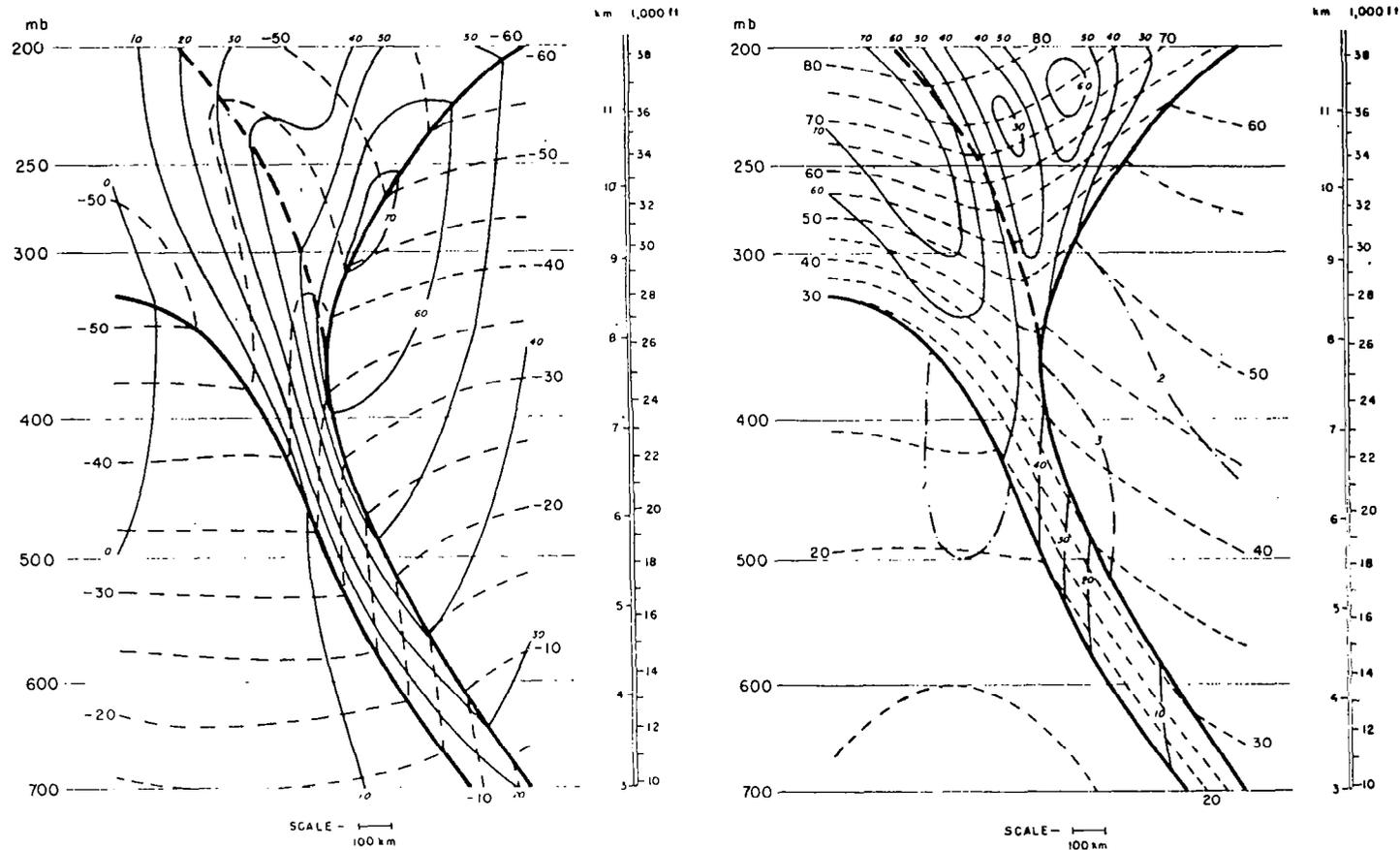
Figure 3. Composite fronts of Reed and Danielsen (1959). On the left: temperature
(°C, dashed) and isotachs (m sec^{-1}) of the geostrophic flow normal to the
section; on the right: isentropes (°C, dashed) and potential vorticity
(x 10^{-9} c.g.s.).

flux is one of heating above the level of maximum wind and cooling below the level. This increase of the static stability coupled with the increase of vorticity due to the horizontal convergence results in the creation of a region of anomalously large values of potential vorticity. These values "descend into the troposphere beneath the decelerating exit region of the jet during frontogenesis and are partially dissipated by turbulent mixing in the frontal layer."

Some of the most striking results of several analytic studies of frontogenesis have come from the models of Hoskins (1971). He considered a Boussinesq, rotating, inviscid fluid bounded at the top and bottom by rigid surfaces with an initial specified field of potential temperature. A horizontal field of deformation is allowed to act on the system. In the case of a single rotating stratified fluid, Hoskins obtains results similar to those of Sanders' (1955) low-level fronts (see figure 4). The front becomes more shallow and less intense aloft. The circulation is in a direct sense. Latent heat is frontogenetic in that it increases the buoyancy, and hence the upward motion, of the warm air. Friction within the Ekman Layer causes convergence, which is frontogenetic. However, divergence above the Ekman Layer is frontolytic, and the net effect of friction is uncertain. This is also discussed by Eliassen (1966).
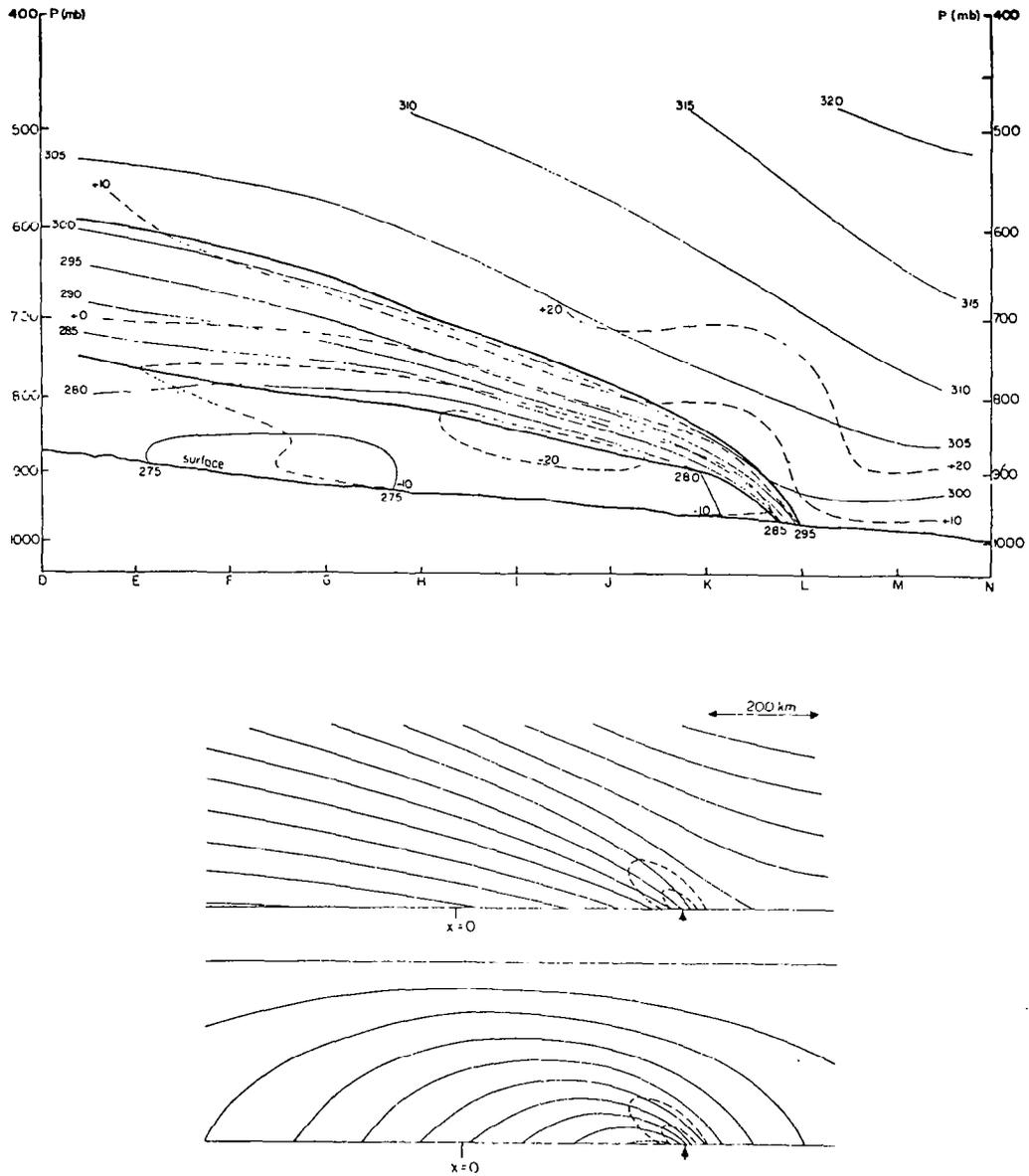
Figure 4. Top: low level front from Sanders (1955). Isentropes (°K, thin, solid lines) and isotachs (m sec⁻¹) of flow normal to the section. Isentropes (middle) every 2.4 K and isotachs (bottom) of long front velocity every 4 m sec⁻¹ from model front from Hoskins (1971).

Hoskins also examined a two fluid case, with an upper region of high potential vorticity (the stratosphere) separated from a lower region of low potential vorticity (the troposphere) by a discontinuity surface (the tropopause). When a height-independent deformation field acted on the system, a downward kink in the tropopause formed. The circulation in this feature was indirect. Simultaneously, a wind maximum developed near the level of the tropopause (see figure 5). A low-level baroclinic zone with direct thermal circulation also appeared. Although the depth of the upper "front" and the intensity of the "jet stream" are both underdone, and the simplicity of the model is unlike the real atmosphere, the similarities of Hoskin's results to observed structures is noteworthy.

Summary

Atmospheric fronts may be classified according to the following categories:

Upper Level Fronts

These are fronts that extend from the lower stratosphere into the upper or middle troposphere. Near the tropopause, they lack a thermal gradient and are zones of large horizontal cyclonic shear; away from the tropopause they are regions of both shear and baroclinity. The air in these fronts is very dry and has values of potential
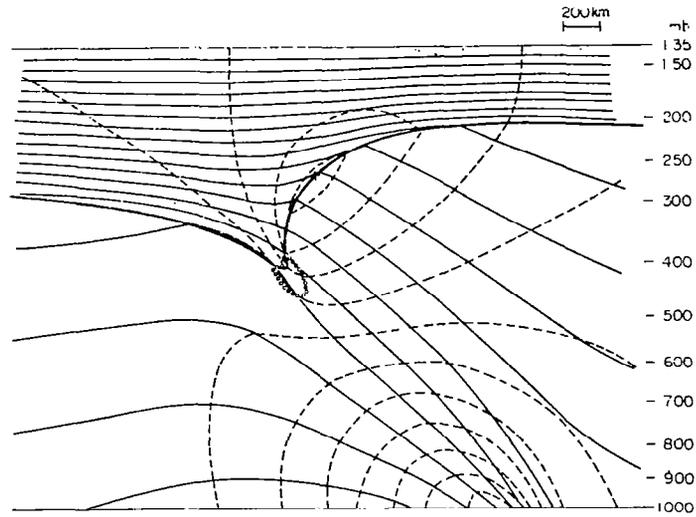
Figure 5. Model front from Hoskins (1971). Isentropes
(solid) every 7.8 K and isotachs (dashed) of long
front velocity every 10.5 m sec^{-1}.

vorticity, radioactivity, and ozone concentrations of com-
parable magnitude with the air of the stratosphere. The
circulation in these fronts is thermally indirect, with the
strongest subsidence near the warm edge of the front. The
air in at least the upper portion of such fronts is of
stratospheric origin. Below the level of maximum wind,
these transverse differences in vertical velocity are very
important for frontogenesis. Near the level of maximum
wind confluence is a more important frontogenetic effect.
The horizontal flow is nearly parallel to the isotherms for
upper fronts, and its speed is greater than that of the
phase speed of the front. These fronts are more common on
the west wide of upper troughs and the temperature
gradients become most intense as the fronts reach the axis
of the trough.

Low-Level Fronts

This type of front is typically found to extend from
the surface to 700 or 600 mb. It is most intense at and
near the surface and weakens rapidly with increasing height.
The width of the front also increases upwards, and the
front becomes parallel to the surface. Low-level fronts
separate air masses of different origins, and form where a
horizontal field of deformation acts upon a region of
temperature gradient. The circulation about these fronts
is thermally direct. Strong across-the-front gradients of

24

vertical velocity where the front intersects the surface
,are frontogenetic ahead of the front near the surface, and
frontolytic aloft. The effects of confluence are similar.
The release of latent heat of condensation in the ascending
warm air acts in a frontogenetic manner. Friction near the
surface causes convergence, which is frontogenetic, but
this is accompanied by frontolytic divergence at higher
altitudes.

Troposphere-Spanning Fronts

Both upper and lower-level fronts are able to exist in
the absence of the other. However, fronts are observed
which reach unbroken from the surface to the tropopause.
Examples of such fronts are found in Newton (1954) and
Palmén and Newton (1963), among others (see figure 6).
Such fronts are commonly depicted, but usually not studied
as a separate class. They would appear to be instances in
which an upper-level front and lower-level front become
linked together. This would seem to occur after an upper-
level front has propagated to the east side of an upper
trough, where the likelihood of there being confluent sur-
face winds and low-level fronts is greatest. However, ex-
cept for Petterssen (1956) (see figure 7), the author is
unaware of any study showing the development of this type
of front. As Petterssen's cross-sections through the front
are twenty-four hours apart, there is inadequate time
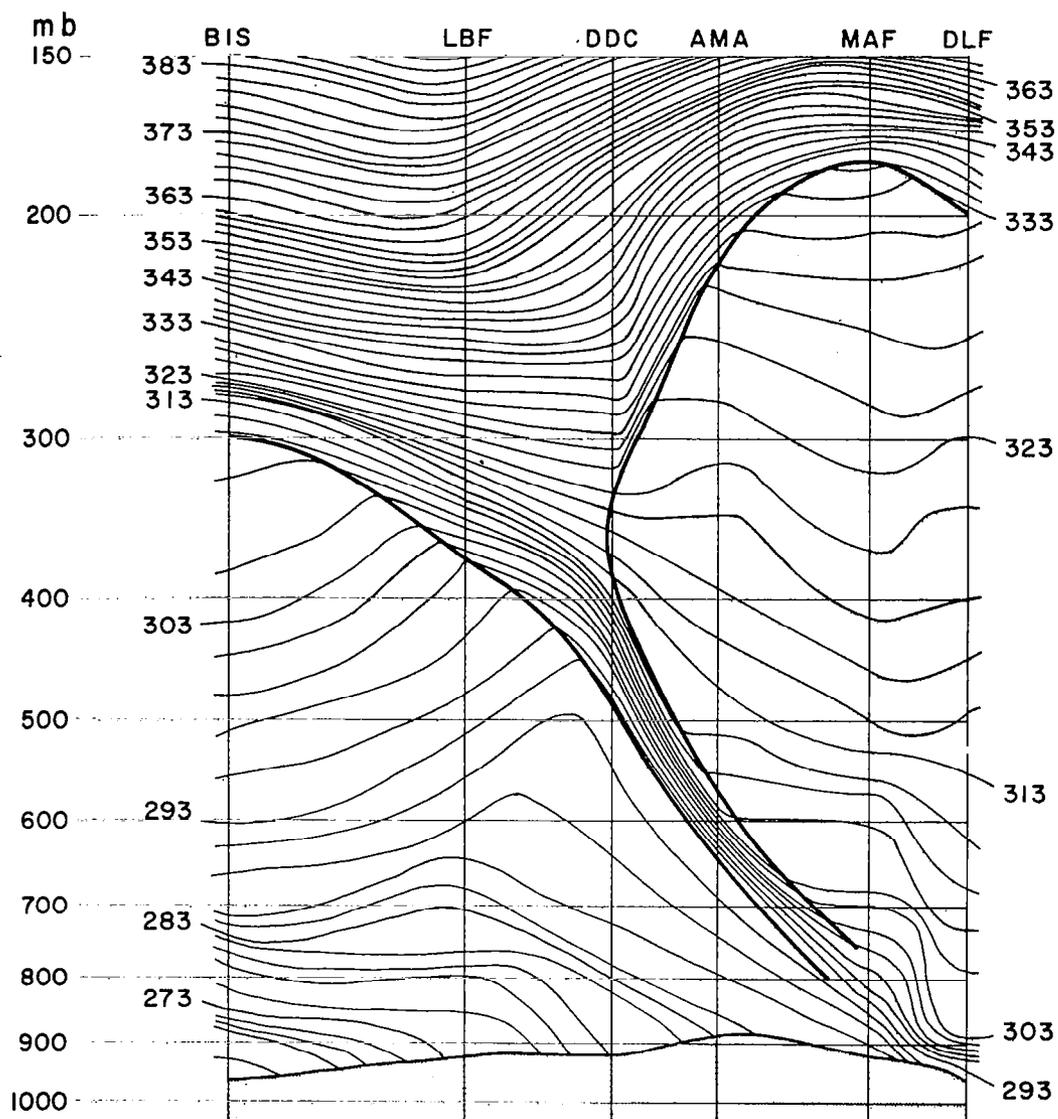
Figure 6. Isentropic cross section from Staley (1960) show-
ing an example of a troposphere-spanning front.
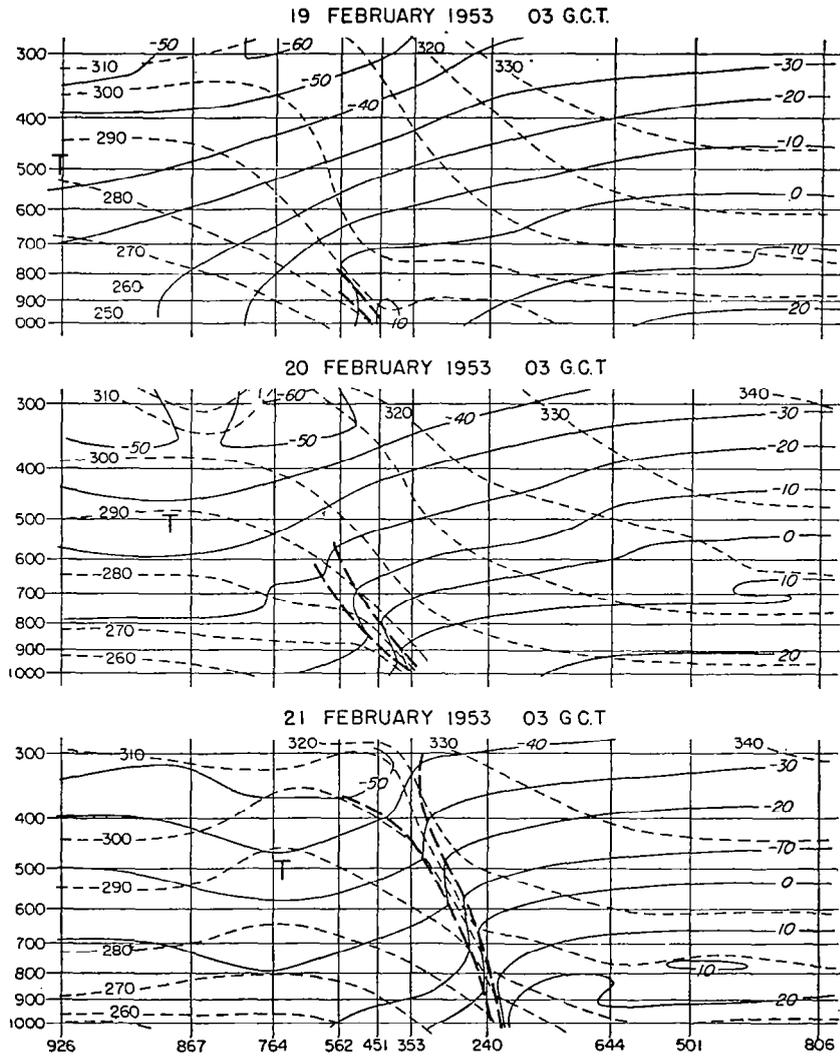
Figure 7.   Cross sections through a zone of frontogenesis
            from Petterssen (1956). Temperature (°C, solid)
            and potential temperature (°K, dashed).

resolution to clearly depict the processes involved in its formation. The manner in which such fronts evolve is un-known and deserving of careful study. This study will focus its attention on an upper-level hyperbaroclinic zone that extends to the low troposphere as time passes. Several con-trasts between this study and others are worth noting.

First, the time resolution of the data is four times better than that of conventional observations, and it is believed that this may reveal aspects of frontal structure and development that normally are unobservable.

Second, the system being studied is felt to be more typical of average fronts than the cases studied by other investigators, particularly Reed (1955) and Reed and Sanders (1954).

The upper-level front is on the east side of the trough. Many of the cases of upper-level fronts presented in other papers occur on the west side of the trough.

Unlike some papers, the cross-sections presented here will extend through the whole troposphere. Attention will be paid to changes in the lower troposphere that occur as the upper front develops.

Horizontal analyses will be performed on surfaces of constant potential temperature. The usefulness of isen-tropic coordinates for the study of fronts has been dis-cussed by Bosart (1970) and LaSeur (1974). The subsidence in upper-level fronts and the small magnitude of turbulent

diabatic effects away from the level of maximum winds implies that entropy will be quasiconservative in such fronts. Also, vorticity on an isentropic surface changes less rapidly with time and is more easily resolved spatially than vorticity on a pressure surface. As fronts are zones of near discontinuities of potential vorticity, they should be more easily examined in isentropic than in pressure coordinates.

THE SYNOPTIC SITUATION

To study the surface weather during the period 1200 UT 11 May to 1200 UT 12 May, 1974, WBAN Forms 10A and 10C were obtained from the National Climate Center. Observations were plotted for every hour, and analyses of surface wind streamlines, cloud cover, and present weather were performed for every three hours from 1200 UT 11 May to 0500 UT 12 May. Data for 0600 to 1100 UT 12 May were unavailable due to lack of funds. Observations for 1200 UT 12 May were obtained from the Northern Hemisphere Data Tabulation Series. Simplified versions of these analyses are presented in figure 8.

As figure 8 shows, the weather in the eastern half of the United States during the above-mentioned 24 hours was dominated by two low pressure areas. One of these lows moved northeastward from the Louisiana coast to northwestern Georgia, maintaining a central pressure of about 1000 mb. This low was unattended by fronts and had widespread, sometimes moderate precipitation ahead of it.

The other storm moved northeastwards from south-central Minnesota to a position north of Lake Superior. Its pressure rose from 992 to 994 mb in the 24 hour period. A typical system of fronts accompanied the storm. Precipitation around the low center and ahead of the warm front was widespread, but generally light. There was extensive
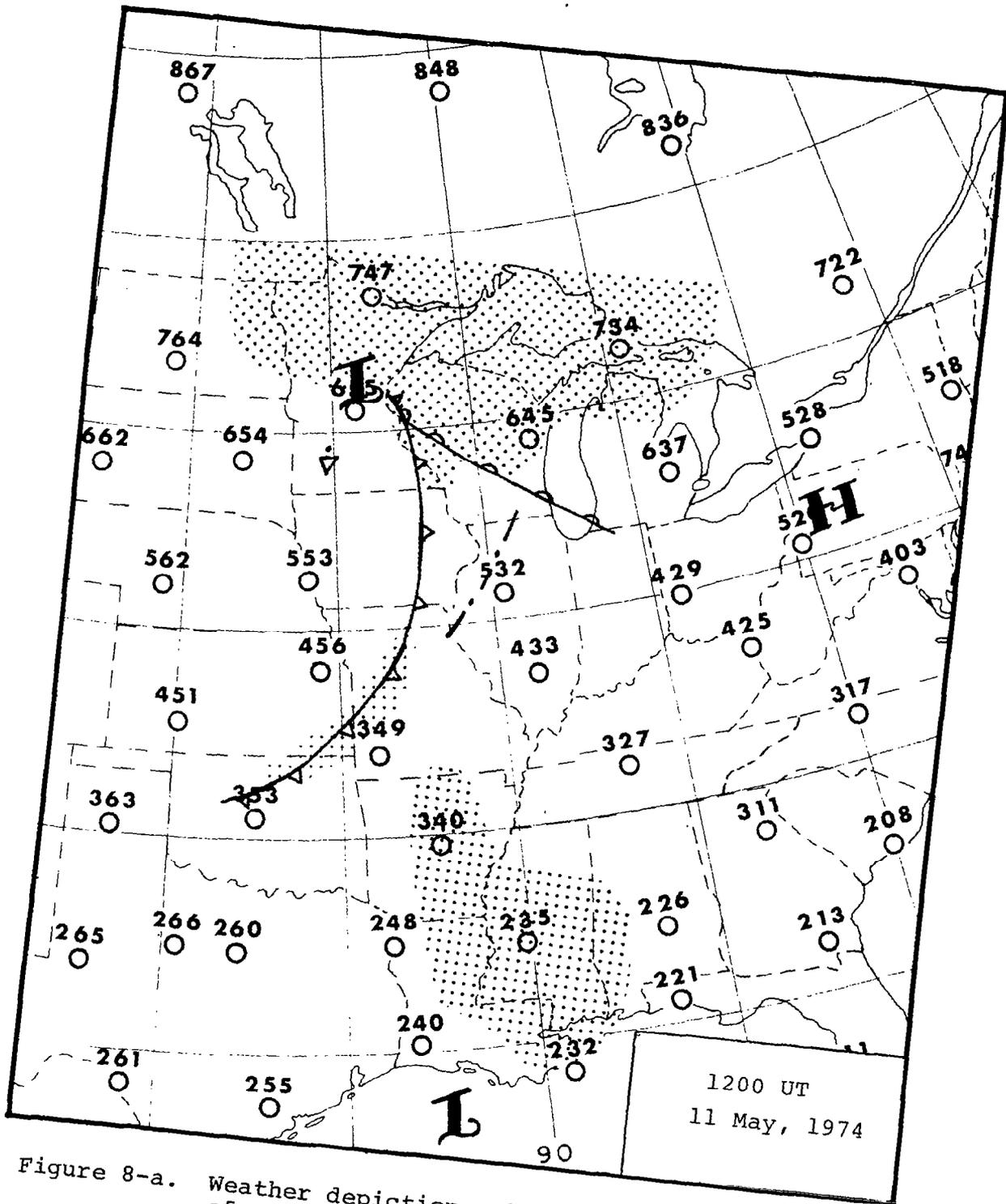
Figure 8-a. Weather depiction. Stippling indicates areas of steady precipitation.
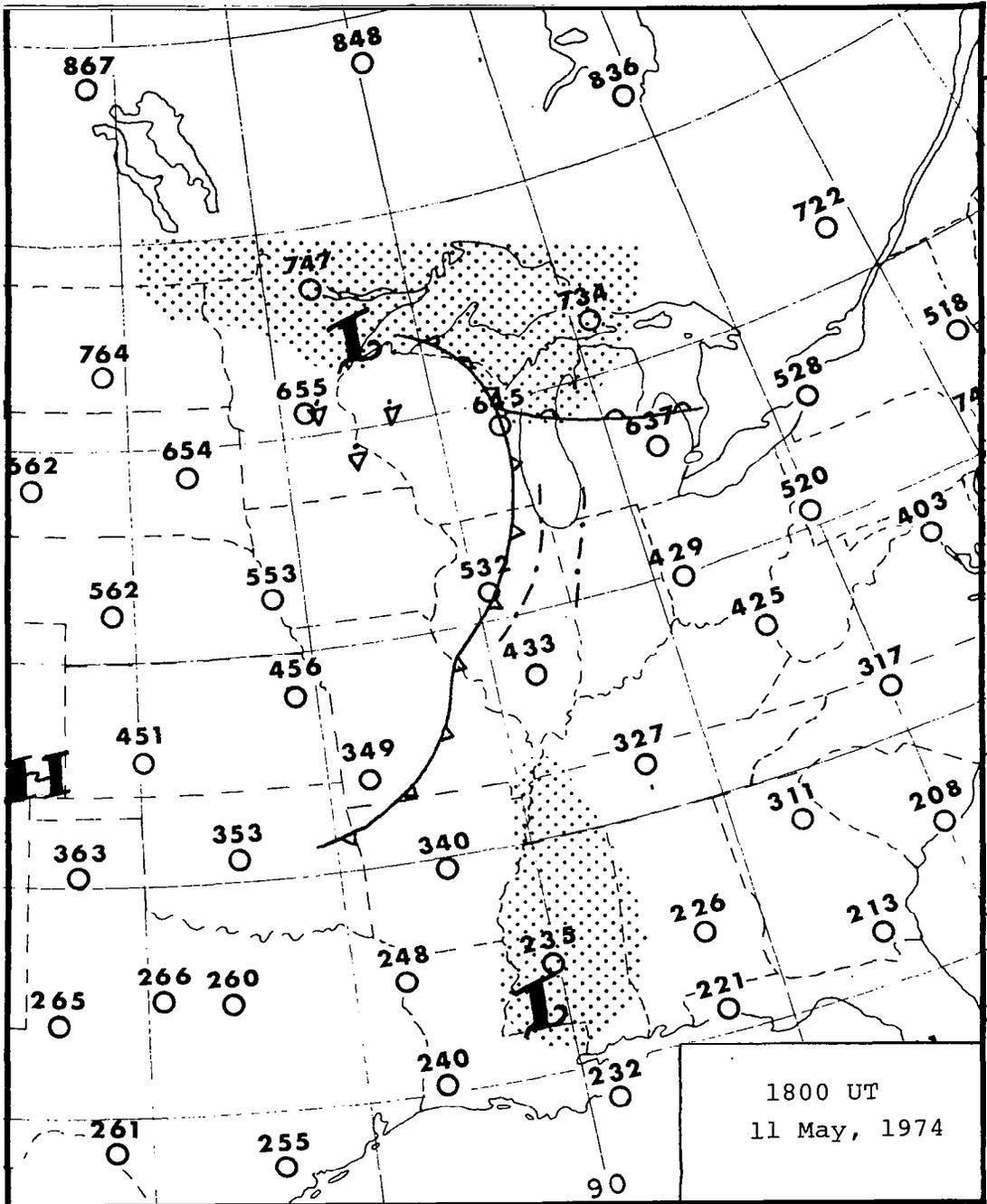
Figure 8-b.
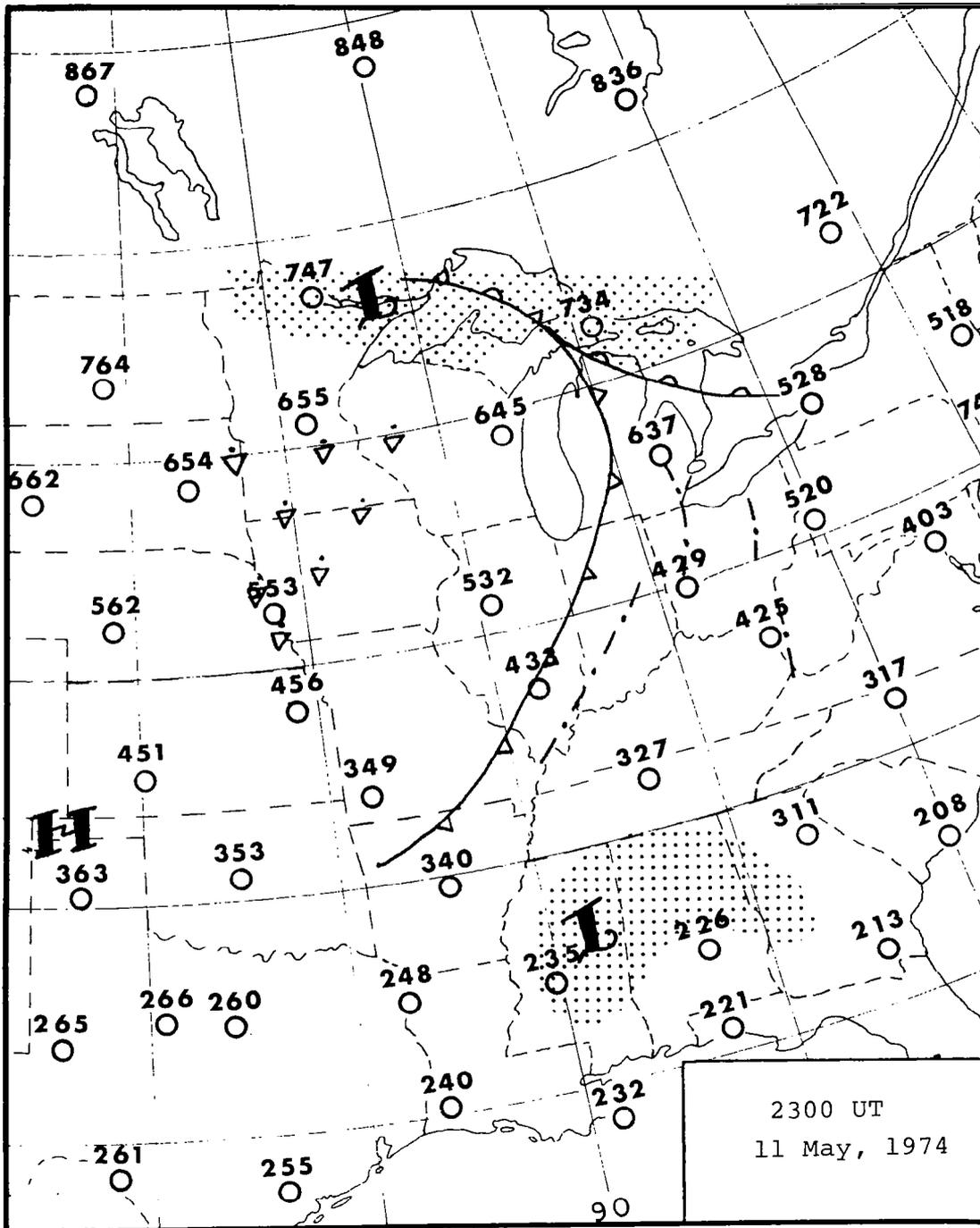
Figure 8-c.

Figure 8-d.

34
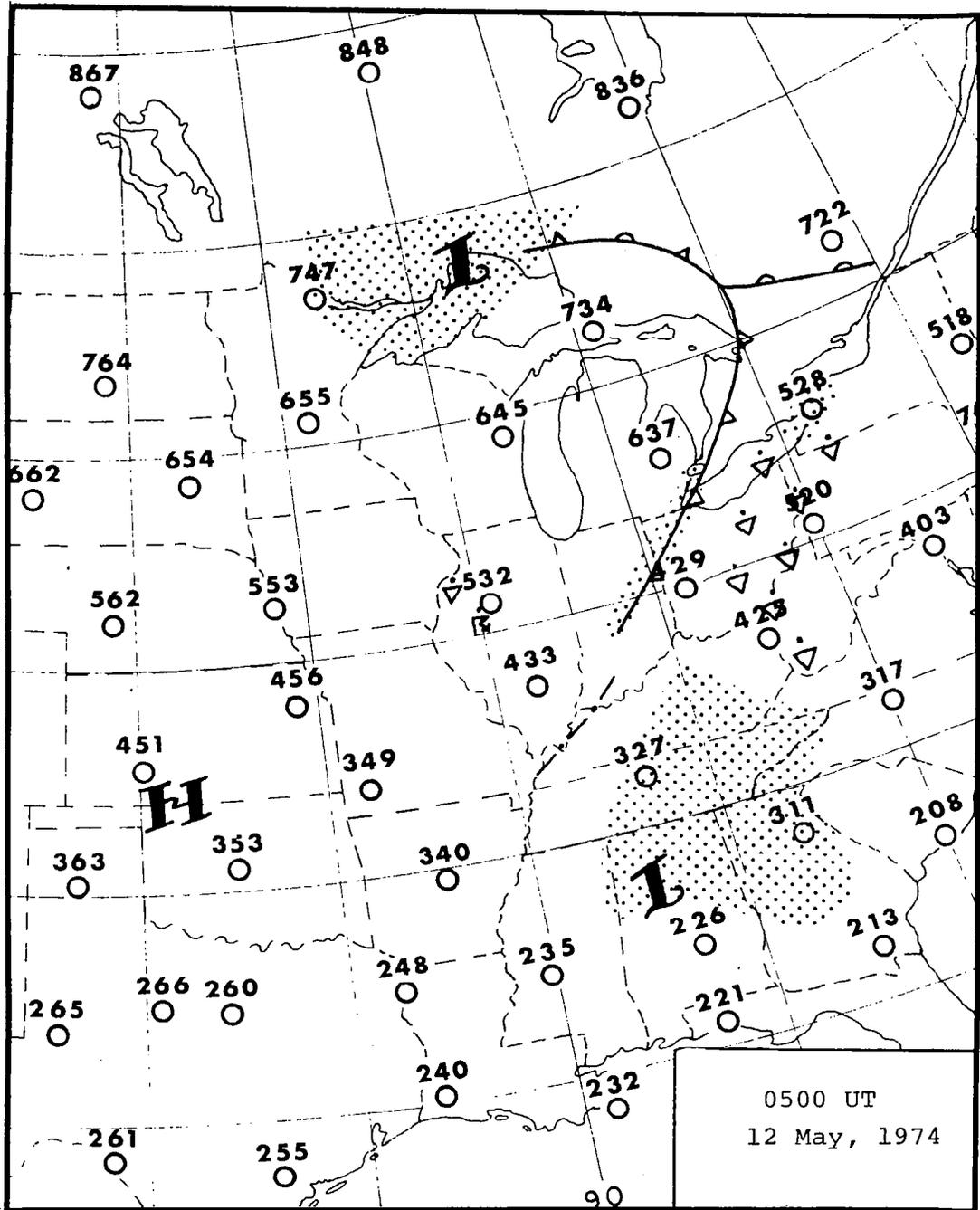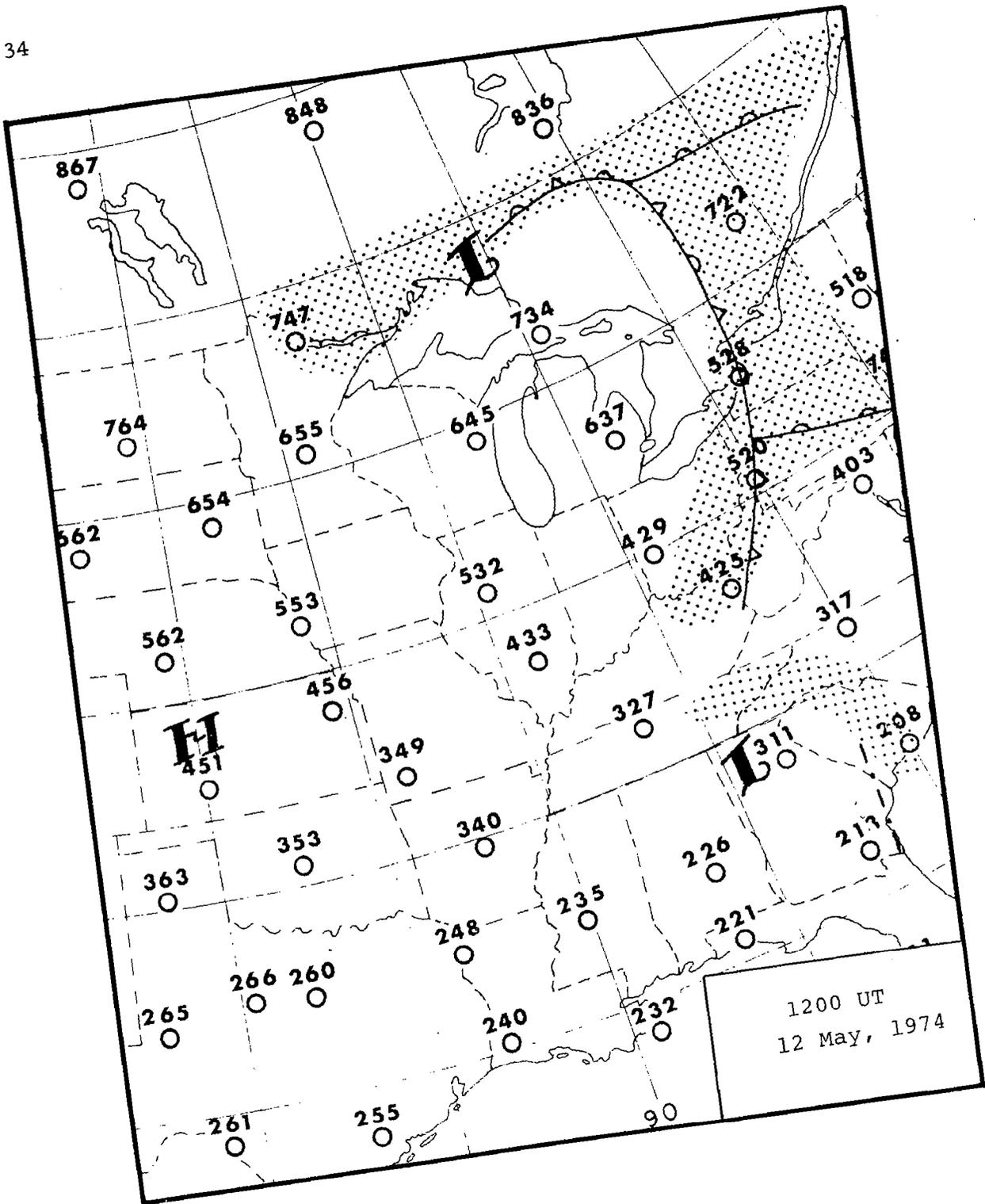
Figure 8-e.

convection ahead of the cold front for much of the period under consideration. The most severe weather occurred from north-central Ohio to south-central Michigan between 2000 UT 11 May and 0200 UT 12 May. Five tornadoes, several funnel clouds, winds up to 70 knots, and one and one half inch hail were reported between these times (Storm Data, 1974). A large area of convection also broke out to the south and west of the low center between 2000 UT 11 May and 0300 UT 12 May. Small hail and winds near 50 knots were reported by several stations in the area from eastern Nebraska to southern Minnesota. The cold front itself had little precipitation along it until late in the period under consideration.

It is noteworthy that neither the cyclone nor the accompanying fronts were of extraordinary intensity. This system is a more typical one than most of those that appear in the literature of fronts.

DESCRIPTION OF THE DATA

During the above-mentioned 24 hours, the National Aero-
nautics and Space Administration conducted a special obser-
vational program called the Atmospheric Variability Experi-
ment (AVE). This particular set of observations was the
first in the second series of such experiments and its full
title is the AVE II Pilot Experiment. During the experi-
ment, 54 rawinsonde stations in the eastern half of the
United States took soundings every three hours instead of
at the conventional 12 hour interval (see figure 9). The
data were processed by the NASA Marshall Space Flight Cen-
ter, Aerospace Environment Division. Values of the data
every 25 mb (Scoggins and Turner, 1974) and data for every
pressure contact were provided courtesy of NASA.

The data for thermodynamic variables used in this
study were computed for every pressure contact. Winds were
computed for one minute intervals and then interpolated to
the pressure contacts. The pressure difference between
pressure contacts is about 12 mb at 850 mb, 8 mb at 500 mb,
and 5 mb at 250 mb. The pressure difference over a one
minute interval at these same pressure levels is about 30
mb, 15 mb, and 10 mb, respectively.

Estimates of the root mean square error for the thermo-
dynamic variables are as follows (Scoggins and Turner, 1974):

Figure 9. Stations participating in AVE II pilot experiment
and locations of cross sections.

Parameter	Approximate RMS Error
Temperature	1 C
Pressure	1.3 mb surface to 400 mb; 1.1 mb between 400 and 100 mb; 0.7 mb between 100 and 10 mb
Humidity	10 percent
Pressure Altitude	10 gpm at 500 mb; 20 gpm at 300 mb; 50 gpm at 50 mb

The errors in the wind observations are more difficult to ascertain but are believed to be as follows: 2.5 mps at 700 mb with an elevation angle of the balloon of 10°, and 0.5 mps at an elevation angle of 40°; at 500 mb, the errors are 4.5 mps and 0.8 mps for the same elevation angles; at 300 mb, the errors for these same angles are 7.8 mps and 1.0 mps (Scoggins and Turner, 1974).

METHODOLOGY OF THE ANALYSES

The high time resolution of the NASA AVE data provides a rare opportunity for studying the evolution of synoptic and sub-synoptic scale weather systems. Conventional upper-air observations are too far apart in time to reveal in much detail the manner in which changes occur in the structure of fronts. Aircraft data, while increasing spatial resolution, are usually unavailable for sufficiently long periods to greatly improve the resolution in time. Consequently, analyses based upon such data are often enhanced by the use of models of what a front is believed to be like. However, with the time resolution of the AVE data, the necessity to employ such preconceptions is minimized while the likelihood of producing analyses bearing a close resemblance to the actual state of the atmosphere increases. In this study, therefore, the data will be allowed to speak for itself with as little modeling incorporated into the analyses as possible. Vindication of the accuracy of the resulting picturalization will be sought by obtaining internal consistency among a number of separate, independent analyses.

In order to depict the structure of the fronts for this case, cross sections of potential temperature were constructed for every three hours along the lines indicated in figure 9. A Hewlett Packard 9820A calculator and 9825A

plotter were used to compute and plot from the temperature
and pressure at each pressure contact the pressure of isen-
tropic surfaces every 2K. However, the resulting field of
potential temperature possesses great latitude as to how it
can be analyzed. It is necessary to employ other analyses
to put constraints on the analysis of the cross sections.

Shapiro (1971) has shown that cross sections can be
used to add detail to analyses of temperature on constant
pressure surfaces. It should also be noted that considera-
tion of the pattern of isotherms on an isobaric surface in
a direction normal to the cross section can add detail to
the cross section analysis. For this reason, maps of the
field of potential temperature on the 850, 700, 500, 400
and 300 mb pressure surfaces were prepared for every three
hours. Each set of charts was analyzed independent of the
other, with attention being paid to maintaining continuity
in time of the patterns in the analyses. The cross sections
and isobaric maps were then compared and mutually adjusted
until they were consistent with one another and possessed
good time continuity.

Still further refinement of the cross sections was ob-
tained by constructing maps of the field of pressure on
isentropic surfaces. The technique used to produce these
maps is described by Sanders (1967). Isobars were first
drawn on the lowest isentropic surface. The field of pres-
sure difference between the lower surface and the surface

4K above it was then graphically added to the isobar field
on the lower surface to obtain the pressure topography on
the upper surface. In this way, analyses of the isobars on
isentropic surfaces were obtained every 4K between the 300K
and 336K surfaces. These charts were then compared with the
cross sections and the necessary changes were made in both
analyses so as to produce consistent, temporally continuous
results.

A further check on the location of baroclinic zones in
the cross sections was consideration of the thermal wind
relationship through examination of the vertical shear of
the wind and fields of thickness.

The field of potential temperature was judged to be
sufficiently smooth that time continuity could be obtained
by subjective comparisons of the closely spaced (in time)
analyses. This was not the case for the field of wind on
isentropic surfaces, however. Detailed analyses of the
wind speed on selected surfaces were made using the techni-
que of time-space conversion described by Fujita (1963). A
phase velocity of the patterns in the isotach field was ob-
tained from preliminary analyses. This velocity was then
used to displace "upstream" and "downstream" from the sta-
tion location the wind speed for that station for three
hours after and before, respectively, the time being con-
sidered. This enhanced field of wind speed was then iso-
plethed, and the patterns were made to be continuous in time.

Throughout the process of performing the analyses, care was taken to preserve patterns from one time to the next, and to achieve agreement among the various fields being scrutinized. Due to this synthesis of a variety of independent horizontal and vertical analyses, and due to the small time interval between observations, final analyses are produced which are detailed, internally consistent, temporally continuous, and representative of the actual condition of the atmosphere.

DISCUSSION OF THE CROSS SECTIONS

While isentropes on the cross sections were originally drawn at intervals of 2K, in the interests of economy and to provide an overview of the evolution of this system of fronts, the cross sections for every three hours are here presented with an interval between isentropes of 6K (figures 10 and 11). Also included in these diagrams are: isotachs of the flow normal to the plane of the cross sections at intervals of 40 knots; the position where surface fronts and squall lines intersect the plane of the cross sections; reports of convective activity from stations along the cross sections; and shaded regions indicating where the increase of potential temperature with height is greater than 9×10^{-3} k m^{-1}. This stability criterion was chosen because it is one-half the absolute value of the lapse rate of potential temperature in the mid-tropospheric portion of the hyper-baroclinic zone. This value of frontal stability compares favorably with that obtained by Browning and Harrold (1970). These authors found a lapse rate of wet bulb potential temperature in a warm front of -5×10^{-3} K m^{-1}, much of which lapse is due to the change with height of the potential temperature. In visualizing the three-dimensional appearance of the structures found on the cross sections, it should be noted that the two sections intersect at Saint Cloud, Minnesota (station 655 on figure 9). It will also
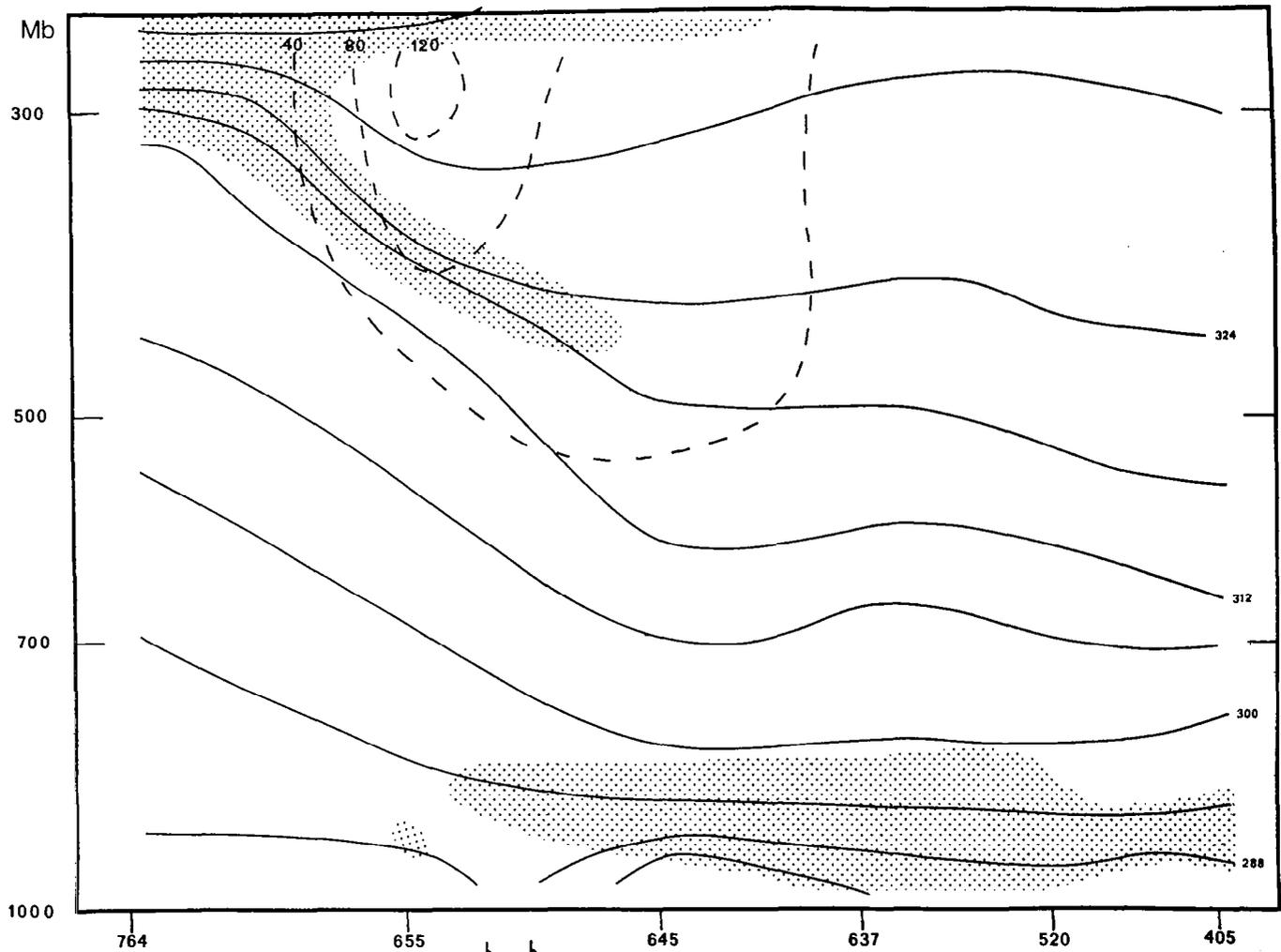
Figure 10a. Cross sections along line A from figure 9. Isentropes (°K, solid) and isotachs (knots, dashed) of flow normal to sections, and stable regions (stippled). 1115 UT, 11 May, 1974.
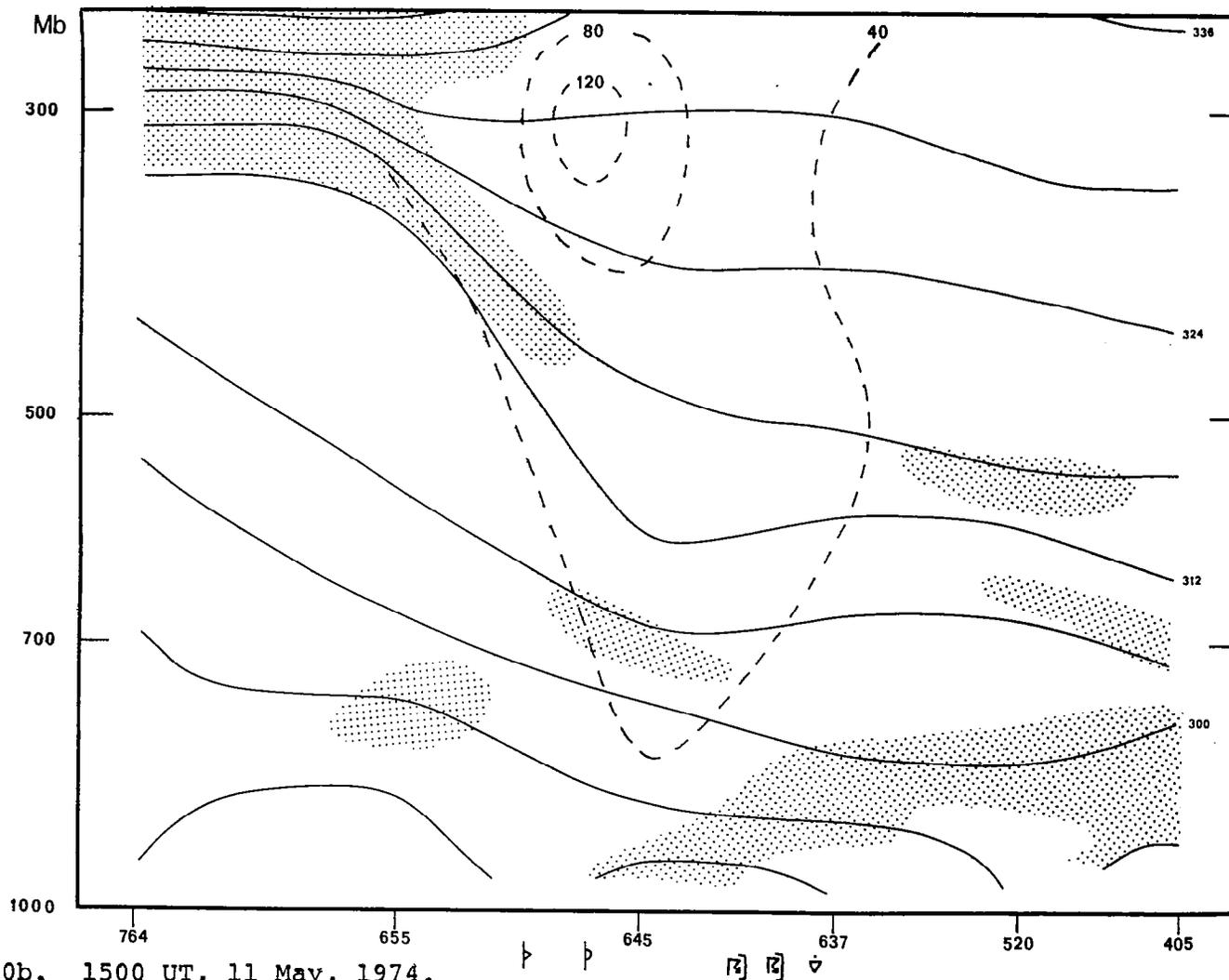
Figure 10b. 1500 UT, 11 May, 1974.
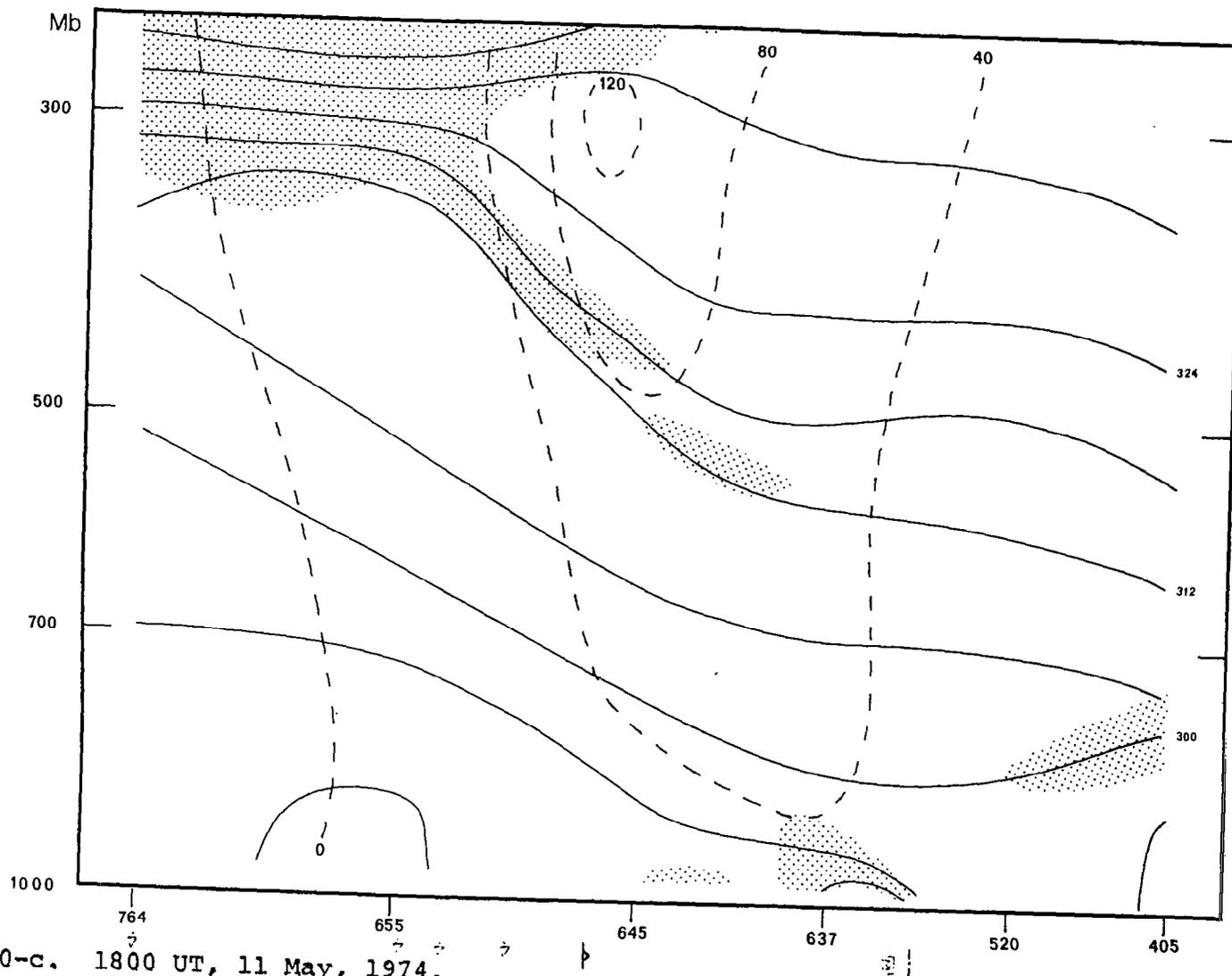
Figure 10-c. 1800 UT, 11 May, 1974.
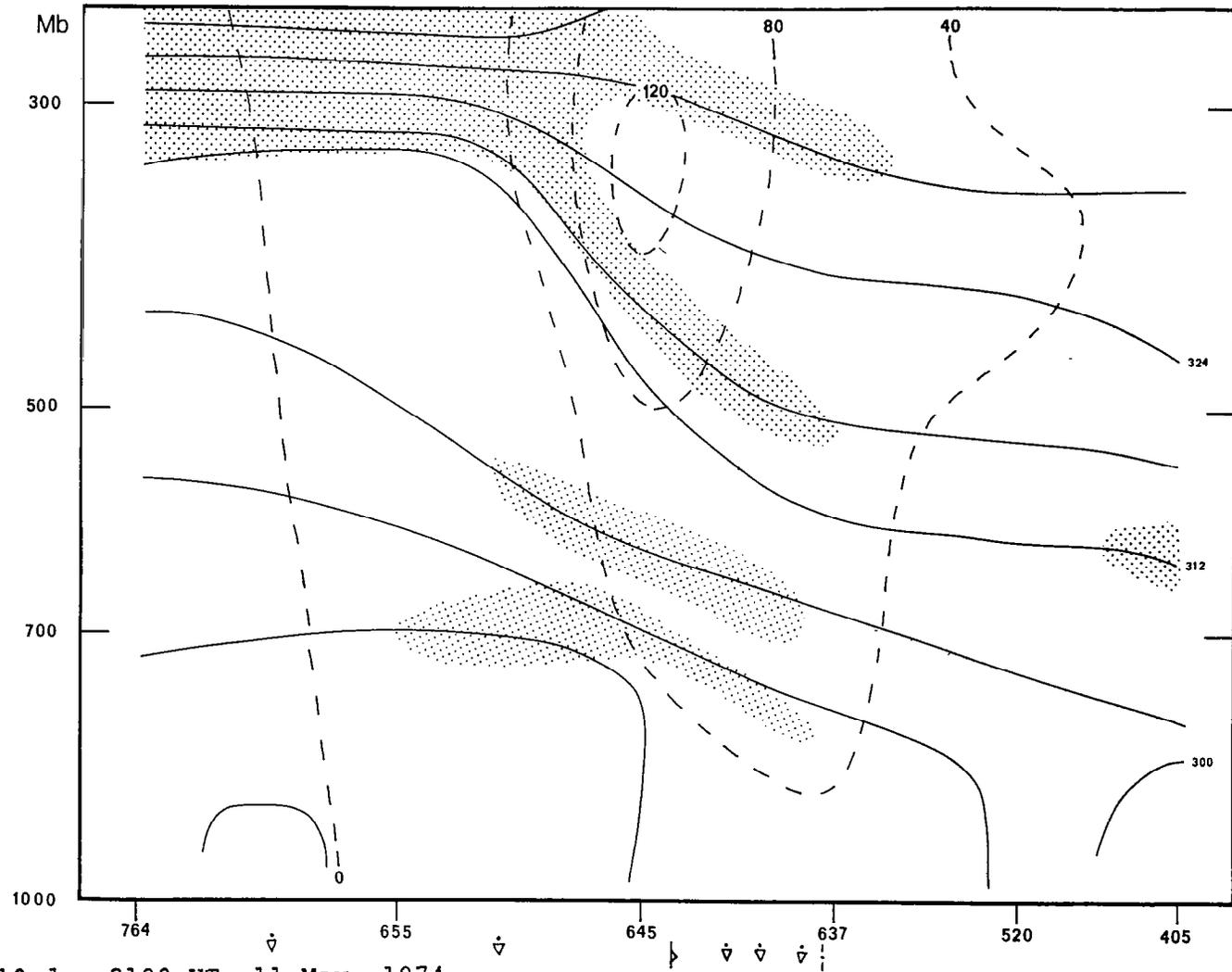
Figure 10-d. 2100 UT, 11 May, 1974.
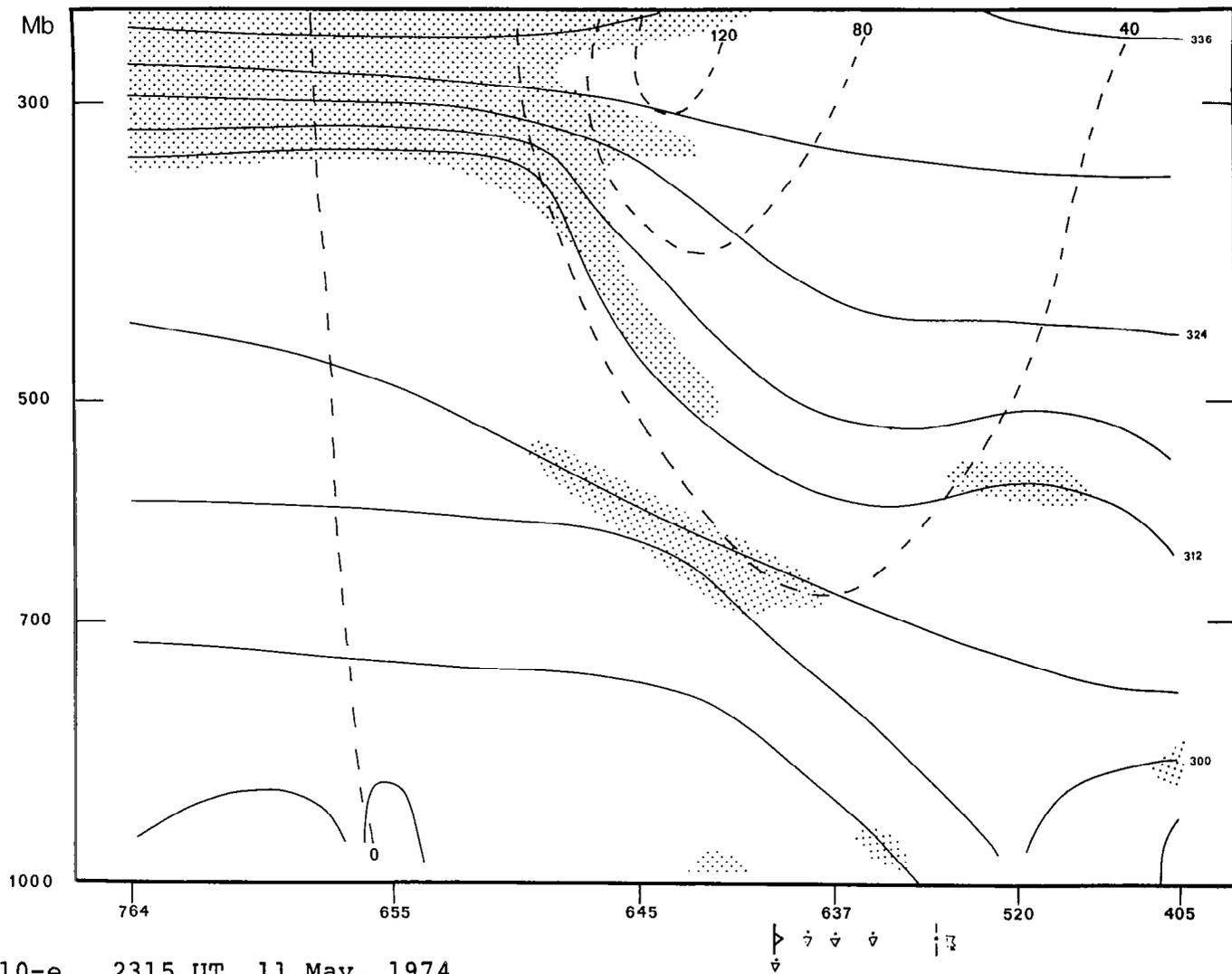
Figure 10-e.   2315 UT, 11 May, 1974.
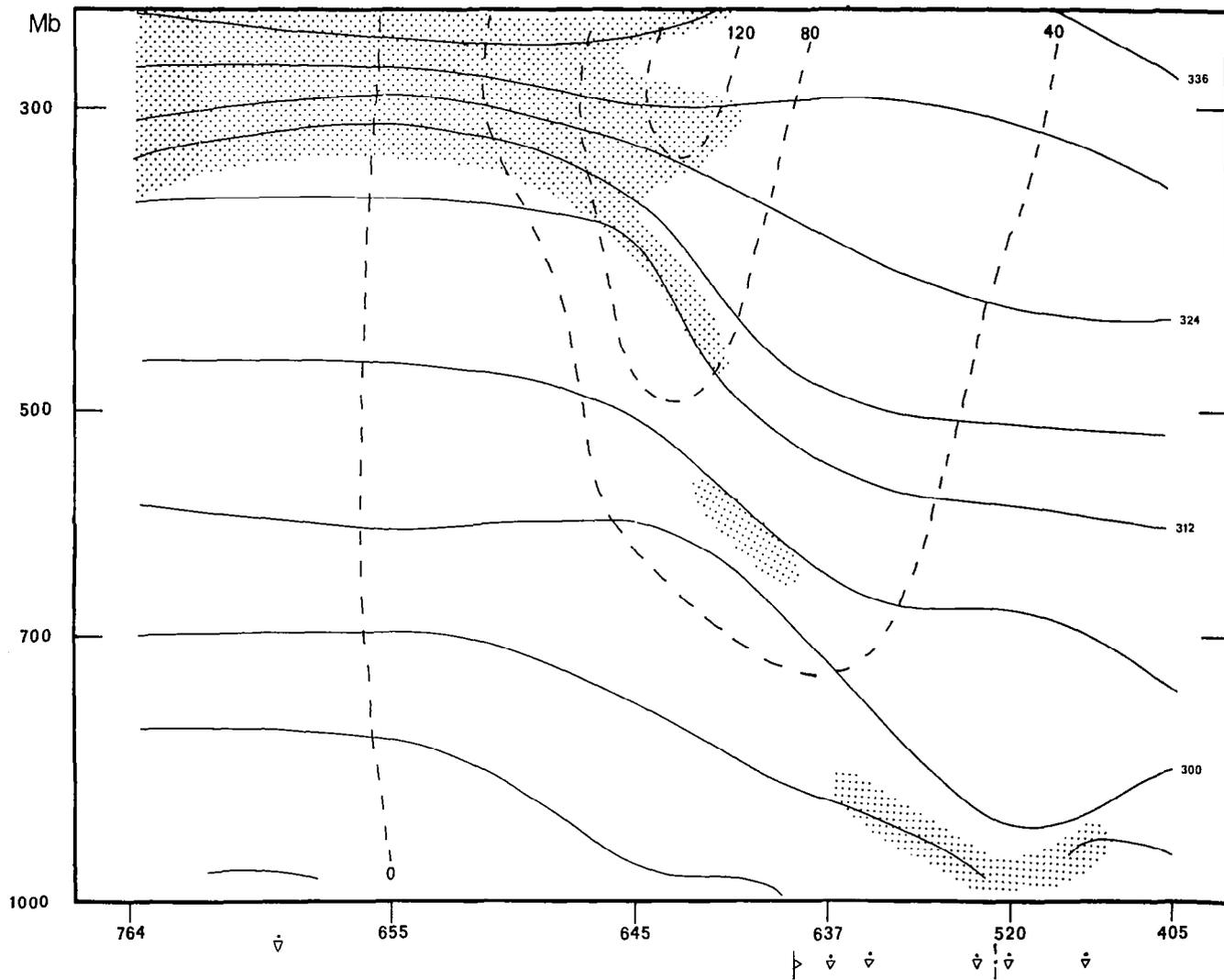
Figure 10-f.   0300 UT, 12 May, 1974.
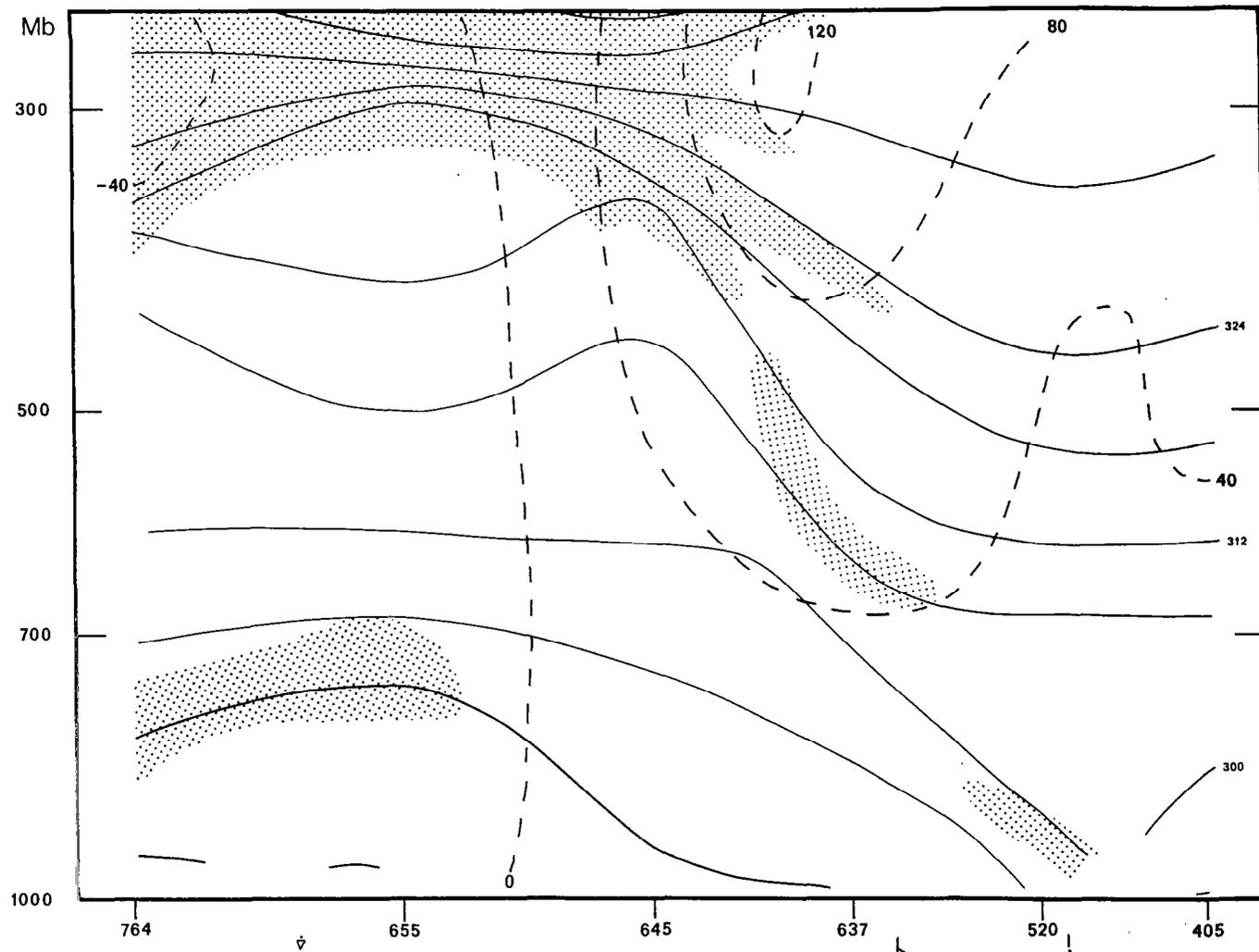
Figure 10-g. 0600 UT, 12 May, 1974.
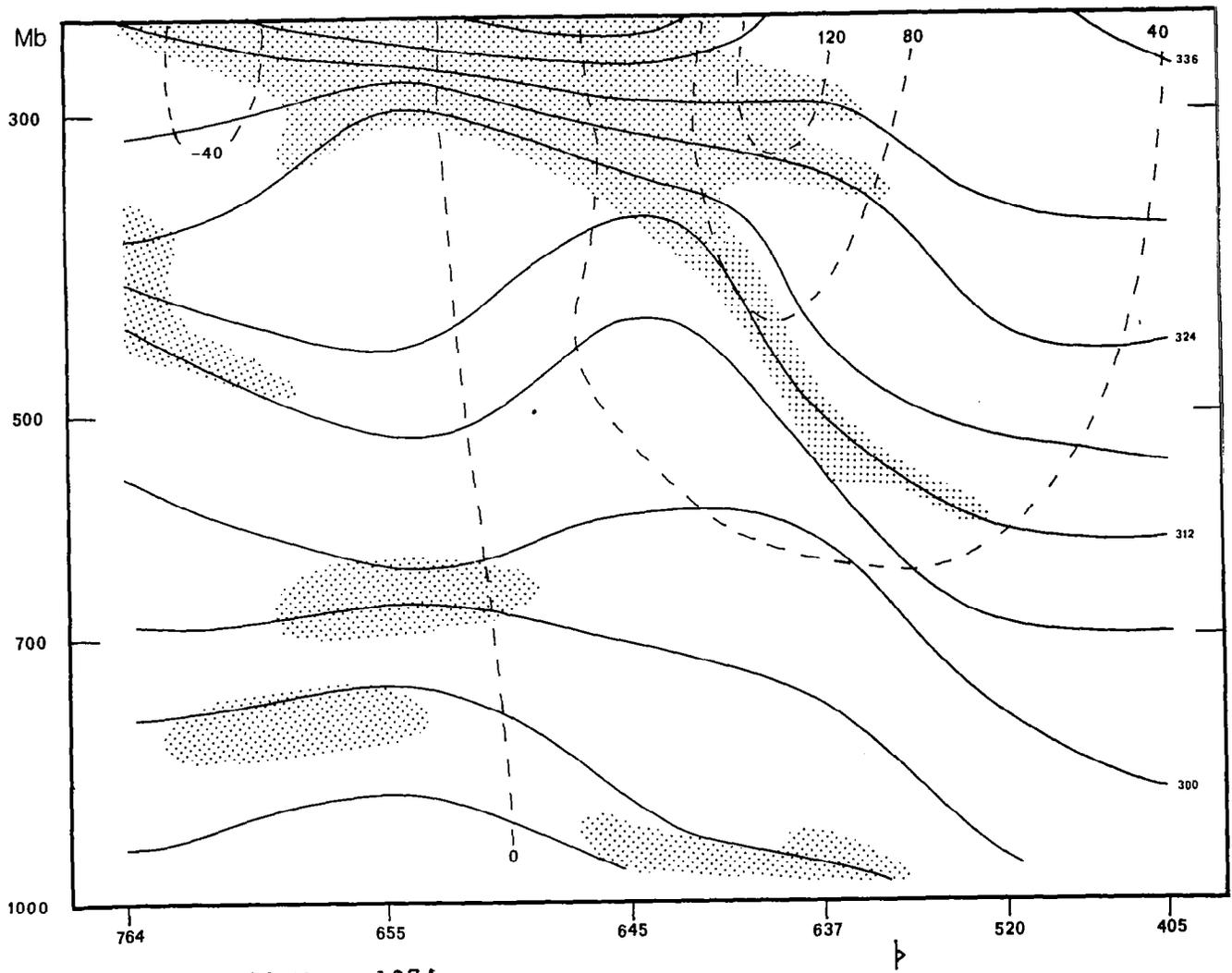
Figure 10-h. 0900 UT, 12 May, 1974.
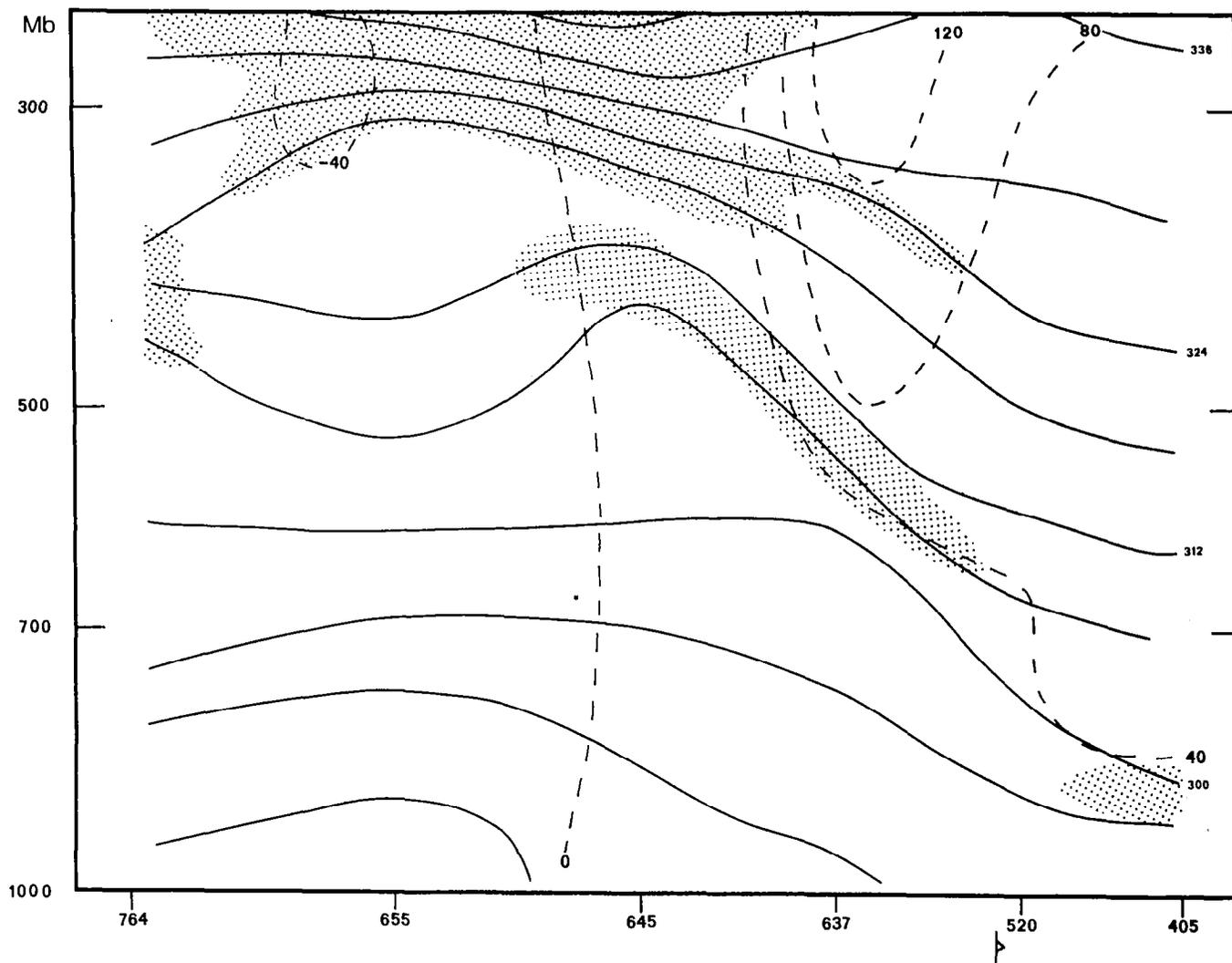
Figure 10-i.   1115 UT, 12 May, 1974.
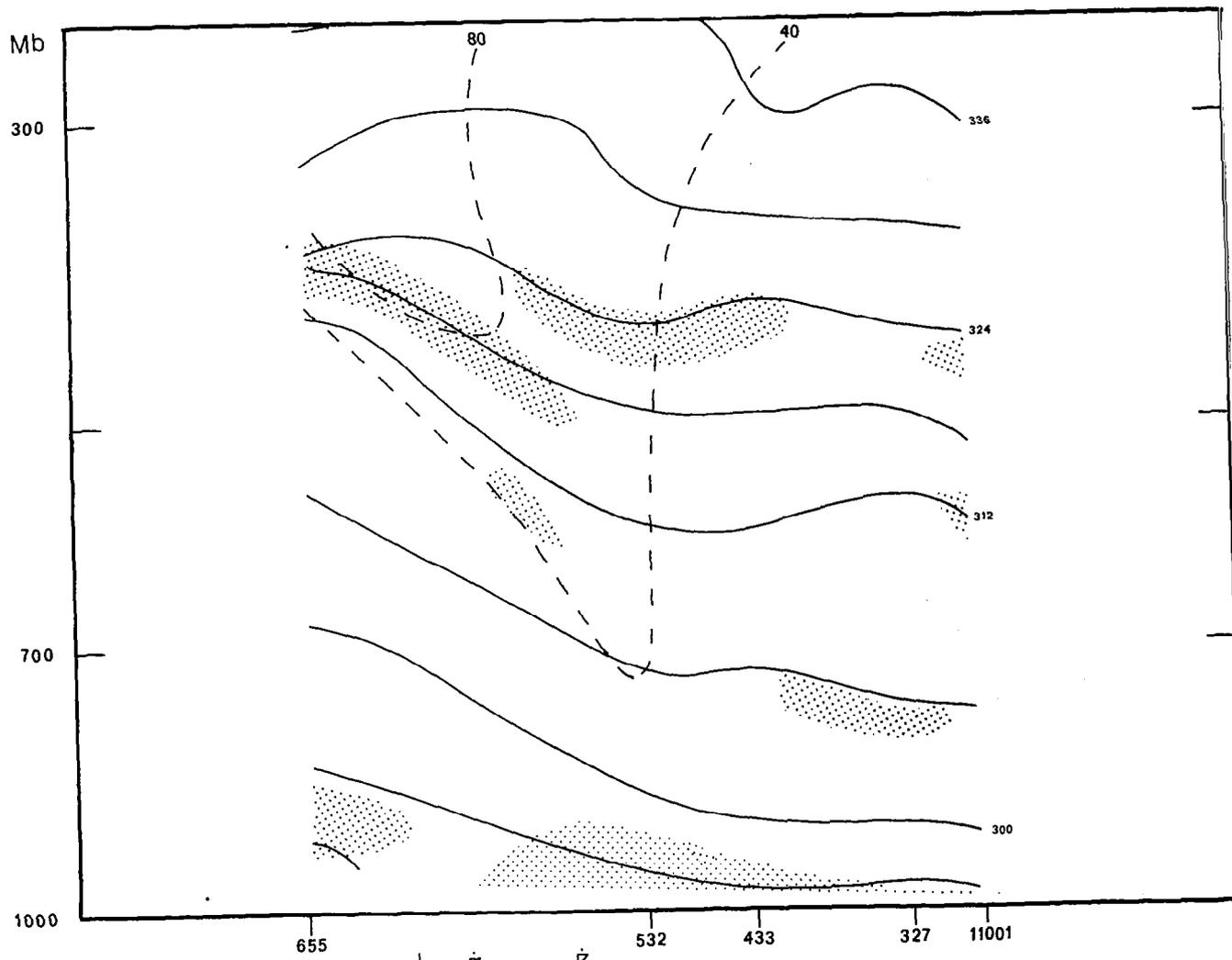
Figure 11-a. Cross sections along line II from figure 9. Notation as for figure 10. 1115 UT, 11 May, 1974.
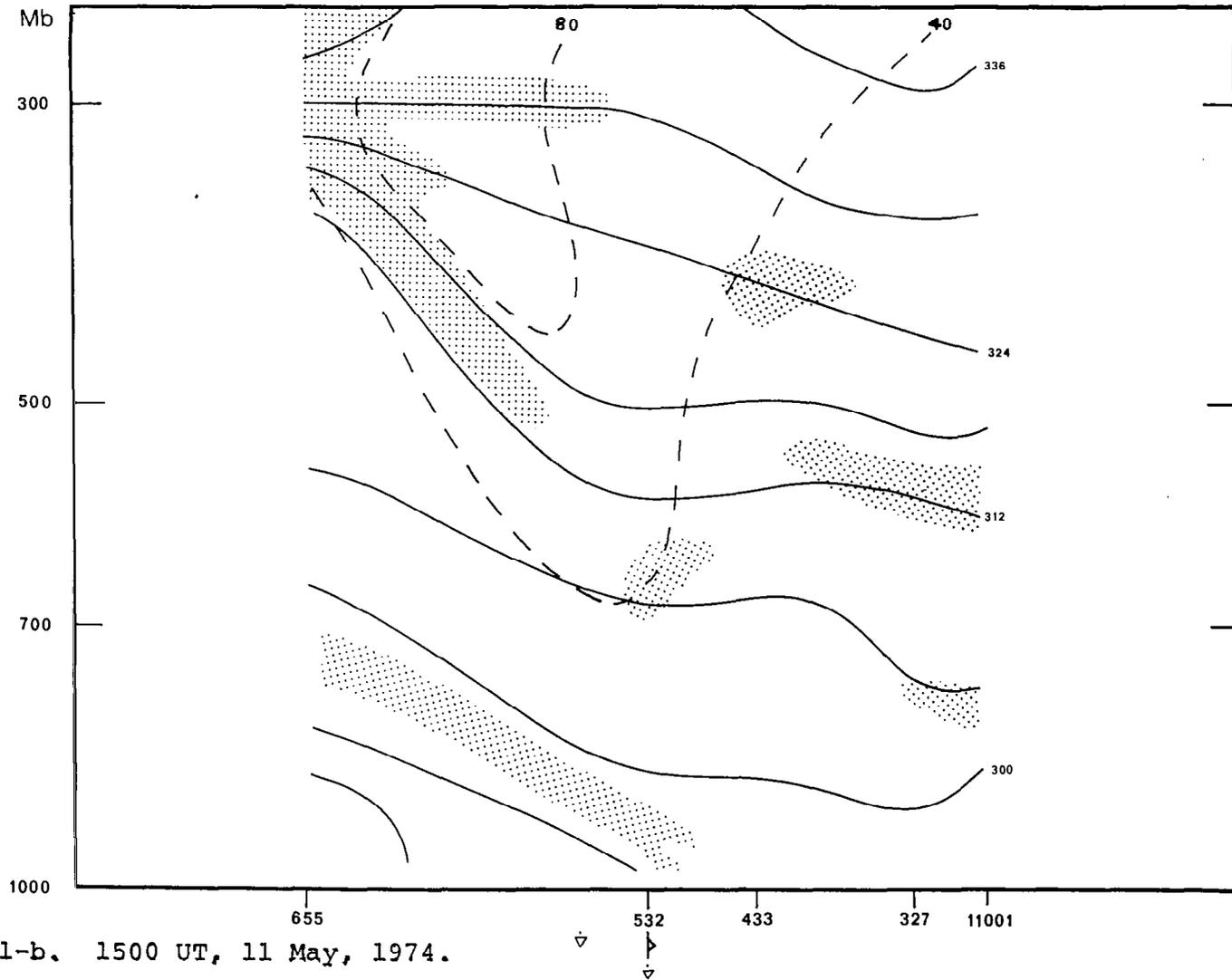
Figure 11-b. 1500 UT, 11 May, 1974.
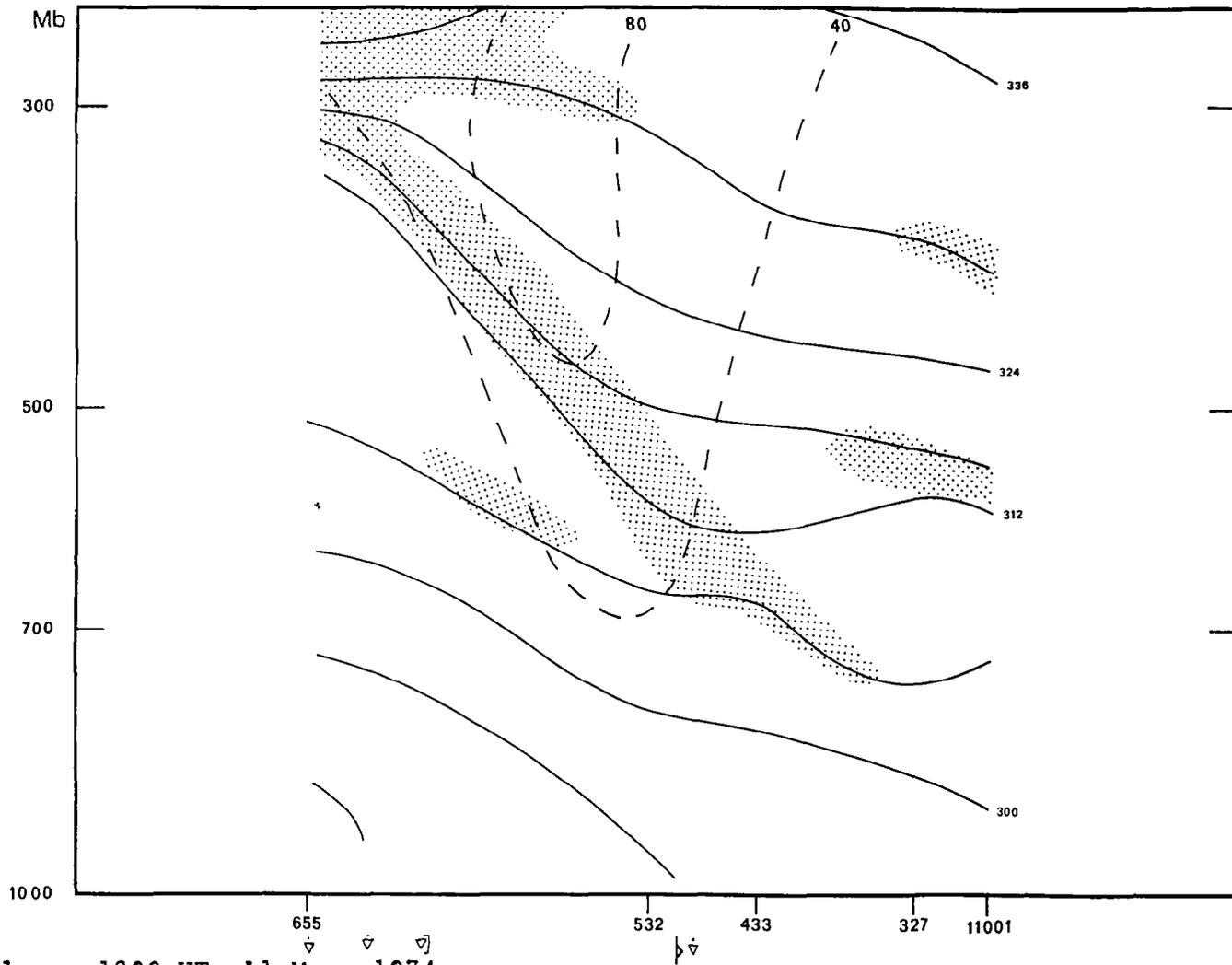
Figure 11-c. 1800 UT, 11 May, 1974.
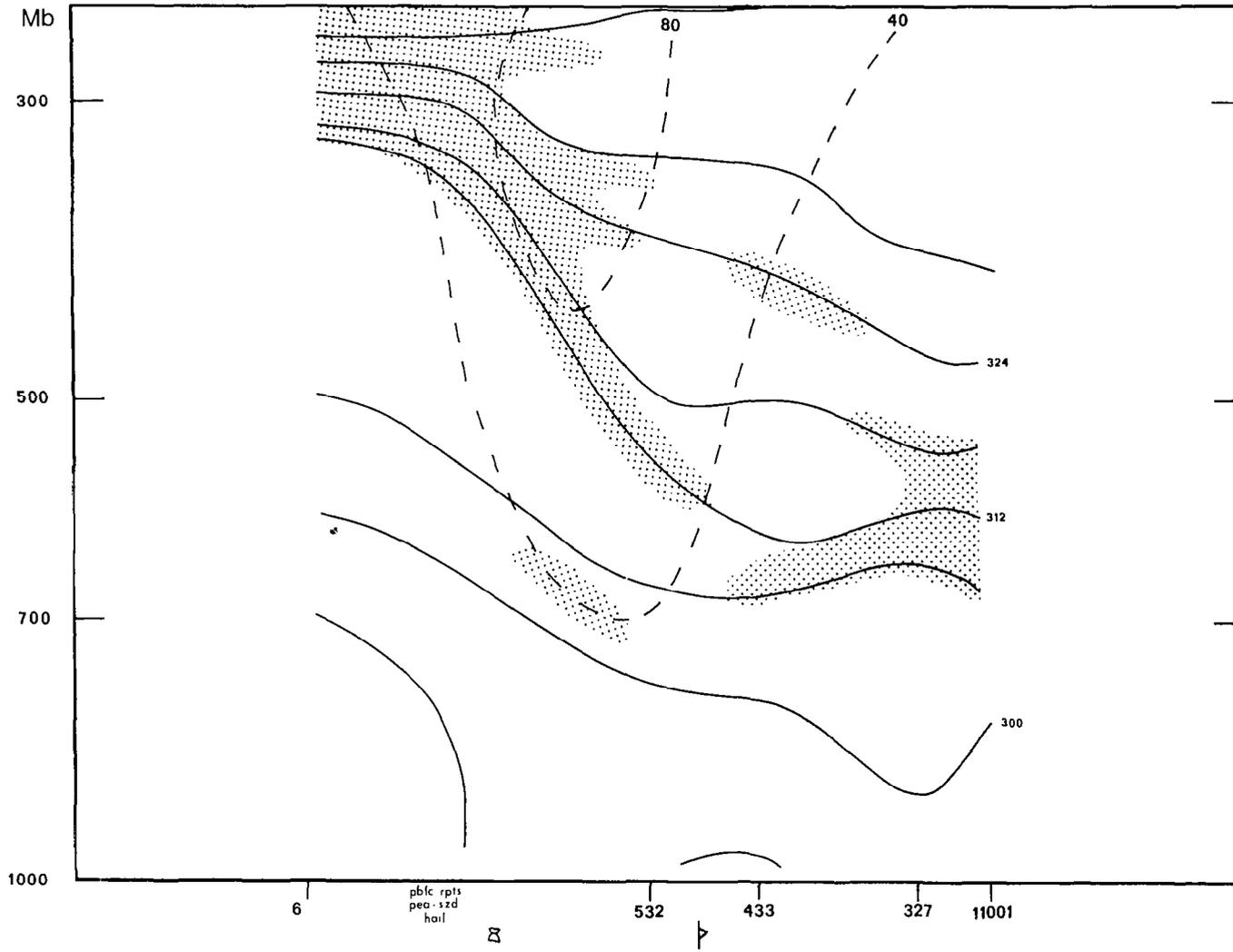
Figure 11-d. 2100 UT, 11 May, 1974.
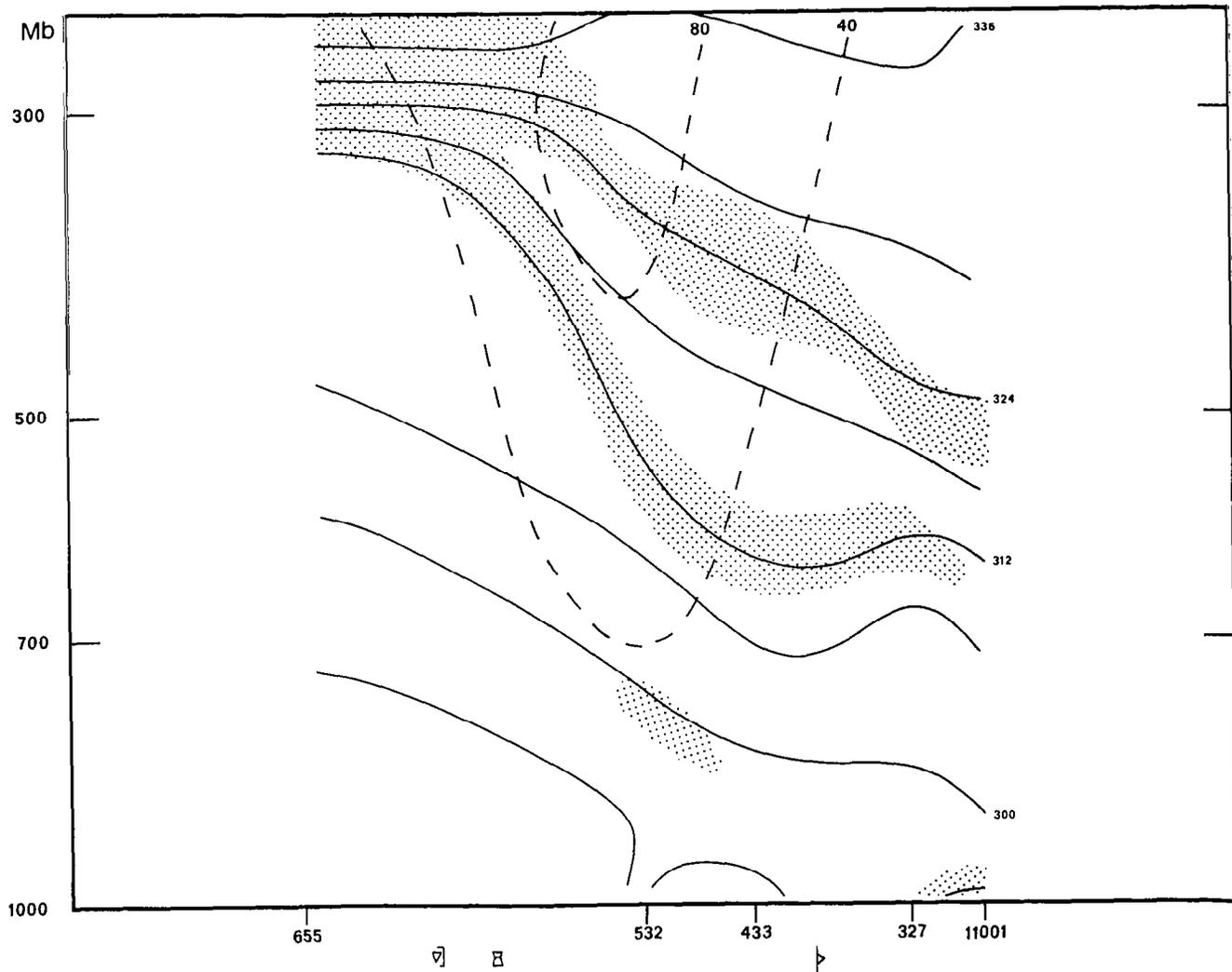
Figure 11-e.   2315 UT, 11 May, 1974.
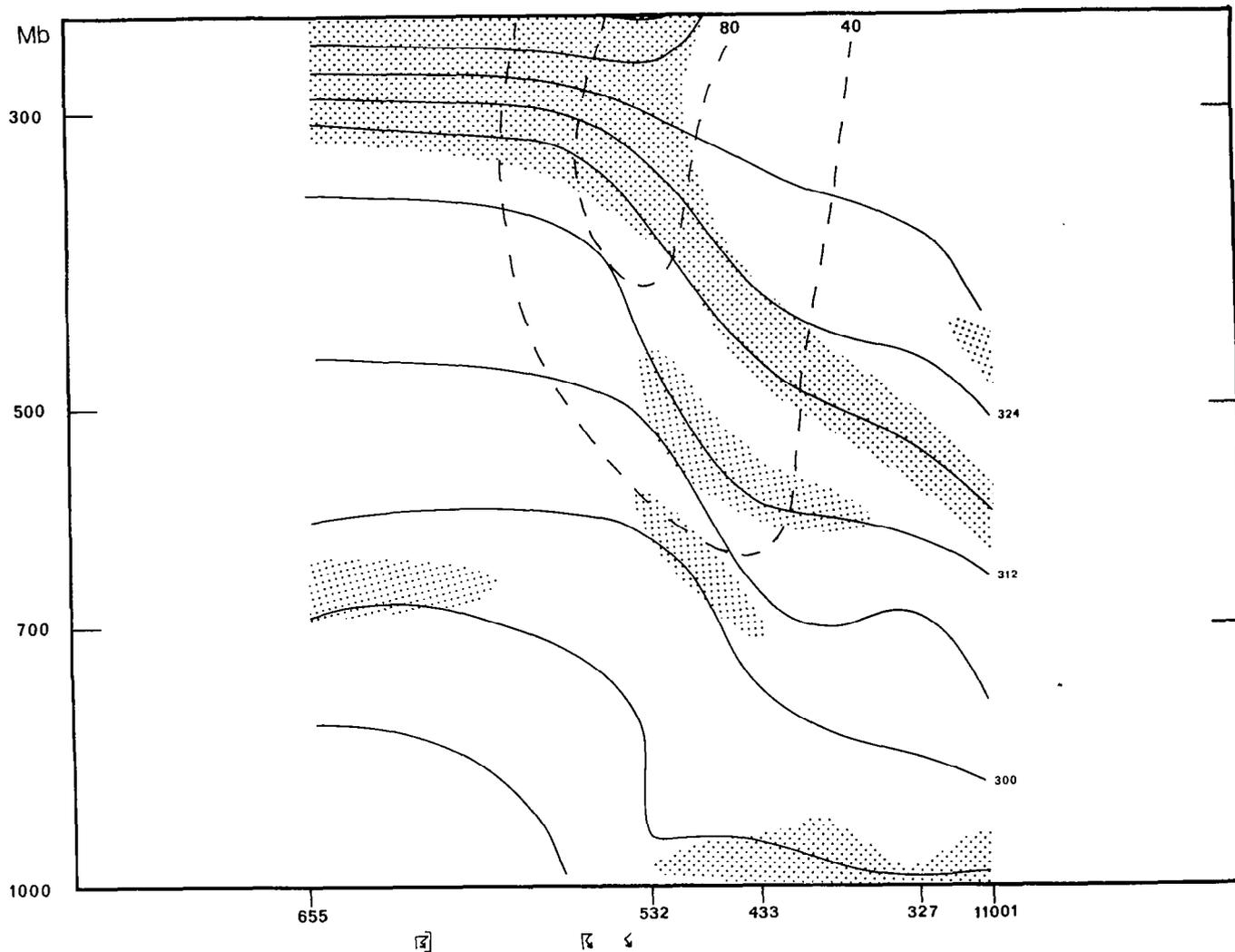
Figure 11-f. 0300 UT, 12 May, 1974.
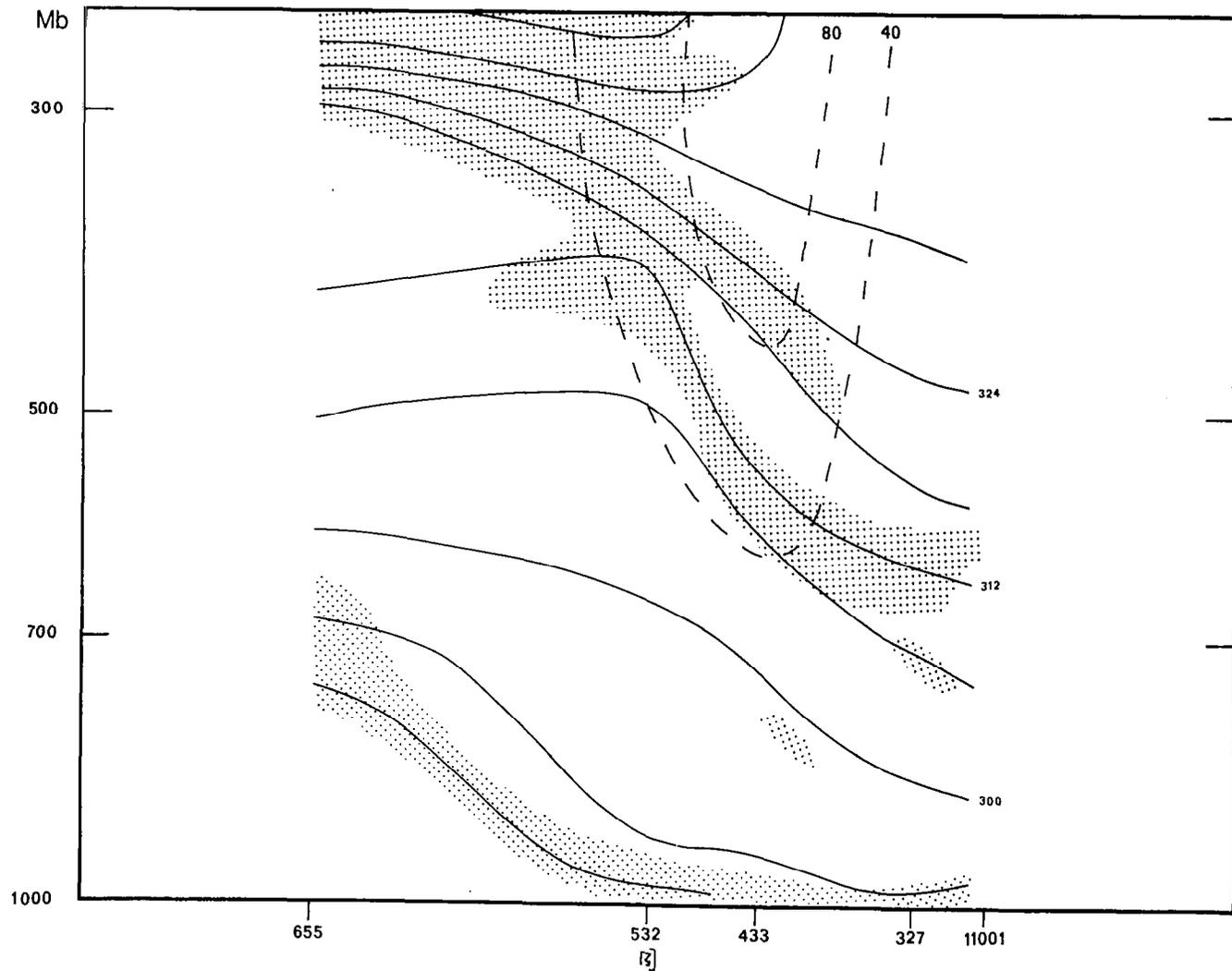
Figure 11-g. 0600 UT, 12 May, 1974.

Mb

300

500

700

1000

120 80   40

324

312

300

532   433   327   11001

655

60
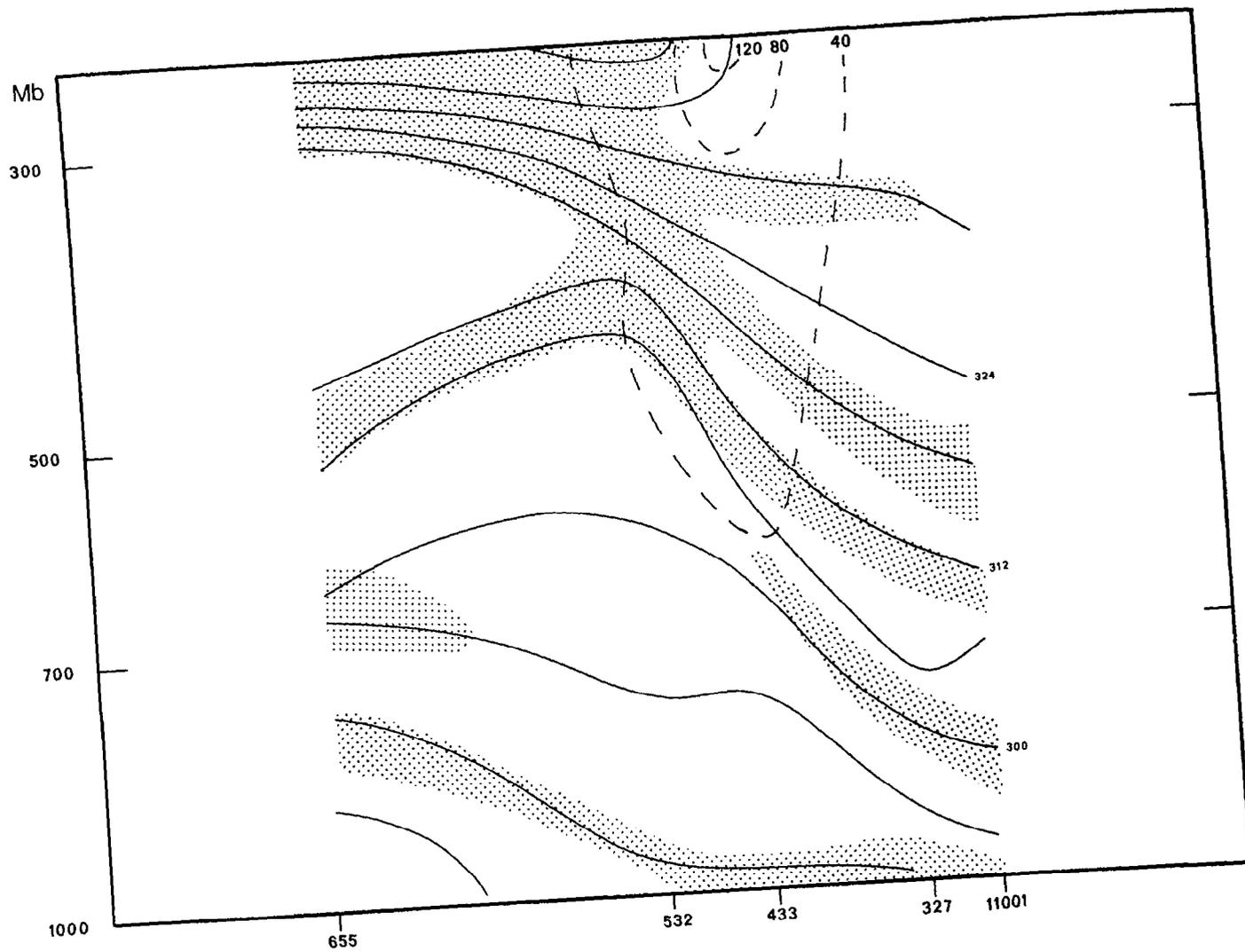
Figure 11-h. 0900 UT, 12 May, 1974.
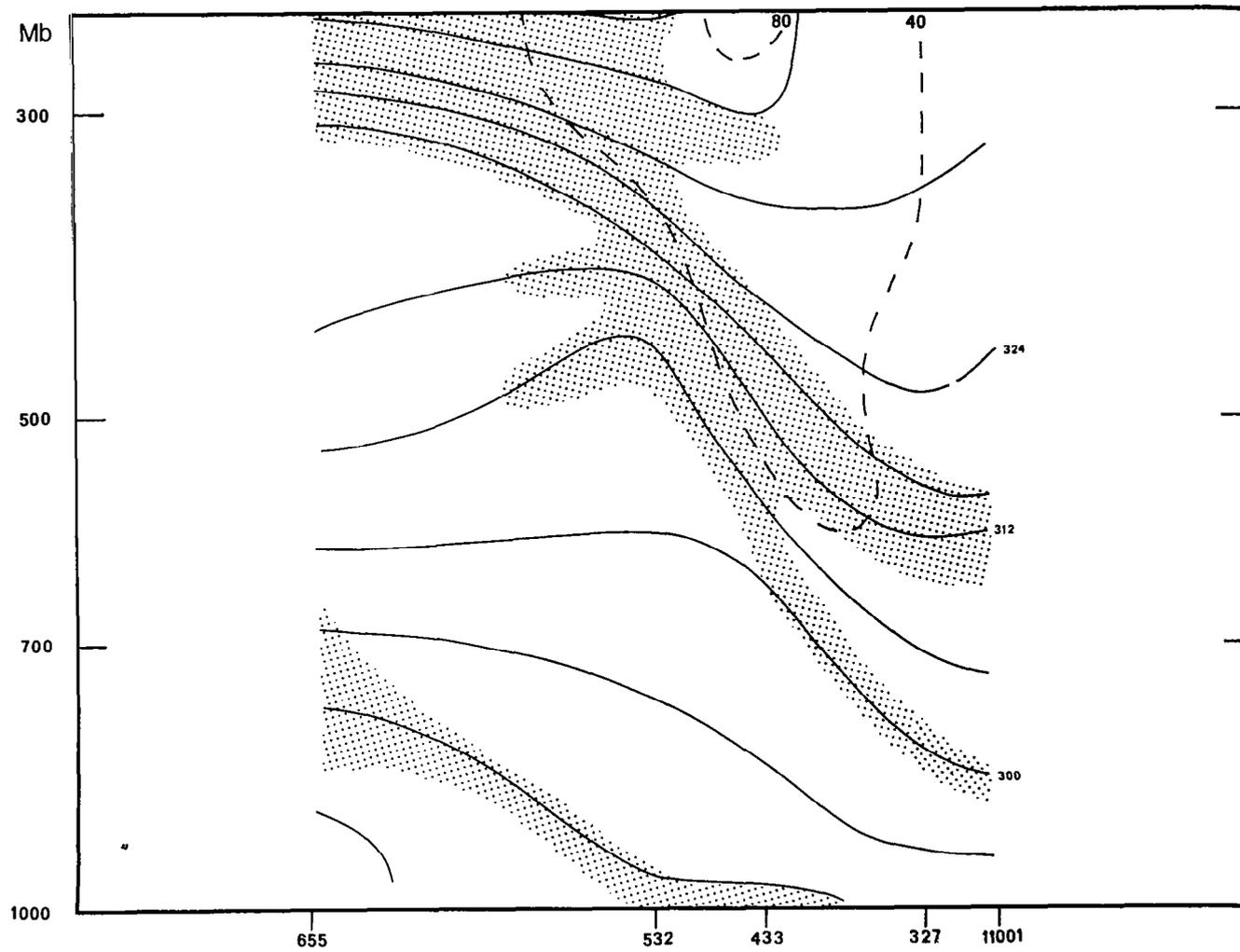
Figure 11-i.   1115 UT, 12 May, 1974.

be found to be helpful to refer to figure 8 during the
course of this discussion. Hereafter, the cross section
from Bismarck, North Dakota (station 764) to Washington,
D.C. (station 405) will be referred to as either cross sec-
tion I or as the northern cross section; the cross section
running from Saint Cloud, Minnesota to Huntsville, Alabama
(station 11001) will be referred to as either cross section
II or the southern cross section (see figure 9).

At 1115 UT, 11 May, 1974, cross section I extended
from the cold air behind the cyclone, through a point just
south of the point of occlusion, and then well to the east
of the weather associated with the Minnesota storm. Cross
section II runs from just south of the low center and into
the warm sector of the cyclone. A hyperbaroclinic zone is
seen to extend from the stratosphere into the upper tropo-
sphere on the northern section. This same zone is also
found on the southern section, but it is not so evident as
it has just begun to enter the plane of the cross section.
The surface fronts are more pronounced on the northern sec-
tion, but on both sections, the surface fronts are seen to
be unconnected with the fronts in the upper levels. The
cold air behind the upper fronts is baroclinic, while the
warm air ahead of the fronts possesses but little tempera-
ture gradient. This is in contrast to Palmén and Newton's
(1948) finding that the air is baroclinic both ahead of and
behind the polar front, and is the opposite of Reed and

Danielsen's (1959) frontal model in which the warm air is baroclinic, while the cold air is barotropic.

The upper front is apparent on both sections at 1500 UT. The greater slope of the front on section II is consistent with the fact that this cross section lies near the axis of the upper level trough. As shown by Palmén and Newton (1963), Margules' formula for the slope of a front, when modified to take into account the curvature of the flow, predicts a larger slope when the flow is more strongly cyclonic than when it is weakly cyclonic or anticyclonic. A further consequence of the variation of the curvature of the flow between the cross sections is the stronger winds found on the northern section. On both sections, the nocturnal cooling inversion erodes from the bottom as the sun begins to heat the surface. The low level cold front shows up well on section II as a sloping stable layer reaching the ground near Peoria, Illinois (station 532).

The continuing growth of the mixed layer at 1800 UT is particularly evident in the western and eastern portions of section I. The deepening of this layer in the cold air behind the storm is due to a combination of cooling aloft and surface heating. Surface fronts are indistinct, and the warm front has moved north of the plane of the cross section, but a squall line gives the appearance of a front in the eastern portion of cross section I. The extension of the upper stable layer to lower levels on section II gives

the mistaken impression that the upper front has also come down to low levels. That this is not the case can be seen by an inspection of figures 11-c and 13-a. The upper front is found to weaken near 600 mb and is underlain there by a stable but flat layer which is itself atop a stable, baroclinic zone to its south and east. The cold air remains baroclinic on both sections. Another persistent feature is the deep layer of low stability found beneath the upper front and above the low level baroclinic zone on both cross sections.

Severe convection is occurring in south central Michigan at 2100 UT. A second area of convective activity is found behind the low center near the borders of Minnesota, Nebraska, and the Dakotas. On both sections, the low level instability associated with this convection is apparent. Relative humidities drop off sharply upwards through the stable layers near 700 mb in the central regions of section I. Such a moisture distribution would be expected to be found in a region where severe local storms are occurring. It is of interest to note that at 1115 UT a layer of low stability was found above the surface inversion on the southern section. This layer may have been a remanant of the previous day's mixed layer. As the mixed layer grew on the morning of the 11th of May, it engulfed this layer, resulting in accelerated growth of the boundary layer.

A major change in the structure of the upper front be-
gins to occur at this time on the southern section. The
front begins to split into two zones, the new zone being
centered around the 324 K isentropic surface. This feature
appears on figure 11-d as a "finger" of high stability
above the primary upper front. By 2315 UT, this structure
has extended a considerable distance into the middle tro-
posphere. Comparison of figures 11-d and e suggests that
this extension occurred as the result of the incorporation
into the front of a preexisting stable layer. Section I
shares this tendency to develop additional upper fronts,
but they do not become as well developed as do those on the
southern cross section. It should be noted that section I
does not exhibit many stable layers in the potential path of
these downward-building fronts. However, where such a
stable layer was found, namely that layer in the middle
troposphere near the center of the chart, the front was ob-
served to extend to lower levels.

Convection is still active in eastern Michigan and
northern Ohio at 2315 UT, with a moderate thunderstorm at
Cleveland. The cold air entering into the plane of sec-
tion I is more barotropic than that earlier found in this
region. The cold air behind the fronts on the southern
section retains its thermal gradient.

Large changes have occurred in the southern section by
0300 UT, 12 May, 1974. In advance of convective activity,

deep instability is found over Peoria, Illinois. This is
associated with strong cooling in the middle troposphere.
The following table of the potential temperature on the 900
and 500 mb surfaces over Peoria shows this effect:

TIME	900 MB	500 MB
2315 UT	294 K	316 K
0300 UT	294 K	306 K

The value of surface potential temperature decreased from
294.1 K to 286.3 K during this same period. However, the
stabilization resulting from this cooling was confined to
a shallow layer near the surface. Examination of the Peoria
surface observations reveals this cooling to be the result
of radiational cooling. The 324 K hyperbaroclinic zone re-
mains well-defined, while the previously sharply delineated
lower zone has become indistinct in its upper portions.
The stability in the upper reaches of this front has de-
creased and the front no longer appears to be connected
with the stratosphere. However, the lower portion of this
front remains strong, and is approaching the baroclinic
zone that has formed as a result of the above mentioned
cooling. A further consequence of the elevation of the
isentropic surfaces has been to reduce the temperature
gradient within the cold air. The northern section shows
few changes from 2315 to 0300 UT.

Schwerdtfeger and Strommen (1964) reported a case where soundings spaced one hour apart revealed cooling taking place simultaneously through deep layers of the troposphere following the passage of a front. He suggested that this was due to an ageostrophic circulation in a direction normal to the front. However, he did not show whether or not this proposed circulation was of sufficient magnitude to lead to the observed cooling. A similar pattern of deep cooling is observed in the present case. Consideration of the cross sections shows that this cooling is due to the nearly simultaneous arrival at different levels of the multiple upper level hyperbaroclinic zones. It is therefore suggested that this same mechanism is responsible for the effect reported by Schwerdtfeger, and is probably found in other instances of frontal passage.

The 312 K hyperbaroclinic zone on the southern section is once again well organized at 0600 UT as is the 324 K zone. Warming is taking place behind the convection of 0300 as shown by the descending isentropic surfaces. This warming combined with continued cold advection to the west, results in the appearance of a secondary low level cold front within what used to be a region of small baroclinity. Aloft, a section of the 0300 mid-tropospheric stability has been absorbed by the 312 K front. A similar process is taking place on the northern section where a downward extension of the upper front occurs as it comes into conjuction with a

middle level stable layer. An additional upper front is now found on this section between the 318 and 324 K isentropes. A weak warm front begins to make its appearance in the upper troposphere on the western side of the cold dome on both sections. Weak low-level stability is found in the western portion of both sections despite the lateness of the hour. Mixing by winds of 15 to 20 knots prevents the formation of a deep or strong surface inversion where skies are clear.

The upper fronts remain well defined on both sections at 0900 UT. On section II however, a merger of the two zones is beginning to take place. A joining of the 312 and 318 K zones has also taken place on section I. The 312 K front continues to extend to lower altitudes as it absorbs stable layers beneath and ahead of itself. A similar descent of this front is found on the northern section, but the resultant structure is neither as deep nor as sharply defined as on the southern cross section. The warm front behind the dome of cold air is better organized at this time. This intensification seems to be associated with a lowering of the isentropic surfaces on the warm side of the front. This is apparently due to subsidence in the warm air, for the mid-tropospheric stability increases as the isentropes lower. Support for this suggested mechanism comes from the rapid decrease in mid-tropospheric relative humidities in this region between 0900 and 1115 UT.

By 1115 UT, the two upper hyperbaroclinic zones of section II have merged, forming a deep, wide front. The lower portion of this front has joined with the stable, baroclinic layer centered around the 300 K surface found on the 0900 chart. The western warm front has weakened somewhat, but is still found on both sections. The northern section is somewhat difficult to interpret. The upper tropospheric fronts on this section have weakened considerably since 0900. While consolidation of the fronts has occurred on section II, the upper front on the northern section has split into two zones. The front near the 330 K isentropic surface has sharpened considerably since the previous section. These changes are associated with warming below the tropopause at Green Bay, Wisconsin (station 645), and with warming near the 350 mb level at Flint, Michigan (station 637). An additional significant difference between this section and others is the widespread precipitation occurring along the front. This ascent on the warm side of the front would result in a weakening of the temperature gradient across the front. The isentropic surfaces in the middle and upper troposphere over Pittsburgh, Pennsylvania (station 520) are higher than at 0900, but this effect does not account for all the observed changes in the structure of this system of fronts.

In summary, the following is revealed by the cross sections:

1. Both sections show fronts in the upper, middle, and lower levels of the troposphere.

2. A hyperbaroclinic zone extends from the lower stratosphere into the upper and middle troposphere on both sections.

3. The warm air ahead of these fronts is only weakly, if at all, baroclinic.

4. The cold air behind these fronts is originally baroclinic, but becomes less so later in the period under study.

5. The hyperbaroclinic zone was not in a steady state, but split into several zones and merged with other zones. This tendency was much stronger on the southern section than on the northern one.

6. The downward extension of the hyperbaroclinic zone appeared to occur as the result of the merger with and tilting of stable layers below and ahead of it.

7. An upper-level warm front formed late in the period on the western side of the cold air, apparently due to subsidence in the warm air.

8. The primary surface fronts were weakly defined and confined to the low levels on both sections.

9. The mixed layer was observed to grow on both sections, attaining its greatest depth in the cold air behind the cyclone.

10. Cooling took place nearly simultaneously through deep layers with the passage of the system of fronts.

PRESENTATION OF THE HIGH RESOLUTION CROSS SECTIONS

The preceeding diagrams have shown the general evolu-
tion of the system of fronts being studied. However, the 6K
isentrope spacing is inadequate to reveal the details found
on the original diagrams. To show these details, the cross
sections for both the northern and southern lines are here
presented with a spacing between isentropes of 2K. Presen-
tation of every section would be an inordinate amount of
work and could confuse the reader by supplying an overabun-
dance of detail. Therefore, the sections are provided for
every six hours, beginning with the 1800 UT cross sections
(figures 12 and 13). Included on these charts are isotachs
of the flow normal to the plane of the cross section, drawn
at intervals of 40 knots. Isentropes are drawn every 2K,
except in the stratosphere, where a spacing of 10K is used.
Values of potential vorticity in units of 10^{-6} K $m^{-1}mb^{-1}$ on
selected isentropic surfaces are plotted on the southern
cross sections. Considering the discussion of the previous
section, further itemization of the temporal development of
the system would be redundant. Therefore, in accordance
with the principle that an isentropic cross section is worth
at least a thousand words, remarks in this section will be
confined to pointing out features on the sections that are
of significance, allowing the diagrams to speak for them-
selves.
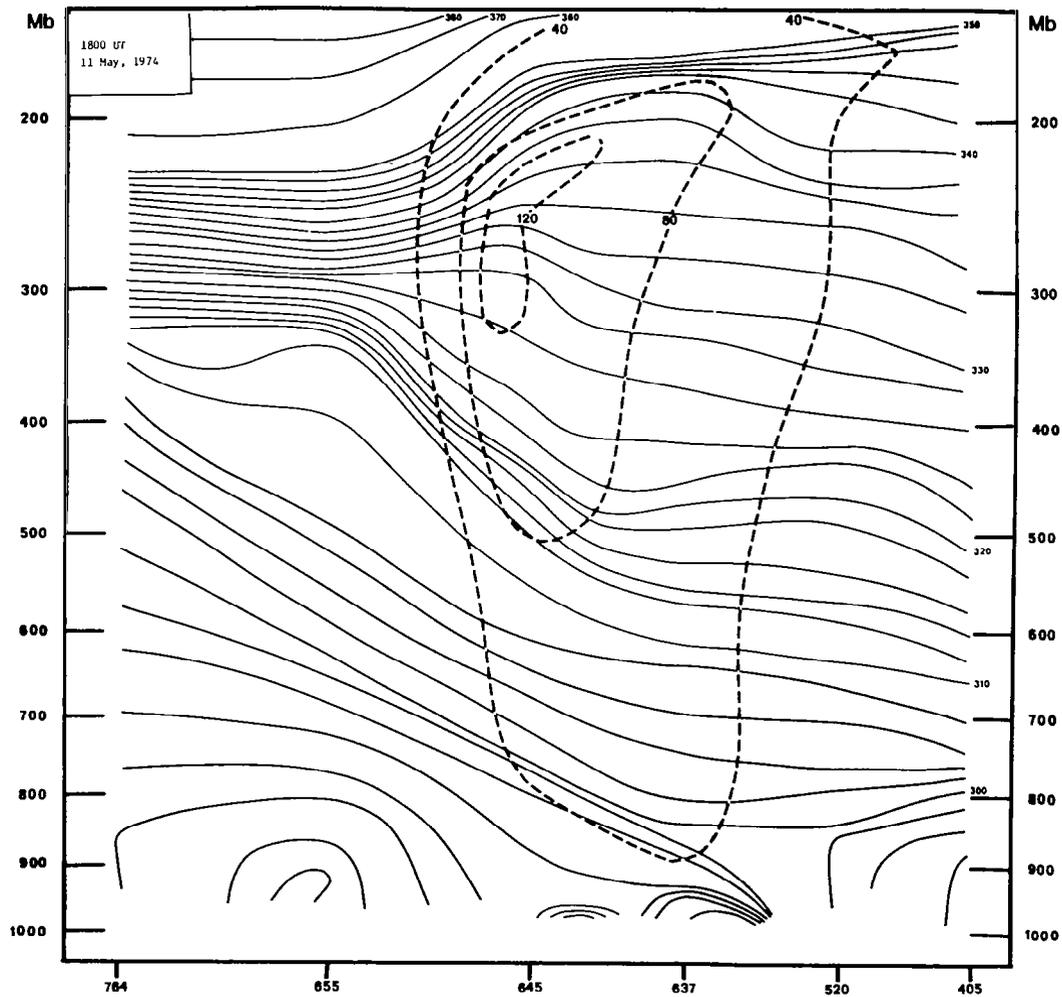
Figure 12-a.   High resolution cross sections along line I from Figure 9.   Isentropes (°K, solid) and isotachs (knots, dashed) of flow normal to section. 1800 UT, 11 May, 1974.
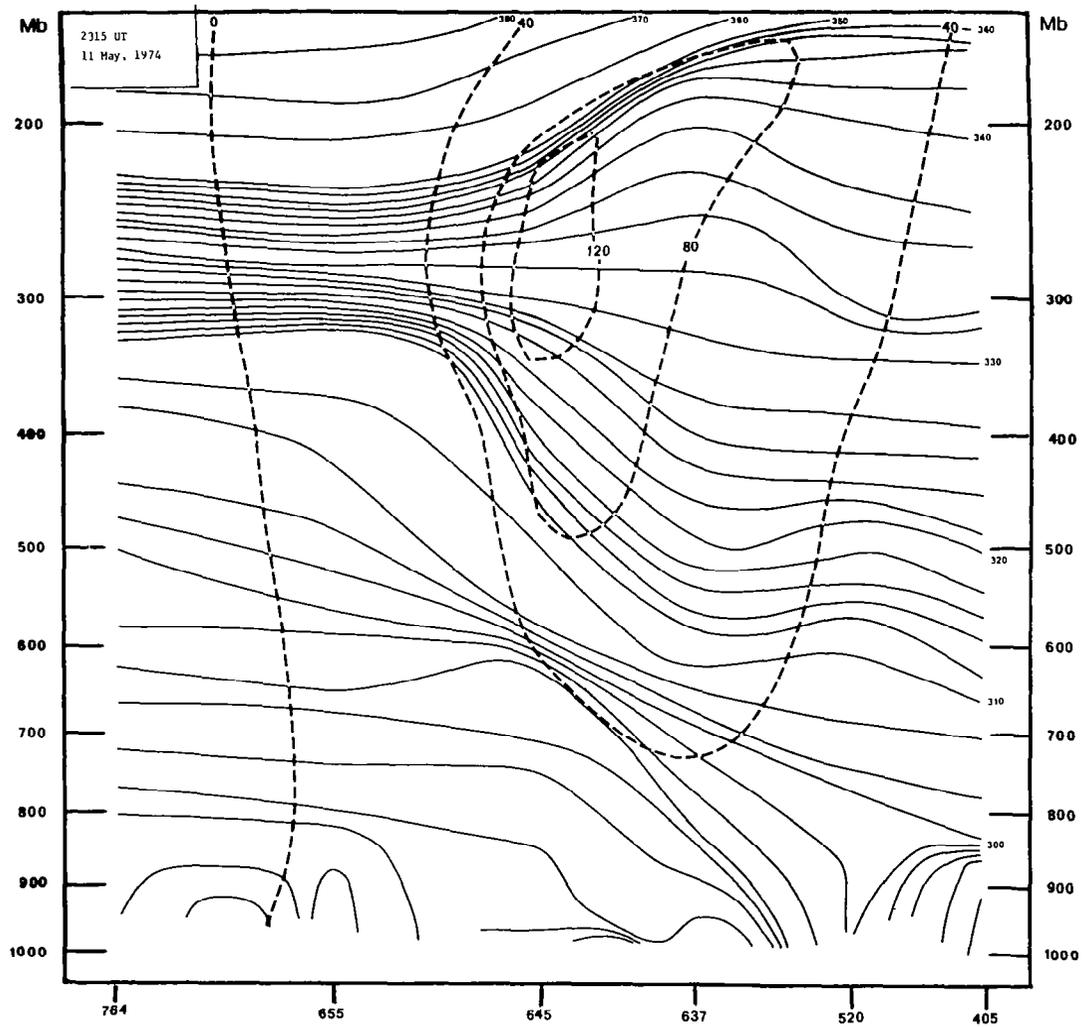
Figure 12-b.   2315 UT, 11 May, 1974.

Figure 12-c.   0600 UT, 12 May, 1974.
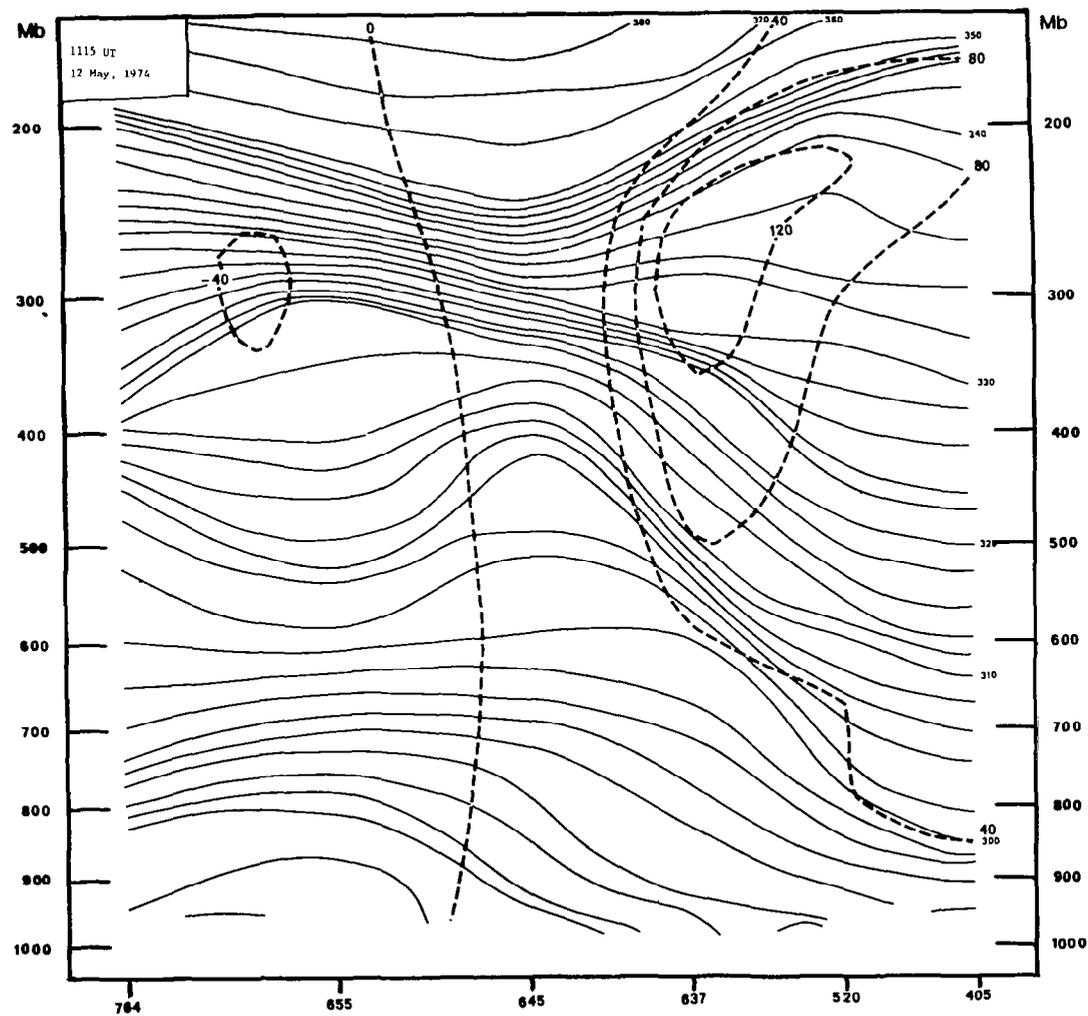
Figure 12-d.   1115 UT, 12 May, 1974.

On both the northern and southern sections, the tropo-
pause is high over the warm air, low in the cold air, with
its height changing quickly with distance near where the
tropospheric hyperbaroclinic zones encounter the lower
stratosphere. It is characteristic that the change in the
height of the tropopause occurs over a rather small horizon-
tal distance (Defant and Tabba, 1958). This is especially
well illustrated on the southern section for 0600 and 1115
UT, 12 May, 1974. As mentioned earlier in this study, the
atmosphere is in a condition of barotropy in this region
where the tropopause abruptly changes height. This region
is also the level of maximum wind speed. Fronts in this
area, therefore, are not regions of large horizontal tem-
perature gradient, but are zones of large cyclonic wind
shear (Berggren, 1952). This type of structure is found on
both sets of cross sections, although more clearly so on
the northern sections due to the greater wind speeds there.
This shear zone, and also a sloping zone of temperature
gradient are observed to slope upwards and eastwards from
the region of tropopause discontinuity. Such an extension
of the front into the lower stratosphere is very similar to
analyses produced by Palmén (1958) and Shapiro (1976).

Also, these sections clearly show the splitting and
coming together of the upper tropospheric fronts. These
fronts are shown to be not in a steady state, but constantly
undergoing changes in their structure and their relation to
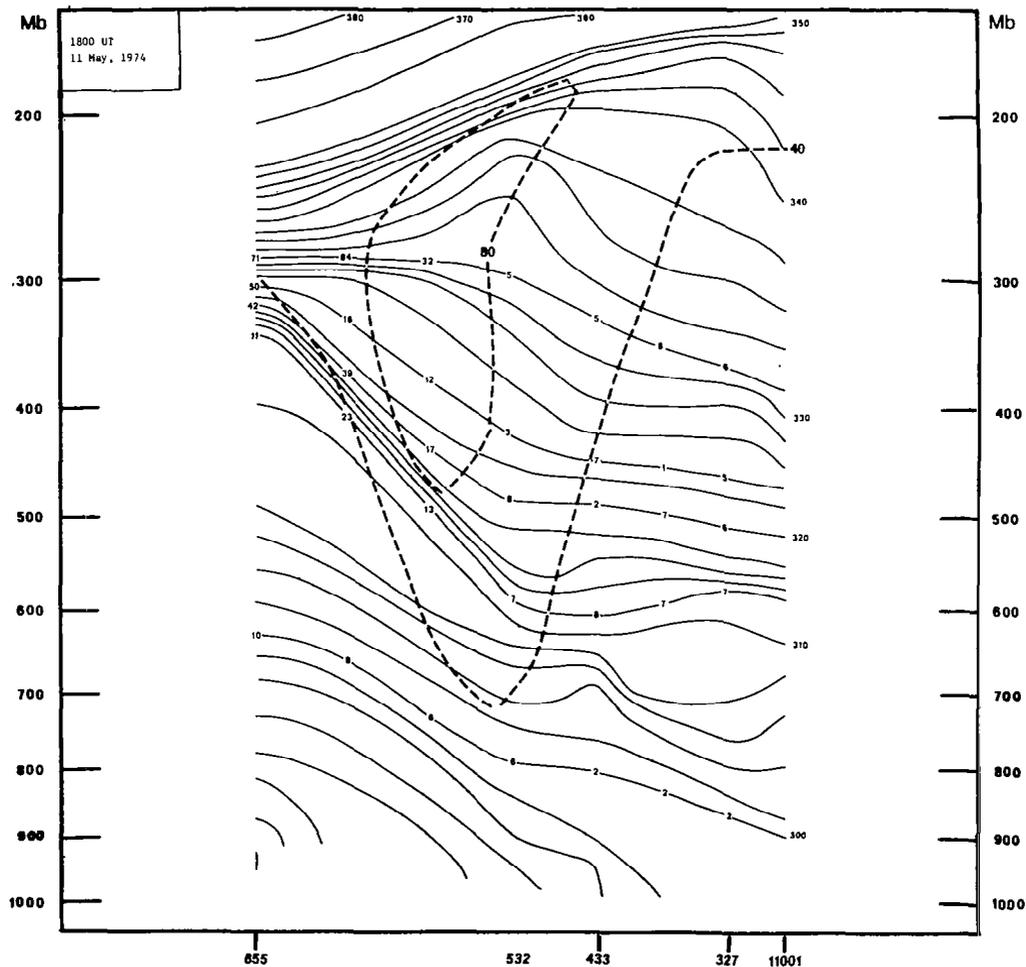
Figure 13-a.   High resolution cross sections along line II from Figure 9.   Notation
as per figure 12 with addition of values of potential vorticity
$(x\ 10^{-6}\ k\ mb^{-1}\ sec^{-1})$ plotted on selected isentropic surfaces.   1800
UT, 11 May, 1974.
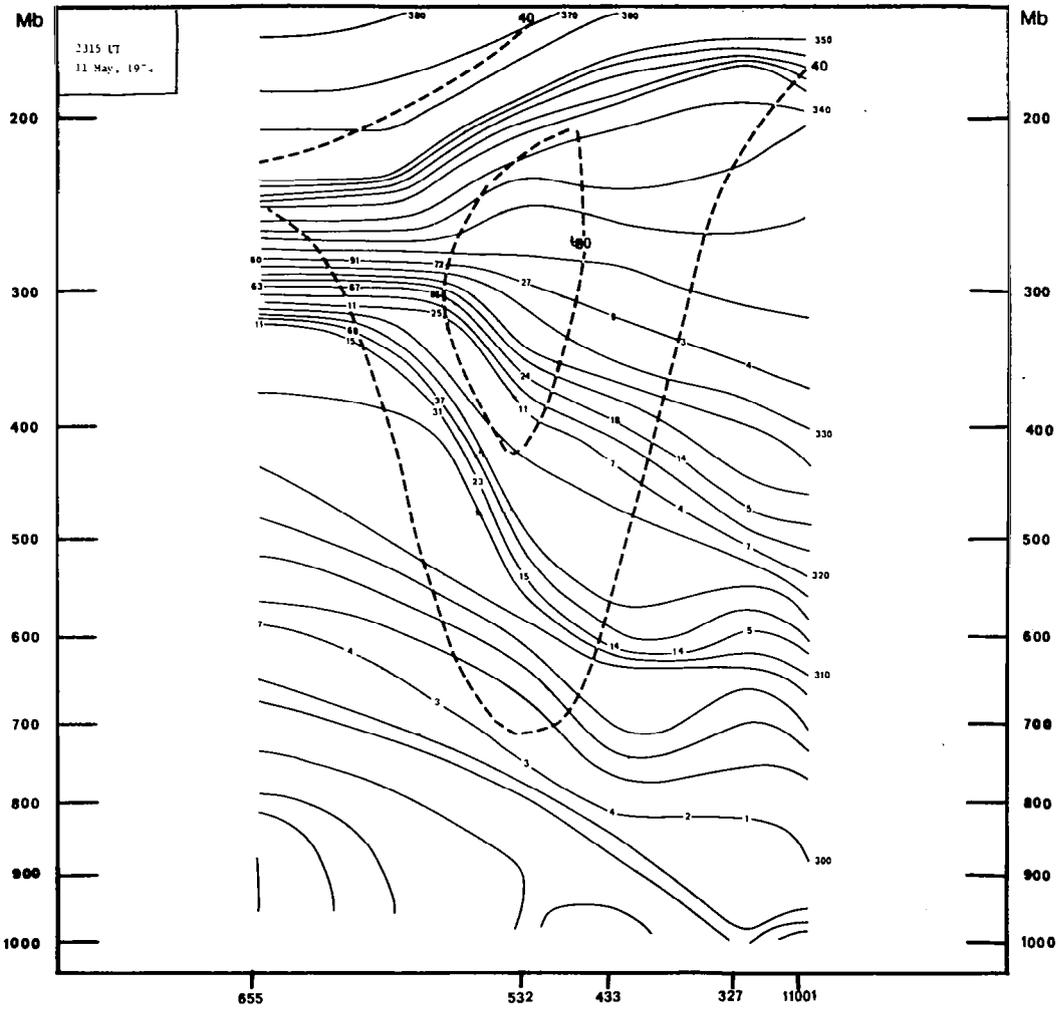
Figure 13-b. 2315 UT, 11 May 1974.
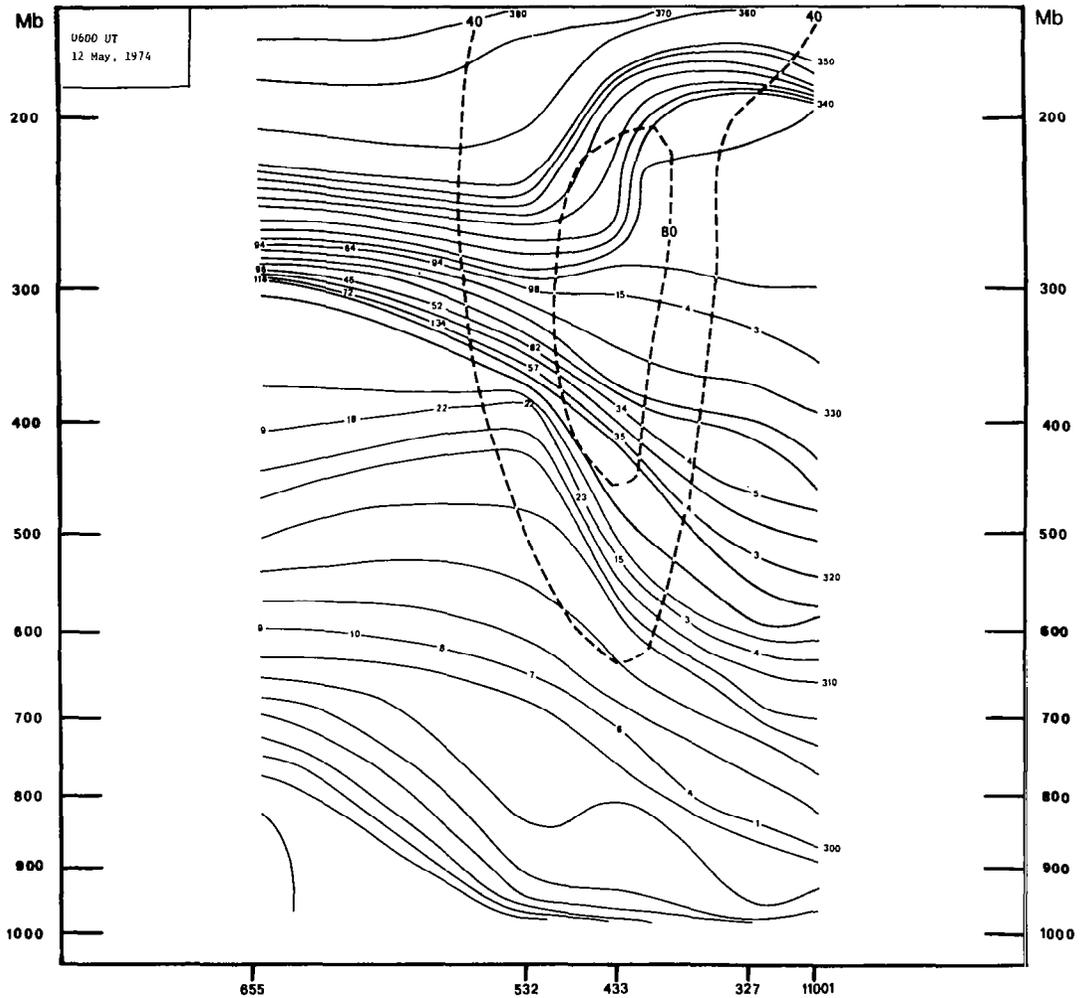
Figure 13-c.   0600 UT, 12 May, 1974.
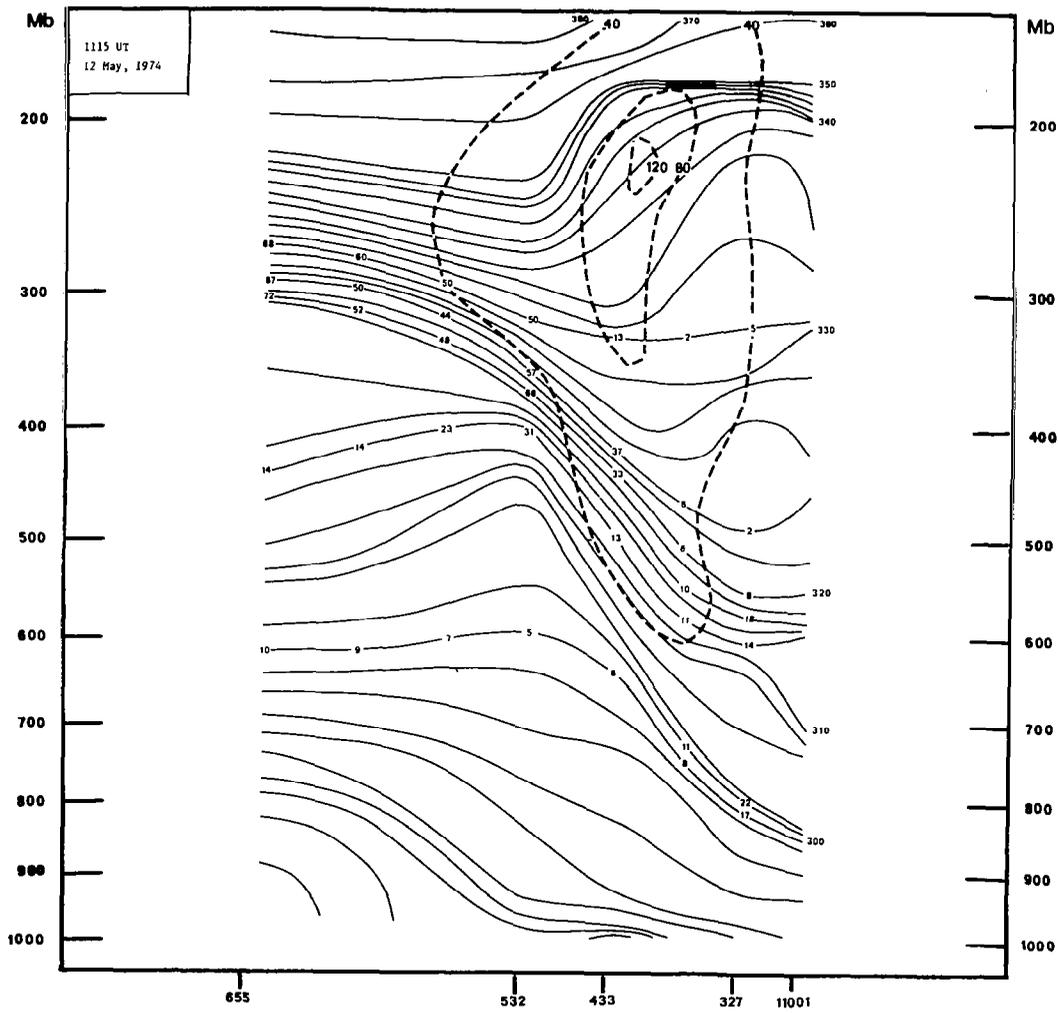
Figure 13-d. 1115 UT, 12 May, 1974.

the surrounding environment. On the southern section, frontal splitting appears to result from destabilization within a layer resulting from an upward increase in the time rate change of temperature, and frontal recombination seems to be associated with stabilization due to warming aloft and cooling at lower elevations or an upward decrease in the time rate change of temperature. Similar processes are found on the northern sections (i.e., compare Flint, Michigan between 2315 and 0600 UT), but the relative weaknesses of these changes on the northern sections makes it difficult to draw a definite conclusion.

The downward extension of the upper fronts is seen to involve preexisting lower stable and/or baroclinic layers, particularly, the upper levels of the midtropospheric baroclinic zone found on both sections. This is an important point and will be treated more fully in the next section of this paper. That this descent of the fronts is due to actual lowering of the fronts and not to advection of low level baroclinity is indicated by consideration of analyses of pressure and wind on isentropic surfaces. There was inadequate upstream baroclinity for advection to account for the observed changes in frontal structure.

The primary surface fronts are weak, shallow, and unconnected to the middle and upper level fronts. A well-developed secondary cold front forms in the cold air behind the leading cold front in the southern section between 2315

and 0600 UT. This front first appeared following the passage of convective activity at Peoria, and seemingly resulted from a combination of cold air advection to its north and west and warming following the passage of the convection. Maintenance of the front is apparently due to continuing cold advection in its rear. The front blends into the surface nocturnal cooling inversion.

DISTRIBUTION OF POTENTIAL VORTICITY

Potential vorticity, values of which are included on the southern cross sections, is defined as

$$P = -\frac{\partial \theta}{\partial P} (\zeta_\theta + f)$$

where ζ_θ is the relative vorticity on a surface of constant entropy. In natural coordinates, this relative vorticity is

$$\zeta_\theta = (\frac{\partial V}{\partial N} + \frac{V}{R})_\theta$$

where $\frac{\partial V}{\partial N}$ is the vorticity due to horizontal shear, and $\frac{V}{R}$ is the contribution from the curvature of the flow, both taken on an isentropic surface.

In order to compute the potential vorticity, maps of the field of wind speed and of streamlines of the flow were constructed. As mentioned earlier, the isotach analyses were enhanced through use of the technique of time-space conversion. The streamline field was less complicated than that for the wind speed, so no formal time-space conversion was employed in these analyses. Time continuity was subjectively incorporated into the streamline analyses by consideration of adjacent (in time) charts. Values of the horizontal shear and of the curvature of the flow were then estimated from these diagrams. Values of the thermal

stability were obtained from the cross sections. Potential vorticities were computed for seven points on the 300, 312, 320, 324, and 332 K isentropic surfaces. In locations of interest where the shear and curvature varied but little with height, supplementary values were computed by interpolation of the value of the relative vorticity.

Since potential vorticity is conserved during a dry adiabatic process, it can be used as a tracer of air parcels. Many authors have used the distribution of potential vorticity to show that the air in upper tropospheric fronts is of stratospheric origin (Reed and Sanders, 1953; Reed, 1955; Reed and Danielsen, 1959; et al.). As can be seen from figure 13, stratospheric values of potential vorticity are much greater than tropospheric values, due mostly to the greater static stability of the stratosphere. The values of potential vorticity in the upper portions of the hyperbaroclinic zones are greater than those in the tropospheric air adjacent to the zones, and less than those of the air in the stratosphere. Within the fronts, the potential vorticity decreases with decreasing altitude. Such a distribution suggests that air from the stratosphere is descending into the troposphere in the upper reaches of these fronts. This distribution of potential vorticity is similar to what has been found by other investigators (Reed and Danielsen, 1959; Danielsen, 1964; Shapiro, 1974 and 1976).

The high concentrations of ozone and radioactive particles found within upper fronts and the dryness of the air in these zones is compelling evidence to believe that air from the stratosphere descends into the troposphere within upper tropospheric fronts. However, there is disagreement as to the depth to which this extrusion of stratospheric air descends. Surface based observations do show increases in the concentrations of ozone and radioactive particles following the passage of upper fronts, but this does not necessarily indicate that air from the stratosphere is being extruded directly down to the surface. Rather, stratospheric air may be brought part way into the troposphere and then be taken to lower levels through mixing and precipitation processes.

The fact that the value of potential vorticity decreases downwards in the fronts implies that the stratospheric extrusion is of limited vertical extent. These lower values indicate that either this air is not of stratospheric origin, or, if it is, it has been subjected to mixing which has destroyed its previously large values of potential vorticity.

The large values of potential vorticity found near 800 mb on the 1115 UT section should not be interpreted as evidence of a deep extrusion of stratospheric air. This increase is due to a diabatic increase of static stability accompanying the development of the 300 K front. As has

already been mentioned, this front was in a nascent state
on earlier sections as a middle-level baroclinic zone. It
should also be noted that none of the isentropes making up
this front extend into the stratosphere. This means that
stratospheric air could reach into this front only through
a diabatic process. Such a process or processes (i.e.,
turbulence or convection) would likely destroy the extru-
sion as a separate entity.

The air in this lower front is much drier than the
air below it. However, examination of cross sections of
mixing ratio shows that a region of dry air at these alti-
tudes existed earlier to the west of the future front, and
moved into the region where the front formed.

A further argument against the extrusion of strato-
spheric air to very low altitudes in this case is the man-
ner in which the low level front formed. As has already
been mentioned, this front formed due to the interaction of
the upper front and an already existing lower level baro-
clinic zone. This is clearly seen by inspecting the 0600
and 1115 UT sections. This observation is in accord with
Palmén and Newton's (1969) criticism of Reed's 1955 conclu-
sion. They noted,

> Our interpretation is that a front already
> existed in the troposphere prior to the
> time when... the extrusion of stratospheric
> air to lower levels took place. There is
> no question that strong frontogenesis took
> place... but this appears to have involved

> a sharpening of fronts that were already
> present in the troposphere.

Sawyer (1958) states the same conclusion in a discussion of the characteristics of fronts in the middle troposphere. The occurrence of this process has been mentioned earlier in this study, and can be seen on figures 10 through 13.

Since the intensity of these fronts is weaker than those studied by other investigators, it should not be concluded that deep extrusions of stratosphere air do not occur. Rather, this instance shows that such penetrations are probably not the general case.

COMPUTATION OF FRONTOGENESIS

In order to determine what processes were acting on the fronts depicted in the cross sections, an expression was formulated for the parcel-following frontogenesis on an isentropic surface. Following Haltiner and Martin (1957), frontogenesis is defined to be the total rate change of the magnitude of the temperature gradient on an isobaric surface.

$$F = \frac{d}{dt} |\nabla_p \theta| \qquad [1]$$

In isentropic coordinates, this expression becomes

$$F = - \frac{\nabla_\theta p}{|\nabla_\theta p|} \cdot (\frac{\partial p}{\partial \theta})^{-1} \{ \overset{A}{\nabla_\theta \frac{dp}{dt}} - \overset{B}{(\vec{i} \frac{\partial u}{\partial x} \frac{\partial p}{\partial x} + \vec{j} \frac{\partial v}{\partial y} \frac{\partial p}{\partial y})}$$

$$- \overset{C}{(\vec{i} \frac{\partial v}{\partial x} \frac{\partial p}{\partial y} + \vec{j} \frac{\partial u}{\partial y} \frac{\partial p}{\partial x})} + \overset{D}{\nabla_\theta p (\nabla_\theta \cdot \vec{V})} + \overset{E}{\nabla_\theta p (\frac{\partial}{\partial \theta} \frac{d\theta}{dt})} \quad [2]$$

$$- \overset{F}{\frac{\partial p}{\partial \theta} \nabla_\theta \frac{d\theta}{dt}} \}$$

(see appendix A for the derivation of the above equation).

The terms on the right hand side of equation [2] have the following interpretations:

1) $\frac{\nabla_\theta p}{|\nabla_\theta p|}$ is a unit vector pointing along the gradient of pressure on the isentropic surface.

2) $(\frac{\partial p}{\partial \theta})^{-1}$ is the static stability. Its effect is to modulate the value of the frontogenesis. This is due to the fact that in isentropic coordinates, the gradient of pressure alone does not indicate the intensity of a front; the stability must also be taken into consideration.

3) Term A is the vertical tilting term. This represents the change in the slope of an isentropic surface due to a horizontal gradient of vertical motion. To put it another way, this term is the change in the isobaric temperature gradient resulting from variations across the front in adiabatic warming and/or cooling.

4) Term B is the change in the pressure gradient due to confluence or diffluence of the flow.

5) Term C represents the change in the isentropic pressure gradient resulting from the shear of the flow. See figure 14 for an illustration of how this term acts.

6) The effect of horizontal divergence on altering the mass between isentropic surfaces, and hence the stability is represented by term D.

7) Expression E is the change of stability resulting from the vertical gradient of diabatic heating or cooling.
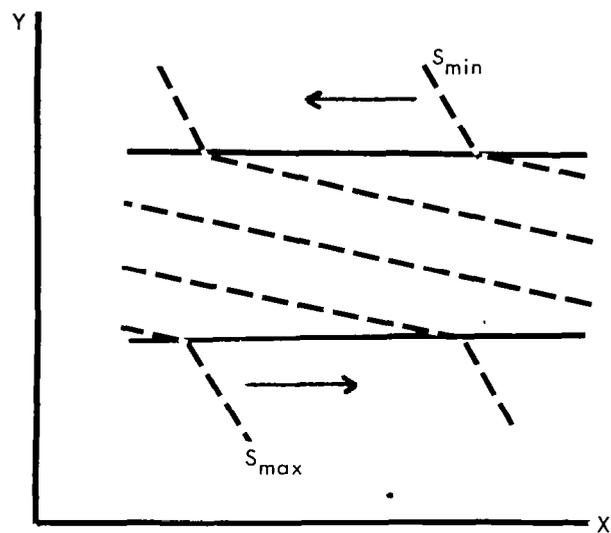
Figure 14. Illustrating the effect of horizontal shear in concentrating isopleths of conservative property S.

8) Term F is the change in horizontal temperature
gradient due to diabatic temperature changes across
the front.

In evaluating the frontogenesis for the fronts under
study, these last two terms were ignored, that is, motion
was assumed to be adiabatic. This assumption is justifiable
for the upper tropospheric fronts, where the air is charac-
teristically quite dry. A subjective assessment of the pos-
sible effects of these terms on the computations of fronto-
genesis will be made in the next section.

Values for the remaining terms in the frontogenesis
equation were readily obtained from the analyses described
earlier in this study. The coordinate system used was a
rectangular coordinate system with the positive x-axis
pointing eastward and the positive y-axis pointing north-
ward. Spatial derivatives were over a distance of two
degrees of latitude (220 km). The total time derivative of
pressure (from the tilting term) was evaluated by Eulerian
methods. That is:

$$\frac{dp}{dt} = \frac{\partial p}{\partial t} + \mathbf{V} \cdot \nabla_\theta p$$

assuming adiabatic conditions. The local time derivative of
pressure was determined using analyses of the pressure on
the isentropic surface six hours apart, centered on the time
in question; the advection term was evaluated using the wind
and pressure analyses for the time being considered.

Values of the frontogenesis were computed at three points across the front on the 312K and 320K isentropic surfaces for both cross sections at 0600 UT, 12 May, 1974. The frontogenesis equation was also evaluated for a point on the 300K surface on both sections for this same time. Figures 15 and 16 show the fields of pressure and wind on these three surfaces at this time, and also show the points at which the frontogenesis was computed. Figure 17 shows the values of frontogenesis at the above points and also the vertical velocity (dp/dt) about these points. Finally, figure 18 depicts the values of the individual terms of the frontogenesis equation at each point where the equation was evaluated.

The diffluence ahead of the jet streaks shown on figure 16a-c is noteworthy. Namias and Clapp (1949) showed that diffluence was found ahead of mean wind maxima and confluence occurred behind these regions. The diffluence in this case was present before the arrival of the jet maximum, which moved into the region of diffluence. The diffluent zone then moved so as to remain ahead of the jet streak. This pattern was observed at all levels and at all times.

One additional comment about the wind distribution is in order. The usefulness of working in isentropic coordinates became evident when analyses were made of the horizontal distribution of wind speed. The field of wind speed was much more discontinuous in isobaric than in isentropic

...
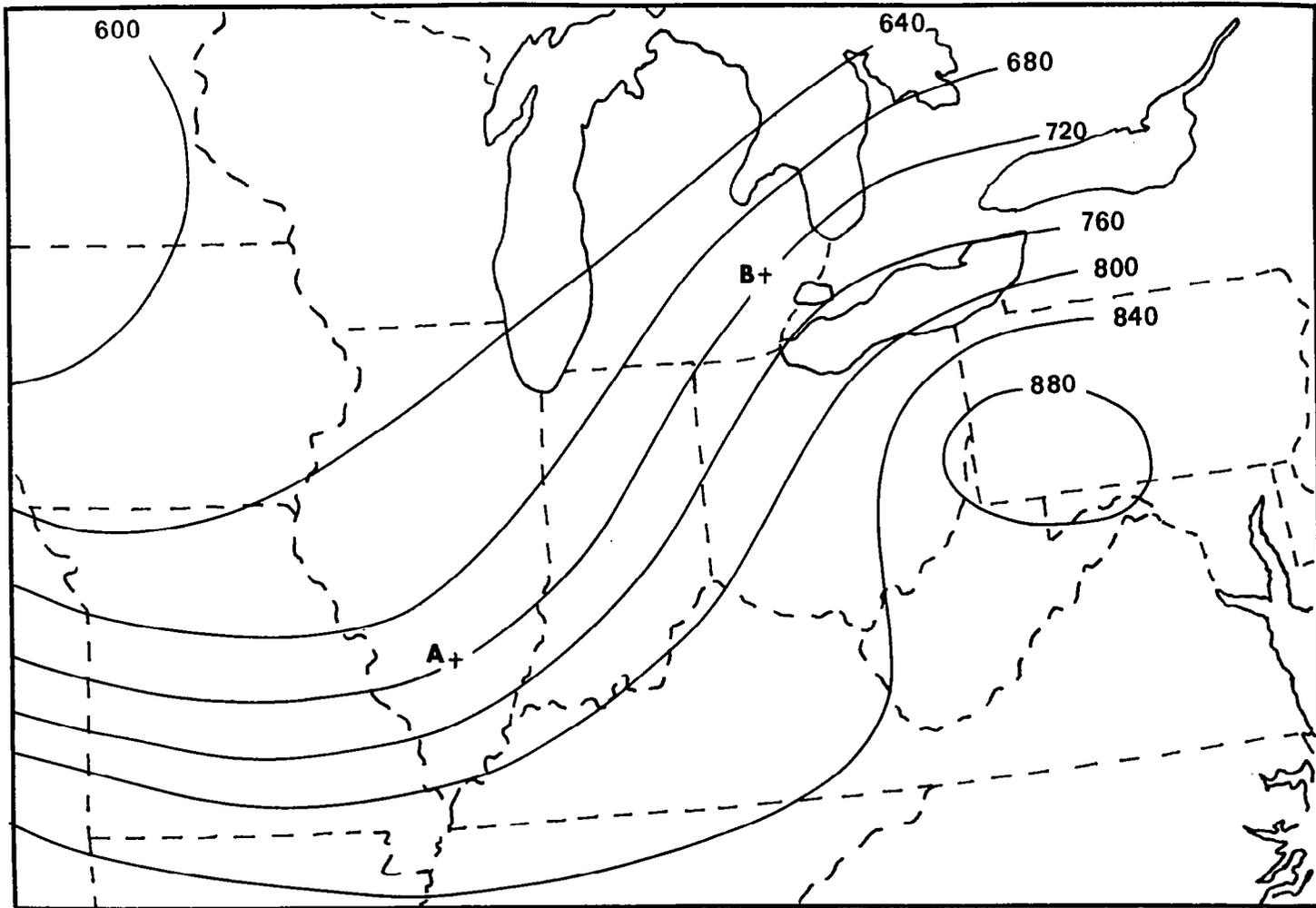
Figure 15-a. Isobars (mb) on isentropic surfaces and locations of frontogenesis computations for 0600 UT, 12 May, 1974. 300 K.
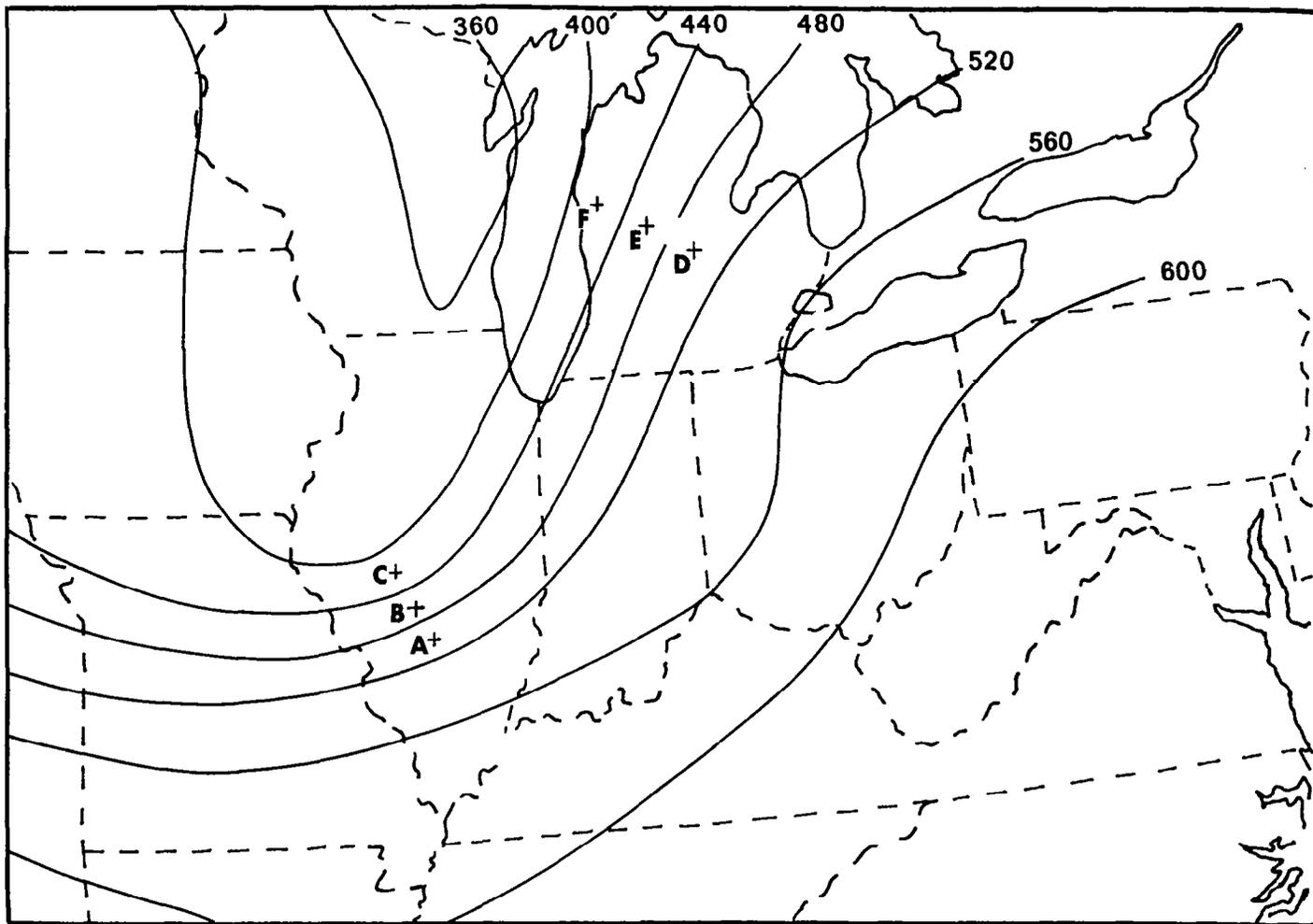
Figure 15-b. 312 K, 0600 UT, 12 May, 1974.
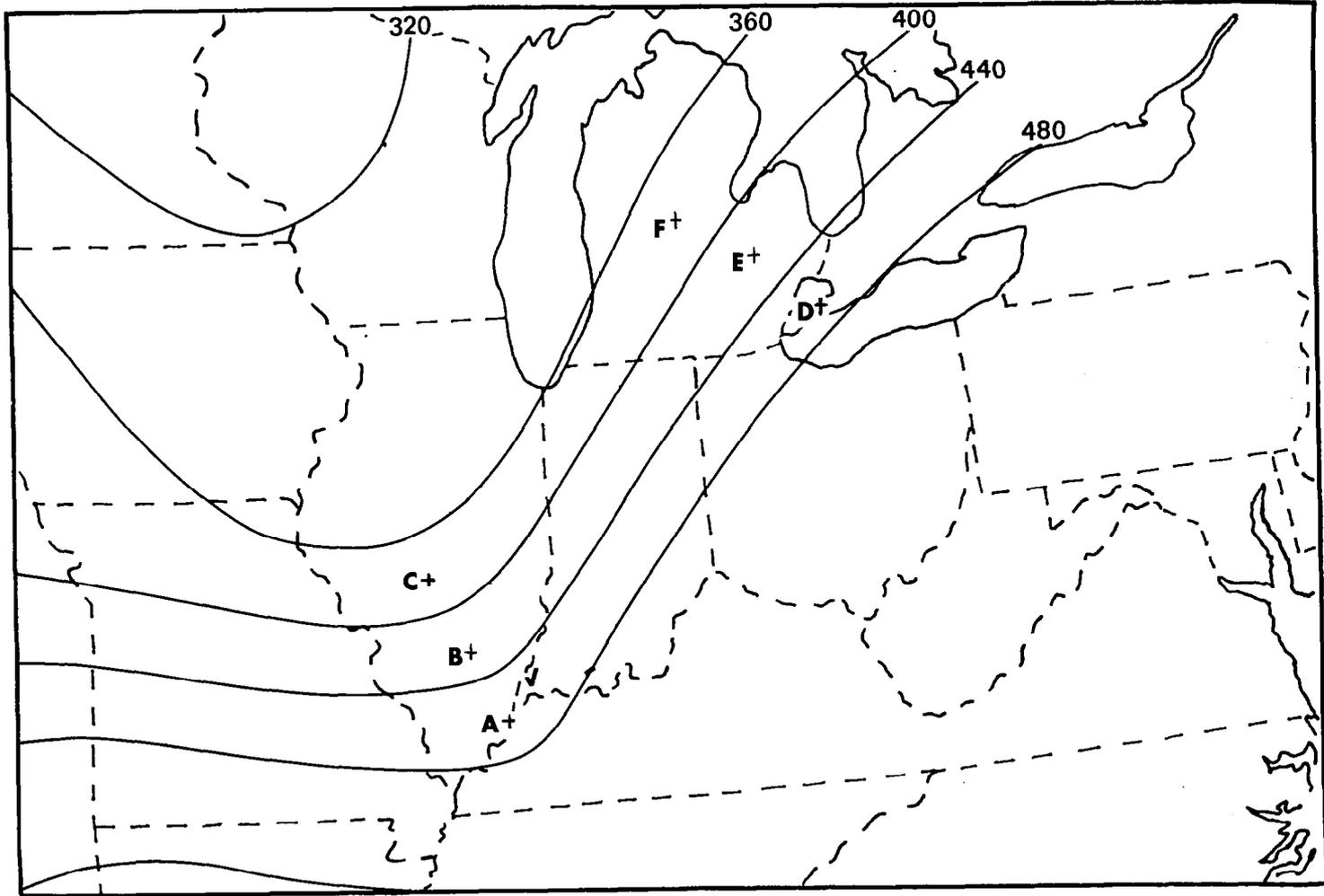
Figure 15-c.   320 K, 0600 UT, 12 May, 1974.
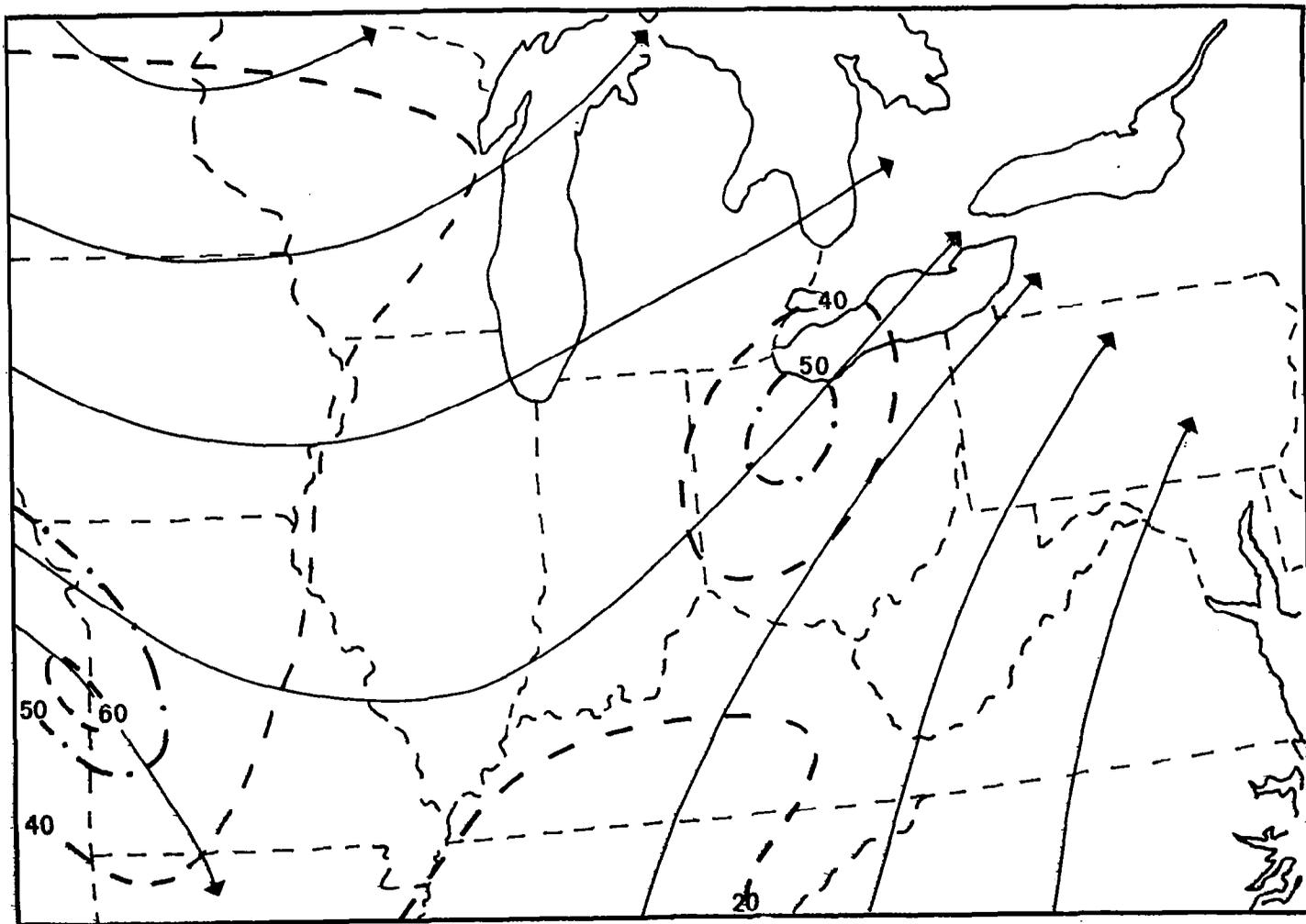
Figure 16-a. Streamlines and isotachs (knots, dashed) on isentropic surfaces for 0600 UT, 12 May, 1974. 300 K.
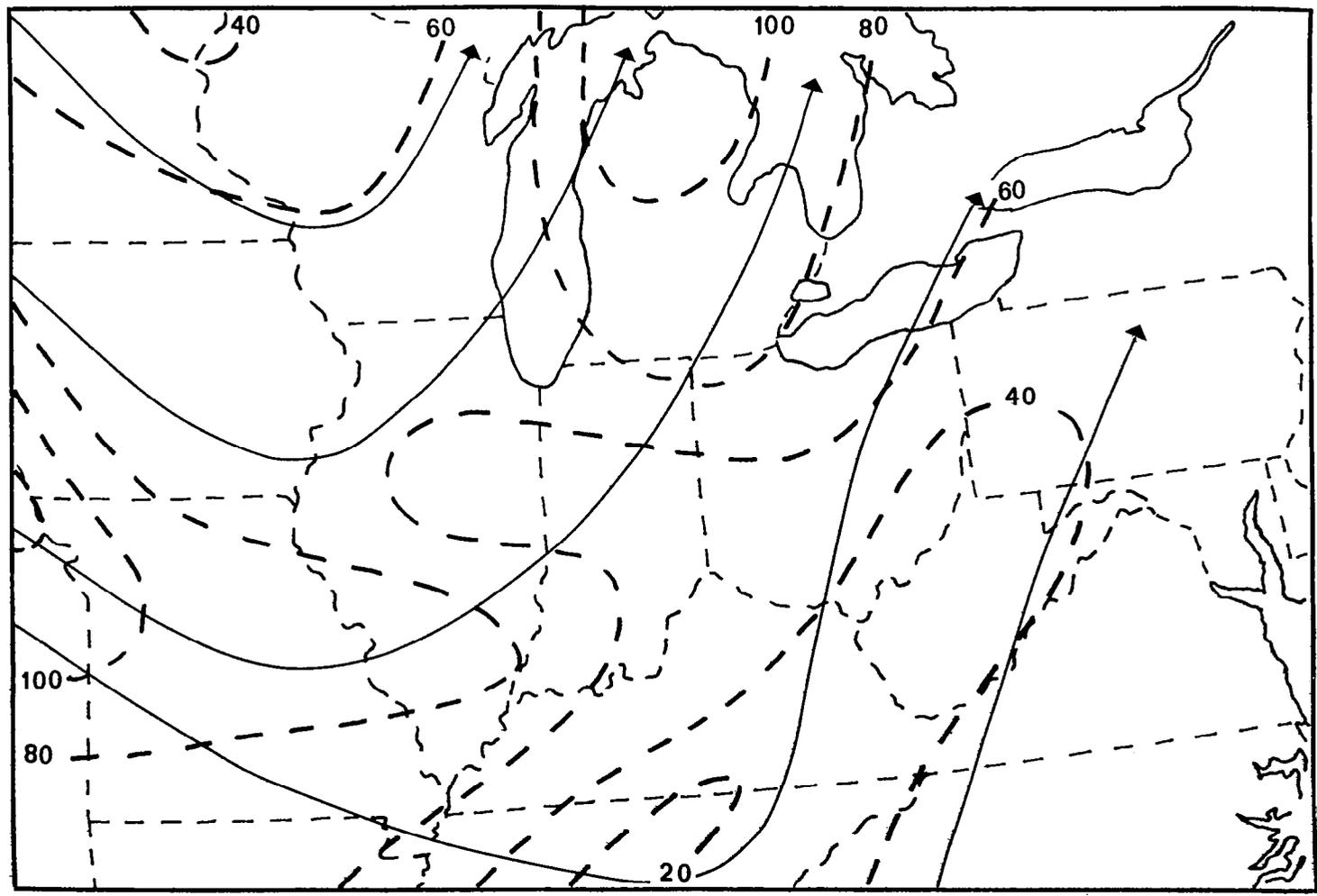
Figure 16-b.   312 K, 0600 UT, 12 May, 1974.
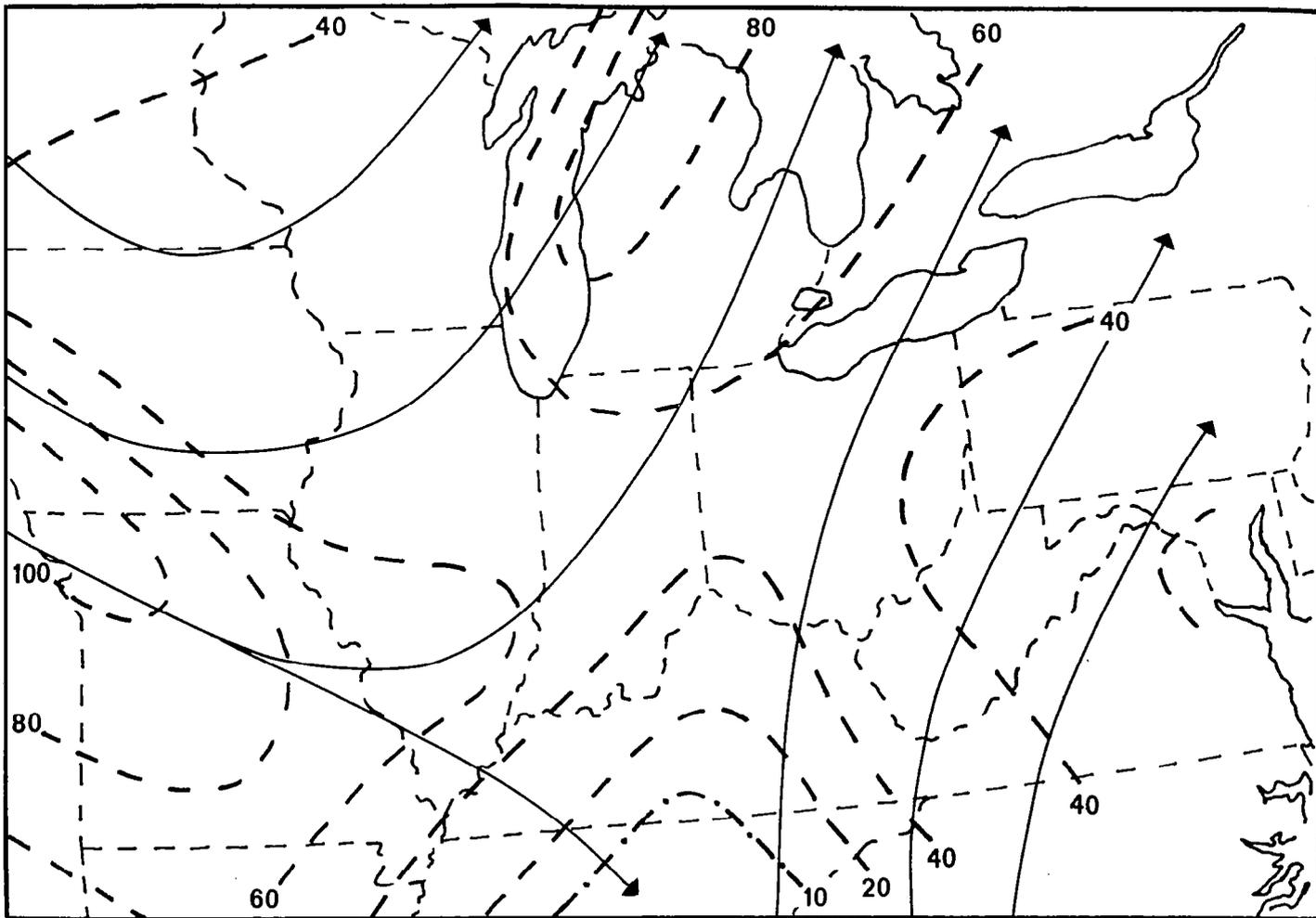
Figure 16-c. 320 K, 0600 UT, 12 May, 1974.
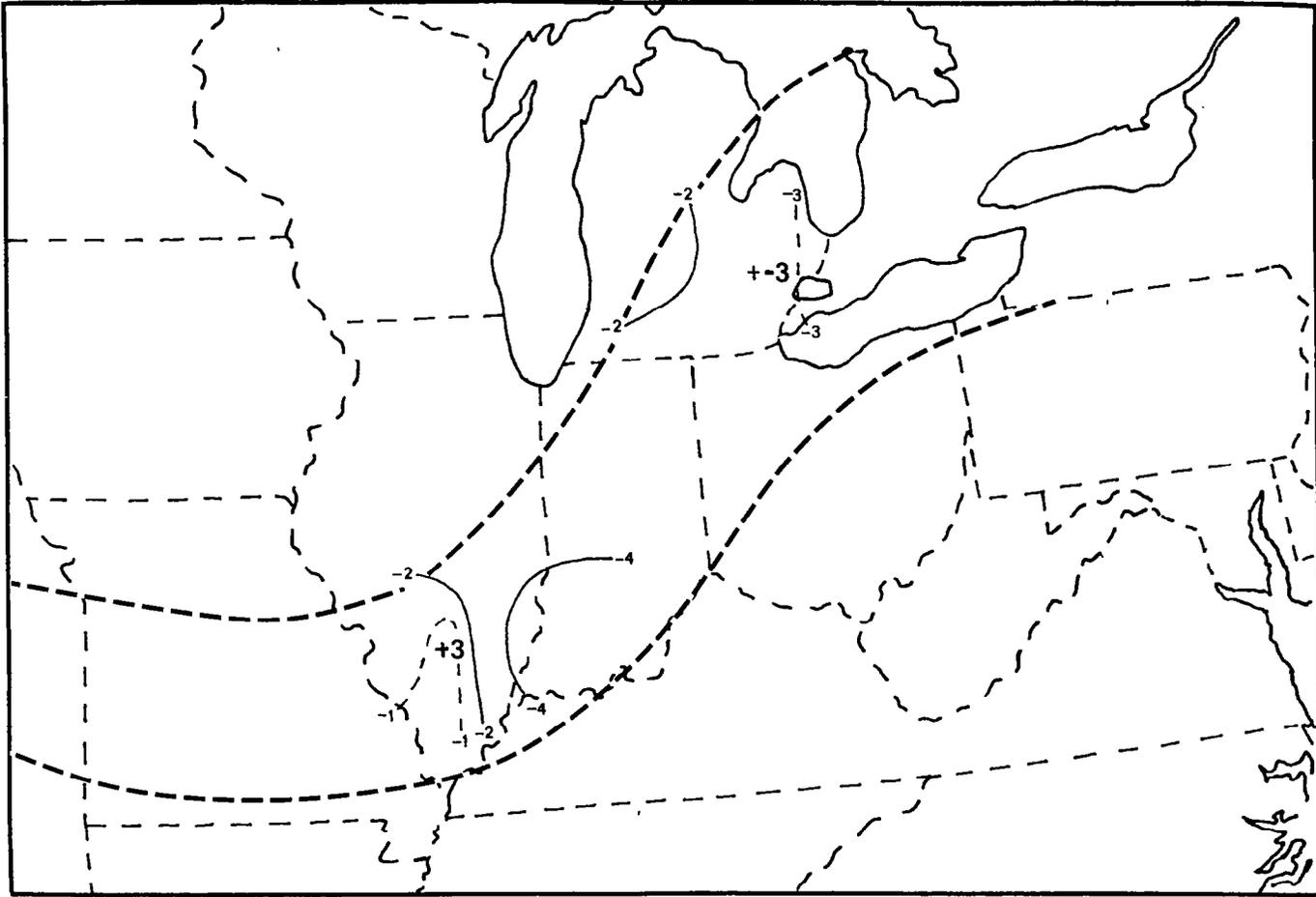
Figure 17-a. Frontal boundaries (heavy, dashed), dp/dt (x 10^{-3} mb sec^{-1}, intermediate values dashed), and computed frontogenesis (x 10^{-10}K m^{-1} sec^{-1}) on isentropic surfaces for 0600 UT, 12 May, 1974. 300 K.
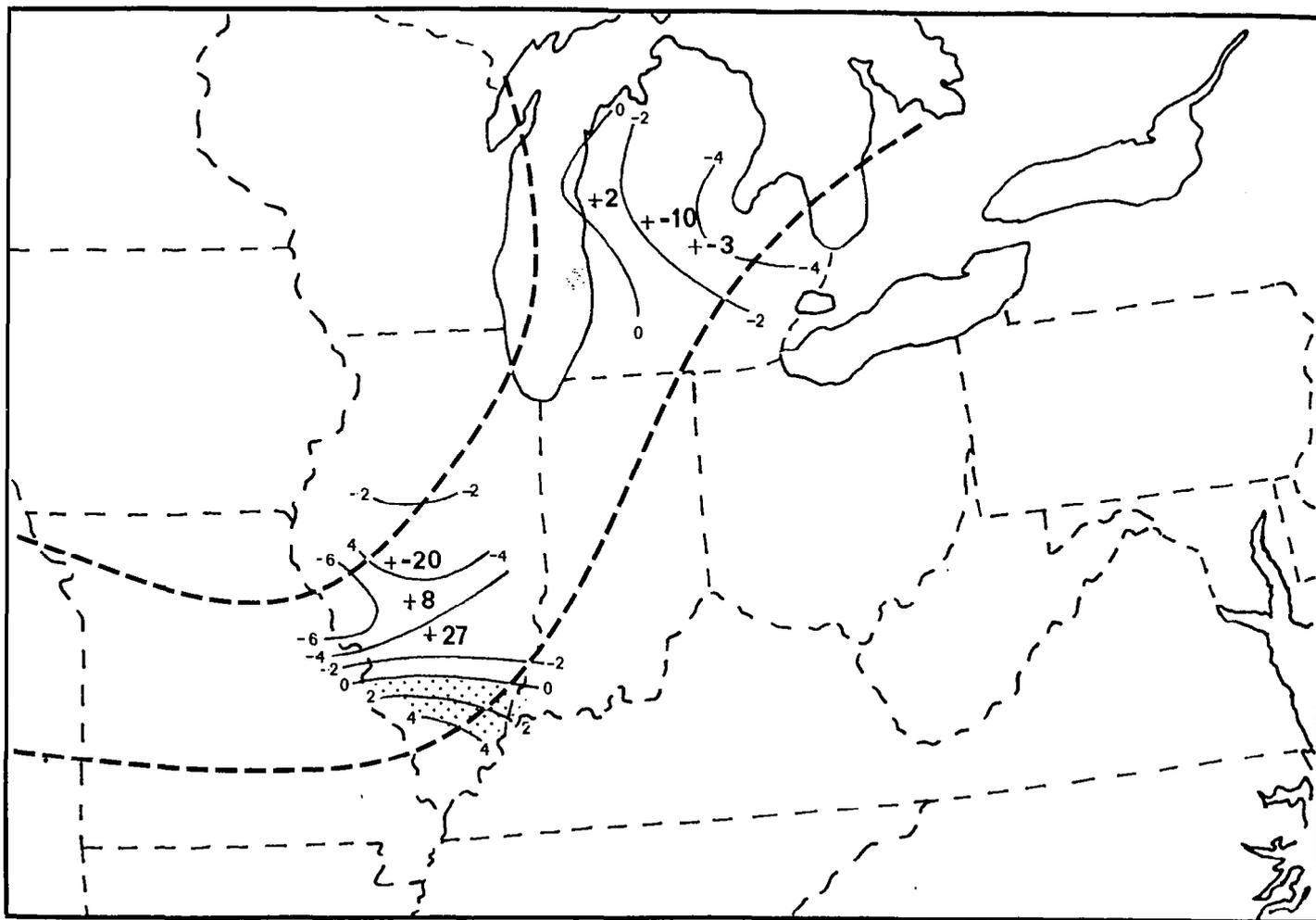
Figure 17-b. 312 K, 0600 UT, 12 May, 1974. Stippling indicates regions of subsidence.
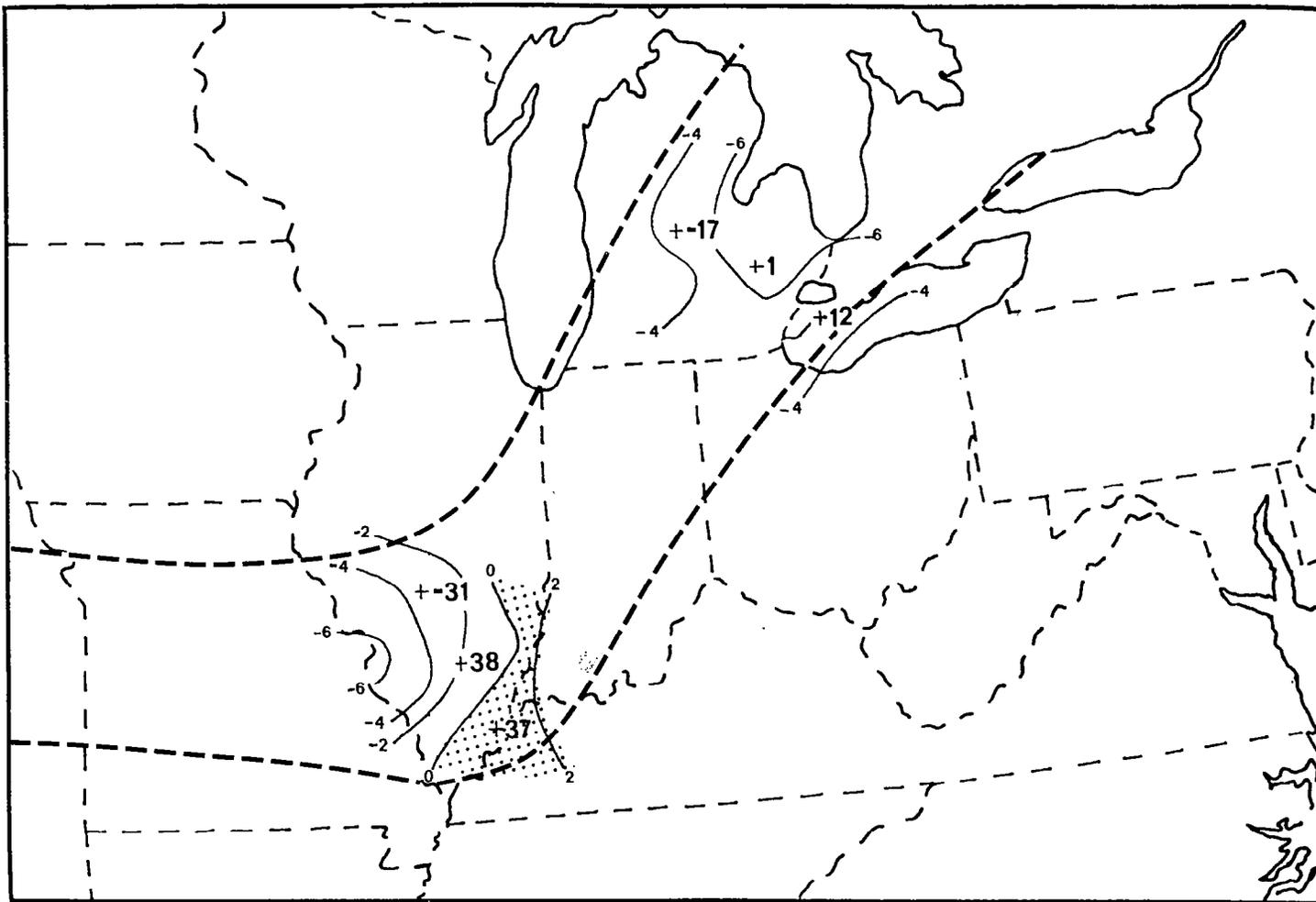
Figure 17-c.   320 K, 0600 UT, 12 May, 1974.
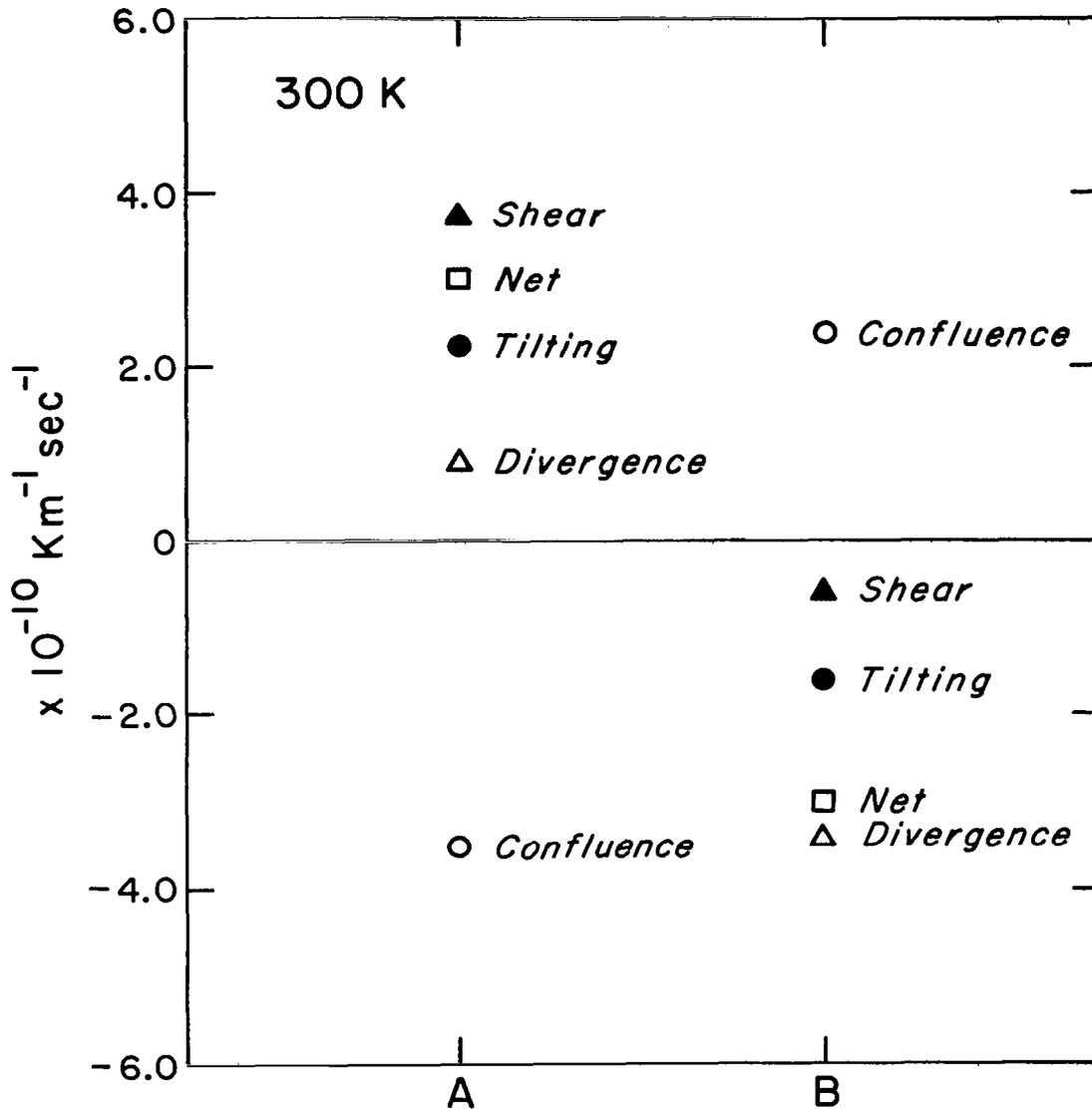
Figure 18-a. Values of terms of equation [2] at points indi-
cated on Figure 15 for 0600 UT, 12 May, 1974.
300 K.
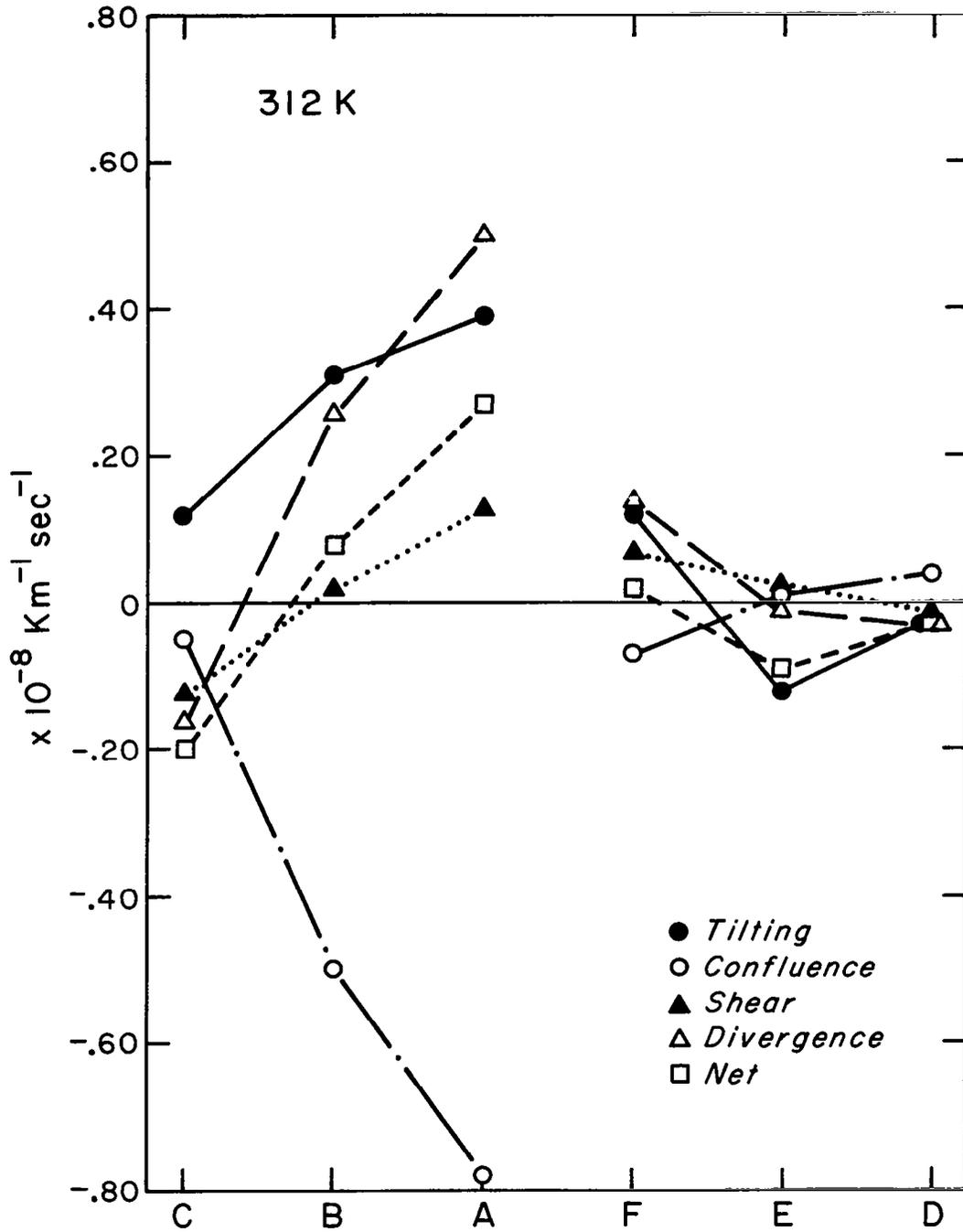
Figure 18-b. 312 K, 0600 UT, 12 May, 1974.
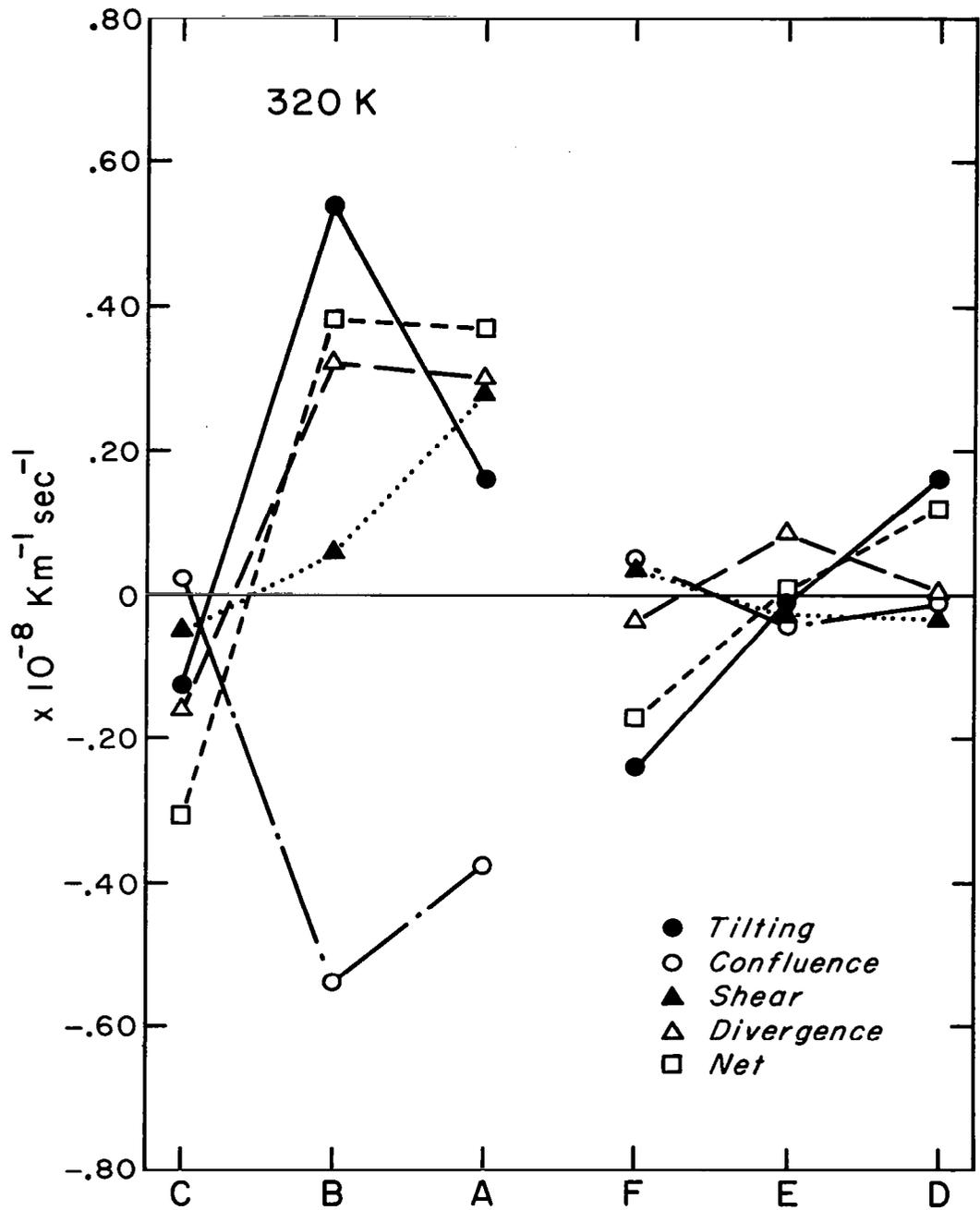
Figure 18-c. 320 K, 0600 UT, 12 May, 1974.

coordinates. Great difficulty arose in obtaining a wind field that possessed good time continuity in isobaric coordinates. Indeed, observations had to be occasionally ignored in order to bring continuity to the field on constant pressure surfaces. No such difficulty occurred in isentropic coordinates.

VERIFICATION OF THE COMPUTATIONS

The pattern of frontogenesis found in figure 17 is in
many ways that which ought to be expected. On all three
surfaces, the magnitudes of the frontogenesis are larger on
the southern section than on the northern one. This is
reasonable given the greater activity of the fronts in this
region. On the 312 and 320 K surfaces there is a tendency
for frontogenesis on the leading edges of the fronts and
frontolysis on the trailing edges. Such a pattern is con-
sistent with the observed movements of the fronts. Bosart
(1970), using similar data found a pattern of frontogenesis
upstream from the region of maximum temperature gradient
and frontolysis downstream from this region. However, the
front in his case was nearly stationary, unlike the steadily
moving fronts studied in this paper. The magnitudes of
frontogenesis computed by Bosart are of the same order of
magnitude as those computed for this case.

Having computed the parcel-following frontogensis at a
variety of points, it was necessary to see how well these
values corresponded with the change in frontogenesis actual-
ly experienced by moving parcels. To do this, trajectories
were constructed to determine the parcel's position three
hours before and after the time of the computation of
frontogenesis. The technique used to determine the trajec-
tories was a kinematic one. As Bosart (1970) has shown,

with such high time resolution data, the kinematic method for constructing trajectories yields results of comparable accuracy to the energy balance techniques of Danielsen (1961). The isentropic pressure gradient at the end points of the trajectories were estimated from the analyses mentioned earlier; the stability was determined by plotting soundings at nearby stations, then subjectively interpolating to the position of the parcel. The frontal intensity at the 0300 and 0900 UT position was then differenced to obtain the parcel-following frontogenesis. Results of this procedure are contained in table 1.

TABLE 1

Surface Point	Computed Frontogenesis $(x10^{-10}K\ m^{-1}sec^{-1})$	Trajectory-Following Frontogenesis $(x10^{-10}K\ m^{-1}sec^{-1})$
300K A	3	15
312K A	27	-66
312K C	-20	-21
320K A	37	- 2
320K C	-31	- 9

Parcel-following values could not be obtained for the northern section as the parcels were outside the data field by 0900 UT.

In comparing the two values of frontogenesis, the errors inherent in the techniques by which the values were

obtained should be taken into consideration. The uncertain-
ty in the analyses employed in computing these values is a
potential source of error. Because of this a difference be-
tween the computed and trajectory-following frontogenesis of
a factor of two or three is a practical limit of the accu-
racy of the techniques used. Taking this caveat into ac-
count, though, the disagreement between the locally com-
puted and trajectory-following frontogenesis is still sub-
stantial. One possible solution to this discrepancy is
that the frontogenesis at the midpoint of the trajectory
may not be representative of the frontogenesis along the
entire path of the parcel. To test this possibility, fronto-
genesis was computed at the beginning and end points of par-
cel A on the 312 K surface. Leibnitz' Rule was then used
to integrate the frontogenesis over the length of the tra-
jectory. The parcel was found to undergo frontolysis at
the beginning and end points of its path, with an integrated
frontogenesis of near zero. This still yields a large dif-
ference with the trajectory-following value of frontogene-
sis, but is a step in the right direction and demonstrates
that nonlinearities in the field of frontogenesis need to be
taken into account.

An additional source of error is the trajectories them-
selves. According to Bosart (1970), the maximum uncertain-
ty of a trajectory path from similar data is one grid
interval (equal to 200 km in his case) over a path length

of 15 to 20 grid intervals. This is also the maximum dif-
ference in parcel position between the kinematic and energy
balance techniques of constructing trajectories from three
hourly observations. In the vicinity of a front (which is
characterized by large gradients of several atmospheric pro-
perties), this small difference could be significant.
Errors of this magnitude were introduced into selected
trajectories. Little change in the magnitude of the pres-
sure gradient on the isentropic surface resulted, but it was
found that the stability could change drastically as a re-
sult of a small change in the position of the parcel. Using
the southern cross section as a guide, the introduction of
reasonable errors into the trajectory of the parcel results
in errors in the stability of about a factor of two. This
reduced the trajectory-following value of frontogenesis for
this parcel from $-66 \times 10^{-10} K\ m^{-1} sec^{-1}$ to $-20 \times 10^{-10} K\ m^{-1} sec^{-1}$.
Evidence that such errors were important comes from con-
sideration of the values in table 1. Notice that the best
agreement between the two values of frontogenesis occurs
for parcels C on the 312 and 320 K surfaces, and that the
worst disagreement is found for parcels A on these same sur-
faces. Parcels C were more in the center of the frontal
zones and hence experienced smaller changes in stability
from any errors in parcel position than did parcels A,
which were on the leading edge of the fronts. Thus, des-
pite the apparently low correlations between the values of

frontogenesis, there is reason to believe that the locally computed values of the parcel-following frontogenesis are indeed meaningful.

Inspection of figure 18 reveals that, in general, none of the terms of the frontogenesis equation can be said to be negligible. The shear term is frequently the smallest, but on the 300K surface in the southern section, it is the largest of the four terms. This lack of dominance of any term or terms is similar to Newton's findings (1954), and unlike the results of Reed (1955) and Reed and Sanders (1953). The reason for this difference is most likely that the fronts in this study and that of Newton are of more moderate intensity than those of the latter two papers.

As would be expected from the earlier-noted fashion in which the front developed by incorporating pre-existing stable layers into itself, the tilting term is important in producing changes in the intensity of the fronts. The vertical velocities on Figure 17 show how this term can affect the frontal intensity by producing variations across the front in the rate of adiabatic temperature changes. The region of the southern section on the 312 and 320 K surfaces shows descending motion along the warm edge of the fronts. This same feature has been noted by other investigators, and is characteristic of a developing upper front. The lack of such descent on the northern section is likely due to the fact that the front here is located in the right

rear quadrant of the jet streak, typically a region of ascending motion. The absence of a subsiding current implies that the fronts in this section are not, at this time, regions of the extrusion of stratospheric air. Examination of the appropriate cross sections lends credence to this conclusion; the fronts are poorly organized, and the 312K zone is no longer an extension of isentropes from the stratosphere.

The strong diffluence present near the southern section on all three isentropic surfaces is noteworthy, for it shows that fronts should not always be regarded as being due to or as representing the juxtaposition of air masses of different origins. That such a process is occurring is apparent from figure 16, but it is happening in a region where individual frontolysis is taking place, i.e. near the northern section. The role of confluent air masses in producing a front is more important in the lower levels of the troposphere, as can be seen from figure 16.

No attempt was made to quantify the effects of the diabatic terms in equation [2]. However, subjective estimates of the signs of these terms can be made from reports of cloud and precipitation and from cross sections of mixing ratios. The latter reveals a large upwards decrease in the mixing ratio through the 300 K front on the southern section. Radiational cooling from the top of this layer (i.e. the base of the front) would increase the stability above

the layer and hence the intensity of the front. This effect
is not so apparent at the other points where computations
were performed.

The other diabatic term involves horizontal variations
in the release of latent heat. In general, precipitation
occurred mostly on the warm side of the front, especially
along the northern section. This would contribute to in-
tensification of the fronts, although the effects would
probably be limited to the middle and lower troposphere.
The occurrence of convection behind the front on the
southern section would be a frontolytic effect, though the
limited extent of this activity would probably minimize
such frontolysis.

COMPUTATION OF VERTICAL VELOCITY

Objections could be raised to the manner in which
vertical velocities were computed, namely the difficulty in
determining the advection of pressure, particularly in the
middle troposphere, where the flow is nearly parallel to
the front. In order to examine this problem, trajectories
were constructed for a number of points at which vertical
velocities had been computed by the method already des-
cribed. The change in pressure between the end points of
the trajectories corresponded poorly with the vertical
velocities computed at the midpoints of the trajectories.
However, when the Eulerian vertical velocities at the mid-
point and end points of a trajectory were integrated using
Leibnitz' Rule to obtain the net displacement, a much better
relationship between the two different techniques was ob-
tained. Figure 19 shows a scatter diagram of values of
vertical displacements computed by these two methods for
several points from different levels at different times.
The correlation coefficient for this sample is .70 signi-
ficant at the 95 percent level as determined by the use of
the F ratio test. This sample is too small for drawing
definite conclusions, but it does demonstrate the useful-
ness of the Eulerian vertical velocities. Additional evi-
dence for accepting the values of vertical velocities ob-
tained by this method is the continuity of the resulting
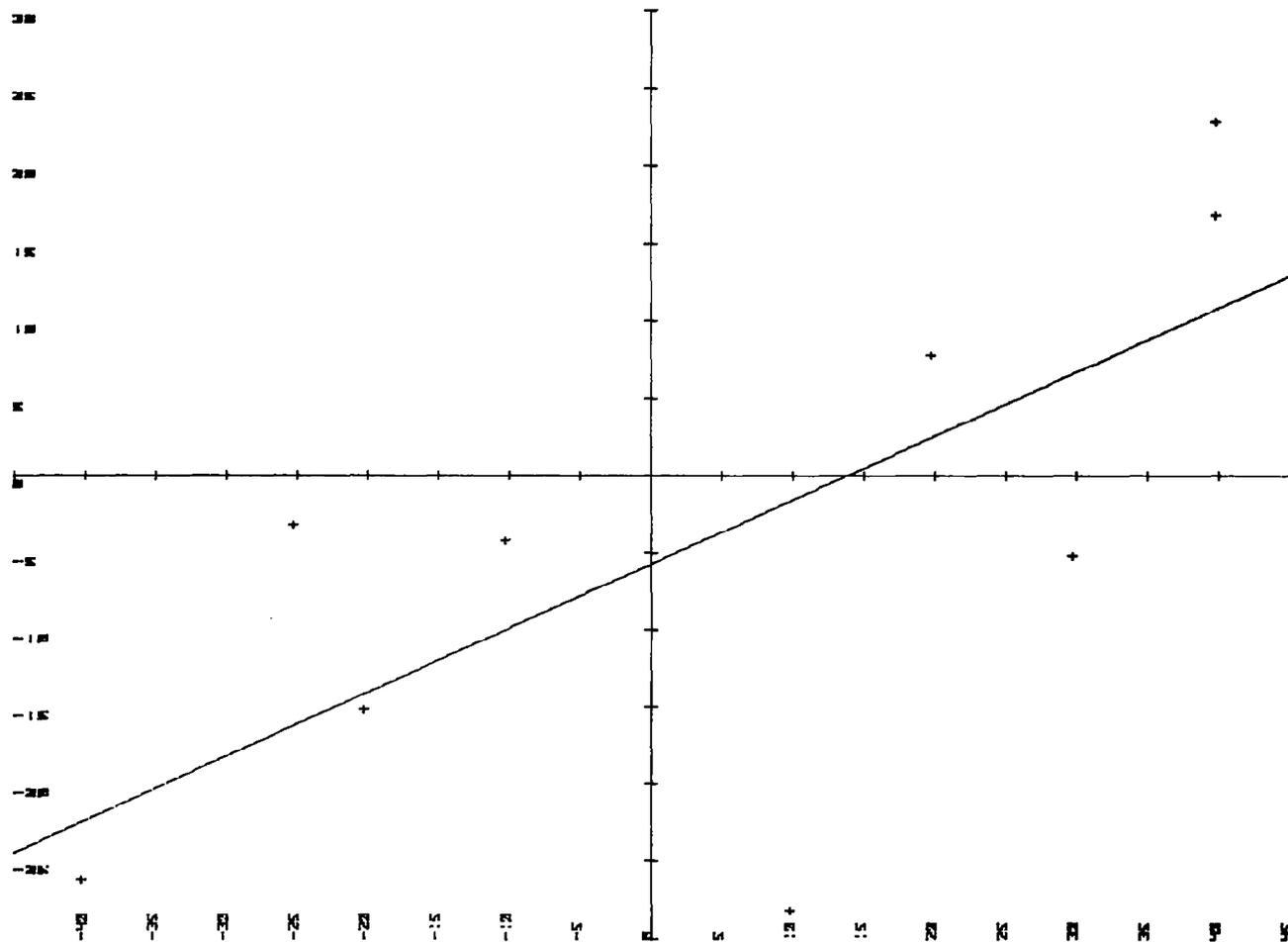
Figure 19. Six hour vertical displacement (mb) following a parcel (abcissa) and
vertical displacement computed by integrating dp/dt over the length of
the trajectory.

fields of vertical motion that it yields (see figure 17).
As a further check of the accuracy of the technique, verti-
cal velocities were computed around the two jet streaks
accompanying these fronts. Figure 20 shows the results of
these computations. As predicted by Murray and Daniels
(1953), there is ascent in the left front and right rear
quadrants of the jet streak, and descent in the right front
and left rear quadrants. This conformity of results to
theory adds confidence to the method by which the vertical
velocities were computed. The high time resolution of the
AVE data is the reason for such apparently accurate re-
sults. The local time rate change of pressure can be
evaluated more nearly instantaneously than with conven-
tional data, and the time continuity available from such
data makes possible more accurate evaluation of the terms
of equation [3].
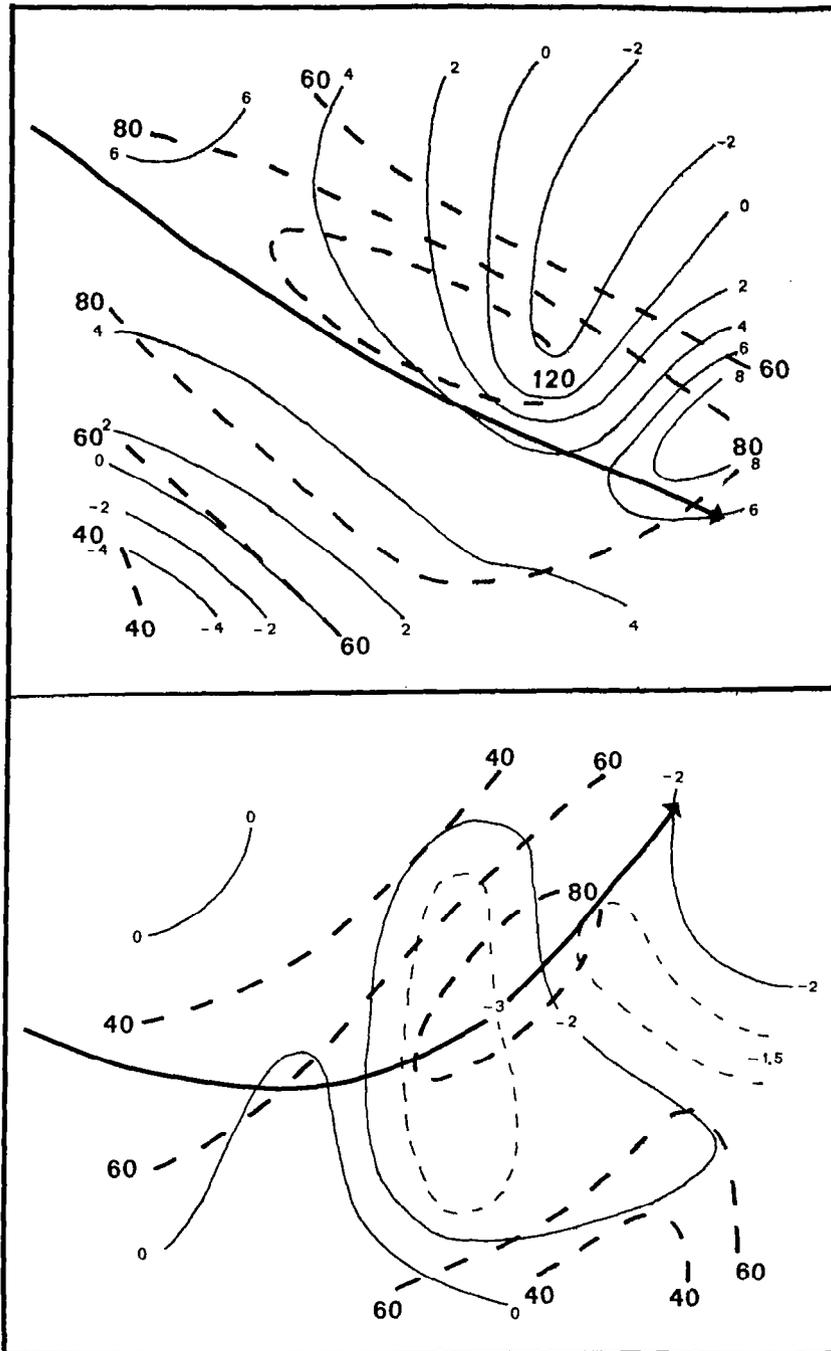
Figure 20. Isotachs (knots, dashed) and dp/dt (x 10^{-3} mb sec^{-1}) about jet streaks. Top: 312 K, 2100 UT, 11 May, 1974, on east side of trough. Bottom: 312 K, 0900 UT, 12 May, 1974, on west side of trough.

SUMMARY AND CONCLUSIONS

A cold front of moderate intensity was investigated using upper air soundings taken every three hours. The front was found to have a complex structure. The front showed up clearly on analyses of surface weather, but isentropic cross sections showed this front to be quite shallow and weak. Hyperbaroclinic zones were found in the middle and upper troposphere above the surface feature, and these zones were of much greater intensity than the surface front. The multiple structure of these zones was observed on all cross sections. These fronts were of greater intensity and showed more activity near the trough axis than to the east of the trough. The fronts were observed to build to as low as 800 mb by incorporation of pre-existing stable layers. Consideration of the distribution of potential vorticity indicates that the air in the upper portion of these fronts is of stratospheric origin. No evidence was found, however, that the extension of the front to very low altitudes was accompanied by the extrusion of stratospheric air. As this system of fronts passed a location, cooling occurred nearly simultaneously through deep layers of the atmosphere.

An attempt was made to compute frontogenesis on isentropic surfaces in the vicinity of the fronts. Poor correlations were found between this computed frontogenesis and that obtained by differencing the frontal intensity at the

endpoints of trajectories on the isentropic surfaces. The
likely reason for this is that inaccuracies in the trajec-
tories in the region of large gradients near the fronts
lead to large errors in the values of frontal intensity.
Consideration of the conservation of total energy along the
trajectory and the construction of additional cross sections
at the endpoints of the trajectories might have helped to
give more accurate trajectories and better estimates of
stability. The field of frontogenesis was found to vary
quite nonlinearly along the trajectories. The size of this
effect with data of such high time resolution casts doubts
on the usefulness of conventional data for the evaluation
of frontogenesis. No single term of the frontogenesis
equation was found to be dominant over the other terms.
This is apparently due to the moderate intensity of this
system of fronts.

Vertical velocities were computed using a modified
adiabatic technique. The field of these velocities is
found, like that of the field of frontogenesis, to be high-
ly nonlinear and nonsteady. A good correlation was found
between these velocities integrated over the path of a par-
cel and the displacement between the endpoints of the tra-
jectory. The field of computed vertical velocities around
the jet streaks accompanying these fronts agrees well with
theory. Again, conventional data would have yielded much
poorer results as these features were of small scale and

were resolved only through consideration of the continuity
of observations closely spaced in time. The poor correla-
tion between instantaneous vertical velocities and that ob-
tained by differencing the pressure at the endpoints of
trajectories casts doubts on the usefulness of the tra-
jectory-obtained values in studies of frontogenesis.

SUGGESTIONS FOR FURTHER RESEARCH

The difference between kinematic and energy-conserving trajectories should be determined. The stability at the end points of the trajectories should be better evaluated. Both of these refinements could then be used to obtain more accurate estimates of trajectory-following frontogenesis for comparison with values of frontogenesis obtained by evaluating the frontogenesis equation.

A knowledge of the history of the air comprising the fronts is useful in understanding the development of the fronts. Therefore, it would be useful to construct isentropic trajectories in order to study the origins of air in different regions of the hyperbaroclinic zones. If the field of stability can be adequately resolved, studying the changes in the potential vorticity along the trajectories might shed light on diabatic processes affecting the fronts.

The use of objective analysis techniques would greatly reduce the time necessary for the construction of analyses or the computation of frontogenesis. This would increase the variety of ways in which the fronts could be studied. For example, maps of the field of frontogenesis at different times could more readily be prepared. Care must be taken, though, to preserve in the objective analyses the detail that is found in the subjectively obtained analyses. A comparison of the differences between analyses and

computations obtained by the two methods could be an interesting and revealing study.

The importance of advection in changing the appearance of the southern cross section cannot be adequately ascertained with the analyses used in this study. To better understand the changes observed on the southern section, particularly the appearance of the low level front late in the period of observation, it would be desirable to construct additional cross sections upstream from the location of the southern cross sections.

Work performed after the completion of this study shows cross sections of baroclinity to be very useful in depicting the development of fronts. Construction of such cross sections could more clearly show the evolution of the fronts studied in this case.

The possible frontogenetic influence of the transport of latent heat in advance of the fronts by the southeast cyclone may merit study. The importance of radiative processes in the low level frontogenesis observed late on the southern section is also worthy of investigation.

123

BIBLIOGRAPHY

Berggren, R., 1952: The distribution of temperature and winds connected with active tropical air in the higher troposphere and some remarks concerning clear air turbulence at high altitude. Tellus, 4, 43-54.

Bergeron, T., 1928: Über die driedimensional verknüpfende Wetteranalyses (I). Geofys. Publikasjoner, Norske Videnskaps - Akad. Oslo 5, No. 6, 1-111.

Bjerknes, J., 1918: On the structure of moving cyclones. Geofys. Publikasjoner, Norske Videnskaps - Akad. Oslo 3, No. 1, 1-18.

Bjerknes, J., and Solberg, H., 1922: Life cycle of cyclones and the polar front theory of atmospheric circulation. Geofys. Publikasjoner, Norske Videnskaps-Akad. Oslo 3, No. 1, 1-18.

Bosart, L. F., 1970: Mid-tropospheric frontogenesis. Quart. J. Roy. Meteor. Soc., 96, 442-471.

Browning, K.A., and Harrold, T. W., 1970: Air motion and precipitation growth at a cold front. Quart. J. Roy. Meteor. Soc., 96, 369-389.

Danielsen, E. F., 1961: Trajectories: isobaric, isentropic, and actual. J. Meteor., 18, 479-486.

_____, 1964: Project Springfield Report. Headquarters, Defense Atomic Support Agency, Washington, D.C., 97 pp.

Defant, F., and Taba, H., 1958: The breakdown of the zonal circulation during the period January 8 to 13, 1956, the characteristics of temperature fields and tropopause and its relation to the atmospheric field of motion. Tellus, 10, 430-450.

Eliassen, A., 1962: On the vertical circulation in frontal zones. Geofys. Publikasjoner, Norske Videnskaps - Akad. Oslo, 24, 147-160.

_____, 1966: Motions of intermediate scale: fronts and cyclones. Advances in Earth Science (P.M. Hurley, ed.), M.I.T. Press, 1966,111-138.

Epsy, J. P., 1841: Philosophy of storms. Boston, 1841.

Faller, A. J., 1956: A demonstration of fronts and frontal waves in atmospheric models. J. Meteor., 13, 1-4.

Fujita, T., 1963: Analytical mesometeorology: a review. Meteor. Monogr., No. 27, Amer. Meteor. Soc., 77-125.

Fultz,D., 1952: On the possibility of experimental models of the polar-front wave. J. Meteor., 9, 379-384.

Godson, W. L., 1951: Synoptic properties of frontal surfaces. Quart. J. Roy. Meteor. Soc., 77, 633-653.

Haltiner, G. J., and Martin, F. L., 1957: Dynamical and physical meteorology. New York, McGraw-Hill, 287-296.

Hoskins, B. J., 1971: Atmospheric frontogenesis models: some solutions. Quart. J. Roy. Meteor. Soc., 97, 139-153.

Howard, L., 1820: The Climate of London, deduced from meteorological observations, made at different places in the neighborhood of the metropolis. Vol. II. London, 1820.

La Seur, N., 1974: The role of vertical motion in the development of upper tropospheric hyperbaroclinic zones. Subsynoptic Extratropical Weather Systems, Vol. I. Lecture notes from a NCAR colloquim, M. Shapiro, coordinator, 20-30.

Matsumoto, S., Ninomiya, K., and Yoshizumi, S., 1971: Characteristic features of "Baiu" front associated with heavy rainfall. J. Meteor. Soc. Japan, 49, 267-281.

Miller, J. E., 1948: On the concept of frontogenesis. J. Meteor., 5, 169-171.

Murray, R., and Daniels, S. M., 1953: Transverse flow at entrance and exit to jet streams. Quart. J. Roy. Meteor. Soc., 79, 236-241.

Namias, J., and Clapp, P. F., 1949: Confluence theory of the high tropospheric jet stream. J. Meteor., 6, 220-226.

Newton, C. W., 1954: Frontogenesis and frontolysis as a three-dimensional process. J. Meteor. 11, 449-461.

Newton, C. W., and Palmén, E., 1963: Kinematic and thermal properties of a large-amptitude wave in the westerlies. Tellus, 15, 99-119.

Palmén, E., 1948:   On the distribution of temperature and wind in the upper westerlies. J. Meteor. 5, 20-27.

_____, 1958:   Vertical circulation and release of kinetic energy during the development of hurricane Hazel into an extratropical storm. Tellus, 10, 1-23.

Palmén, E., and Newton, C. W., 1948:   A study of the mean wind and temperature distribution in the vicinity of the polar front in winter. J. Meteor., 5, 220-226.

_____, 1969:   Atmospheric circulation systems. New York, Academic Press, 603 pp.

Petterssen, S., 1936:   Contribution to the theory of frontogenesis. Geofys. Publikasjoner. Norske Videnskaps – Akad. Oslo, 11, No. 6, 1-27.

_____, 1940:   Weather analysis and forecasting, 1st ed. New York, McGraw-Hill, 505 pp.

_____, 1956:   Weather analysis and forecasting, 2nd ed., Vol. 1, New York, McGraw-Hill, 428 pp.

Petterssen, S., and Austin, J. M., 1942:   Fronts and frontogenesis in relation to vorticity. Papers Phys. Oceanog. Meteor., Mass. Inst. Technol. Woods Hole Oceanog. Inst. 7, No. 2, 1-37.

Reed, R. J., 1955: A study of a characteristic type of upper-level frontogenesis. J. Meteor., 11, 226-237.

Reed, R. J., and Danielsen, E. F., 1959:   Fronts in the vicinity of the tropopause. Arch. Meteor. Geophys. Bioklim., A 11, 1-17.

Reed, R. J., and Sanders, F., 1953:   An investigation of the development of a mid-tropospheric frontal zone and its associated vorticity field. J. Meteor., 10, 338-349.

Sanders, F., 1955:   An investigation of the structure and dynamics of an intense surface frontal zone. J. Meteor., 12, 542-552.

_____, 1967:   Frontal structure and the dynamics of frontogenesis. Final report to NSF, Grant GP-1508, F. Sanders principal investigator, 5.1-5.14.

126

Sawyer, J. S., 1956: The vertical circulation at meteoro-
    logical fronts and its relation to frontogenesis.
    Proc. Roy. Soc., A234, 236-262.

_____, 1958: The free atmosphere in the vicinity
    of fronts. Geophys. Mem., 12, No. 96.

Schwerdtfeger, W., and Strommen, N. D., 1964: Structure of
    a cold front near the center of an extratropical de-
    pression. Mon. Wea. Re., 92, 523-531.

Scoggins, J. R. and Turner, R. E., 1974: Data for NASA's
    AVE II Pilot Experiment. NASA TM X - 64877.

Shapiro, M. A., 1970: On the applicability of the geo-
    strophic approximation to upper-level frontal-scale
    motions. J. Atmos. Sci., 27, 408-420.

_____, 1974: A multiple-structured frontal zone-
    jet stream system as revealed by meteorologically in-
    strumented aircraft. Mon. Wea. Rev., 102, 244-253.

_____, 1976: The role of turbulent heat flux in
    the generation of potential vorticity in the vicinity
    of upper-level jet stream systems. Mon. Wea. Rev.,
    104, 892-906.

Staley, D. O., 1960: Evaluation of potential-vorticity
    changes near the tropopause and the related vertical
    motions, vertical advection of vorticity, and trans-
    fer of radioactive debris from stratosphere to tropo-
    sphere. J. Meteor., 17, 591-620.

U.S. Department of Commerce, 1974: Storm data. National
    Climatic Center, Asheville, N.C.

APPENDIX

DERIVATION OF THE FRONTOGENESIS EQUATION
IN ISENTROPIC COORDINATES

Frontogenesis will be defined as the total time rate of change of the magnitude of the gradient of potential temperature on an isobaric surface

$$F = \frac{d}{dt} \left| \nabla_p \theta \right| \tag{1}$$

Now, for any vector $\vec{a}$

$$\vec{a} \cdot \vec{a} = \left| \vec{a} \right|^2 \tag{2}$$

differentiating with respect to time gives

$$\frac{d}{dt} (\vec{a} \cdot \vec{a}) = 2 \left| \vec{a} \right| \frac{d}{dt} \left| \vec{a} \right| \tag{3}$$

So we have

$$\frac{d \left| \vec{a} \right|}{dt} = \frac{1}{2 \left| \vec{a} \right|} \frac{d}{dt} (\vec{a} \cdot \vec{a})$$

$$= \frac{\vec{a}}{\left| \vec{a} \right|} \cdot \frac{d\vec{a}}{dt} \tag{4}$$

Equation (1) can be rewritten

$$F = \frac{\nabla_p \theta}{\left| \nabla_p \theta \right|} \cdot \frac{d}{dt} \nabla_p \theta \tag{5}$$

128

The transformation from isobaric to isentropic coordinates is

$$\nabla_p \theta = \nabla_\theta \theta - \frac{\partial \theta}{\partial p} \nabla_\theta p$$

$$= -\left(\frac{\partial p}{\partial \theta}\right)^{-1} \nabla_\theta p \tag{6}$$

When (6) is applied to equation (5), the result is

$$F = - \frac{\nabla_\theta p}{|\nabla_\theta p|} \cdot \frac{d}{dt}\left[\left(\frac{\partial p}{\partial \theta}\right)^{-1} \nabla_\theta p\right] \tag{7}$$

The term to the left of the dot product will be neglected for the moment and the total derivative will be expanded to give

$$\frac{d}{dt}\left[\left(\frac{\partial p}{\partial \theta}\right)^{-1} \nabla_\theta p\right] = \overset{A}{\frac{\partial}{\partial t}\left[\left(\frac{\partial p}{\partial \theta}\right)^{-1} \nabla_\theta p\right]} + \overset{B}{V \cdot \nabla_\theta\left[\left(\frac{\partial p}{\partial \theta}\right)^{-1}{}_\theta p\right]}$$

$$+ \overset{C}{\frac{d\theta}{dt} \frac{\partial}{\partial \theta}\left[\left(\frac{\partial p}{\partial \theta}\right)^{-1} \nabla_\theta p\right]} \tag{8}$$

Next, expand terms A, B, and C

$$A = \left(\frac{\partial p}{\partial \theta}\right)^{-1} \frac{\partial}{\partial t} \nabla_\theta p + \nabla_\theta p \frac{\partial}{\partial t}\left(\frac{\partial p}{\partial \theta}\right)^{-1} \tag{9}$$

$$B = \left(\frac{\partial p}{\partial \theta}\right)^{-1} V \cdot \nabla_\theta({}_\theta p) + \nabla_\theta p \, V \cdot \nabla_\theta\left(\frac{\partial p}{\partial \theta}\right)^{-1} \tag{10}$$

$$C = \left(\frac{\partial p}{\partial \theta}\right)^{-1} \frac{d\theta}{dt} \frac{\partial}{\partial \theta} \nabla_\theta p + \nabla_\theta p \frac{d\theta}{dt} \frac{\partial}{\partial \theta}\left(\frac{\partial p}{\partial \theta}\right)^{-1} \tag{11}$$

The first term on the right hand side of (9) can be expanded

$$(\frac{\partial p}{\partial \theta})^{-1} \frac{\partial}{\partial t} \nabla_\theta p = (\frac{\partial p}{\partial \theta})^{-1} [\frac{d}{dt} \nabla_\theta p - \mathbb{V} \cdot \nabla_\theta (_\theta p)$$

$$- \frac{d\theta}{dt} \frac{\partial}{\partial \theta} \nabla_\theta p] \tag{12}$$

The second term on the right side of (12) cancels with the first term on the right side of (10). Next, expand the second term on the right side of (9)

$$\frac{\partial}{\partial t} (\frac{\partial p}{\partial \theta})^{-1} = -(\frac{\partial p}{\partial \theta})^{-2} \frac{\partial}{\partial t} (\frac{\partial p}{\partial \theta}) \tag{13}$$

With the use of the equation of continuity in isentropic coordinates, equation (13) becomes

$$\frac{\partial}{\partial t} (\frac{\partial p}{\partial \theta})^{-1} = -(\frac{\partial p}{\partial \theta})^{-2} [- \mathbb{V} \cdot \nabla_\theta \frac{\partial p}{\partial \theta} - \frac{\partial p}{\partial \theta} \nabla_\theta \cdot \mathbb{V}$$

$$- \frac{d\theta}{dt} \frac{\partial}{\partial \theta} (\frac{\partial p}{\partial \theta}) - \frac{\partial p}{\partial \theta} \frac{\partial}{\partial \theta} \frac{d\theta}{dt}] \tag{14}$$

When expanded, the second terms on the right hand sides of (10) and (11) will cancel with terms in (14). The sum of (9), (10), and (11) will be

130

$$\frac{d}{dt}\left[\left(\frac{\partial p}{\partial \theta}\right)^{-1}\nabla_\theta p\right] = \left(\frac{\partial p}{\partial \theta}\right)^{-1}\left[\frac{d}{dt}\nabla_\theta p - \frac{d\theta}{dt}\frac{\partial}{\partial \theta}\nabla_\theta p + (\nabla_\theta \cdot \vec{V})_\theta p\right.$$

$$\left. + \nabla_\theta p \frac{\partial}{\partial \theta}\frac{d\theta}{dt} + \frac{d\theta}{dt}\frac{\partial}{\partial \theta}\nabla_\theta p\right]$$

$$= \left(\frac{\partial p}{\partial \theta}\right)^{-1}\left\{\frac{d}{dt}\nabla_\theta p + \nabla_\theta p\left[\nabla_\theta \cdot \vec{V} + \frac{\partial}{\partial \theta}\frac{d\theta}{dt}\right]\right\} \quad (15)$$

The first term in the brackets of (15) can be expanded

$$\frac{d}{dt}\nabla_\theta p = \frac{\partial}{\partial t}\nabla_\theta p + \vec{V}\cdot\nabla_\theta(\nabla_\theta p) + \frac{d\theta}{dt}\frac{\partial}{\partial \theta}\nabla_\theta p)$$

$$= \nabla_\theta \frac{dp}{dt} - \nabla_\theta(\vec{V}\cdot\nabla_\theta p) - \nabla_\theta \frac{d\theta}{dt}\frac{\partial p}{\partial \theta} + \vec{V}\cdot\nabla_\theta(\nabla_\theta p) + \frac{d\theta}{dt}\frac{\partial}{\partial \theta}\nabla_\theta p$$

$$= \nabla_\theta \frac{dp}{dt} - \left(\vec{i}\frac{\partial u}{\partial x}\frac{\partial p}{\partial x} + \vec{j}\frac{\partial v}{\partial y}\frac{\partial p}{\partial y}\right) - \left(\vec{i}\frac{\partial v}{\partial x}\frac{\partial p}{\partial y} + \vec{j}\frac{\partial u}{\partial y}\frac{\partial p}{\partial x}\right) \quad (16)$$

$$- \frac{\partial p}{\partial \theta}\nabla_\theta \frac{d\theta}{dt}$$

Substituting (16) into (15) and including the terms omitted from (7) gives the equation for frontogenesis in isentropic coordinates

$$F = - \frac{\nabla_\theta p}{|\nabla_\theta p|}\cdot\left(\frac{\partial p}{\partial \theta}\right)^{-1}\left\{\nabla_\theta \frac{dp}{dt} - \left(\vec{i}\frac{\partial u}{\partial x}\frac{\partial p}{\partial x} + \vec{j}\frac{\partial v}{\partial y}\frac{\partial p}{\partial y}\right)\right.$$

$$\left. - \left(\vec{i}\frac{\partial v}{\partial x}\frac{\partial p}{\partial y} + \vec{j}\frac{\partial u}{\partial y}\frac{\partial p}{\partial x}\right) - \frac{\partial p}{\partial \theta}\nabla_\theta \frac{d\theta}{dt}\right. \quad (17)$$

$$\left. + \nabla_\theta p\left[\nabla_\theta \cdot \vec{V} + \frac{\partial}{\partial \theta}\frac{d\theta}{dt}\right]\right\}$$

1. Report No. NASA RP-1005	2. Government Accession No.	3. Recipient's Catalog No.
4. Title and Subtitle Fronts and Frontogenesis as Revealed by High Time Resolution Data		5. Report Date August 1977
		6. Performing Organization Code
7. Author(s) Albert E. Frank* and David A. Barber*		8. Performing Organization Report No. M-226
		10. Work Unit No.
9. Performing Organization Name and Address George C. Marshall Space Flight Center Marshall Space Flight Center, Alabama 35812		11. Contract or Grant No.
		13. Type of Report and Period Covered Reference Publication
12. Sponsoring Agency Name and Address National Aeronautics and Space Administration Washington, D. C. 20546		
		14. Sponsoring Agency Code

16. Abstract

   Upper air soundings taken every 3 hours are used to examine a cold front of average intensity over a period of 24 hours. Vertical cross sections of potential temperature and wind and horizontal analyses are compared and adjusted until they are consistent with one another. These analyses are then used to study the evolution of the front, which is found to consist of a complex system of fronts occurring at all levels of the troposphere. Low-level fronts are strongest at the surface and rapidly weaken with height. Fronts in the middle and upper troposphere are much more intense. The warm air ahead of the fronts is nearly barotropic, while the cold air behind the fronts is baroclinic through deep layers. A deep mixed layer is observed to grow in this cold air.

   Examination of cross sections of potential temperature and potential vorticity indicates that the air in at least the upper portions of the upper level fronts originates in the stratosphere. No evidence is found, however, of an extrusion of stratospheric air to very low levels. The structure of the upper level fronts is complex. These fronts are observed to split apart, recombine, and descend to low elevations due to the incorporation of pre-existing stable/baroclinic layers.

   An equation for parcel-following frontogenesis in isentropic coordinates is developed and applied. No single process was found to be dominant in changing frontal intensity. Frontogenesis occurs on the leading edge of the fronts and frontolysis on the trailing edge. The magnitudes of the computed frontogenesis decrease downstream from the axis of the upper level trough.

   Isentropic trajectories are constructed to verify the computed values of parcel-following frontogenesis. Poor correlations found between the computed and trajectory-following values of frontogenesis are believed to be due to nonlinearities in the field of frontogenesis and to errors in the trajectories.

   Vertical velocities are computed using a kinematic technique. Reasonable fields of vertical velocity are obtained in the vicinity of the fronts and jet streaks. Good correlations are found between the vertical displacement between endpoints of the trajectories and the value of computed vertical velocity integrated over the path of the trajectory. The field of vertical velocity is also found to be highly nonlinear.

17. Key Words (Suggested by Author(s))	18. Distribution Statement STAR Category 47	
19. Security Classif. (of this report) Unclassified	20. Security Classif. (of this page) Unclassified	21. No. of Pages 136	22. Price $6.00

*For sale by the National Technical Information Service, Springfield, Virginia 22161.

National Aeronautics and
Space Administration

Washington, D.C.
20546

THIRD-CLASS BULK RATE

508 001 C1 U   E 770708 S00903DS
DEPT OF THE AIR FORCE
AF WEAPONS LABORATORY
ATTN: TECHNICAL LIBRARY (SUL)
KIRTLAND AFB NM 87117

MIXED

STATES

NASA